„Loading of total hip joint replacements –

In vivo measurements with instrumented hip implants“

vorgelegt von
Dipl.-Ing. Philipp Damm
geb. in Zschopau

von der Technischen Universität Berlin
Fakultät V – Verkehrs- und Maschinensysteme
zur Erlangung des akademischen Grades

Doktor der Ingenieurwissenschaften
Dr.-Ing.

genehmigte Dissertation

Promotionsausschuss:

Vorsitzender: Prof. Dr.-Ing. Jörg Krüger

Gutachter: Prof. Dr.-Ing. Marc Kraft

Gutachter: Prof. Dr.-Ing. Georg Bergmann

Tag der wissenschaftlichen Aussprache: 08. September 2014

Berlin 2014
D 83

Acknowledgments

First and foremost I would like to sincerely thank everyone who supported me throughout the implementation and evaluation of the very extensive *in vivo* measurements. It has given me great pleasure to work in this unique scientific environment with the opportunity to get a doctorate.

A very special thank you goes out to the patients who volunteered their time and effort to take part in the study. Their enthusiasm and focus during the extensive measurements are greatly appreciated.

This work would not have been possible without the extensive support from Prof. Dr. -Ing. Georg Bergmann who, with his constructive criticism and advice, has been a great mentor throughout my dissertation. I would like to thank him for letting me draw from his profound scientific experience, valuable discussions and encouraging my independent scientific work.

Furthermore, special thanks goes to the entire team of "Instrumented Implants" at the Julius Wolff Institute. It was fantastic to work with you, you have been a great source of collaboration and advice. I would also like to thank all the students who helped evaluating the measurement data.

I am indebted to Dipl.-Ing. Jörn Dymke for his great support during the measurements and Dr.-Ing. Friedmar Graichen for his help with implant fabrication and moral support. I would like to acknowledge Barbara Schiller for her great administrative assistance. A special thanks to Dr.-Ing. Alwina Bender for her assistance with mathematical problems and the needed software support. I would like to thank Dipl.-Sportw. Verena Schwachmeyer for her support and scientific discussions. My personal thanks go to Dr. rer. medic Ines Kutzner; it was fantastic to work with you each day. I want to thank Prof. Dr. Andreas Haider and Dr. Alexander Beier from the Sana Kliniken Sommerfeld for the time-consuming search for study participants and clinical support. Thank you to my sister Sophie Damm for proof-reading the manuscript.

Last but not least I would like to thank my parents who raised me with a love for science and supported me in all my pursuits. Their unconditional encouragement and support have in no small way contributed to who I am today.

Table of Contents

„Die Belastung des Hüftgelenkes –

In vivo Messungen mit instrumentierten Hüftendoprothesen“

von Dipl.-Ing. Philipp Damm

Zusammenfassung

Der totale Hüftgelenkersatz zählt zu den erfolgreichsten Operationen in der Endoprothetik. Jedoch ist das Patientenspektrum in den letzten Jahren immer jünger und aktiver geworden. Dadurch ist der Anspruch im Hinblick auf die Belastbarkeit und Lebensdauer dieser Implantate gestiegen. Bezüglich dieser erhöhten Beanspruchung der Implantate stellt insbesondere der reibungsinduzierte Abrieb der Gelenkpartner noch ein Problem dar. Für die Optimierung der Gleitpartner werden Daten über die *in vivo* wirkenden Reibparameter benötigt, um den Gelenkverschleiß, große Reibmomente an der Pfanne und daraus folgende Lockerungen der Prothesen zu minimieren. Ebenso sind realistische Daten über die auftretenden Gelenkbelastungen während der Rehabilitation bzw. im Alltag erforderlich, um Ärzten und Patienten Hinweise für eine optimale postoperative Nachbehandlung geben zu können.

Eine im Rahmen dieser Arbeit entwickelte instrumentierte Hüftendoprothese mit einer Keramik-Polyethylen Paarung ermöglicht es erstmalig, die Kontaktkräfte und Reibmomente *in vivo* zu messen. 10 Coxarthrose-Patienten wurden mit einem solchen instrumentierten Implantat versorgt.

Beim Gehen wird das Gelenk im Mittel mit einer Kontaktkraft von 248%BW belastet. Durch Unterarmgehstützen war es möglich, die Kontaktkraft um 17% (3-Punkt), 12% (4-Punkt) bzw. 13% beim 2-Punkt Gang zu reduzieren.

Erstmalige *in vivo* Messungen zeigten, dass das Reibmoment beim Gehen während der gesamten Standphase kontinuierlich ansteigt, mit einem mittleren Maximum von 0,22%BWm. Jedoch traten große inter-individuelle Unterschiede auf. Der sich während jedem Schritt ändernde Reibungskoeffizient deutet darauf hin, dass sich die Schmierbedingungen im Gelenkspalt von Mischreibung nach dem Auftreten zu Trockenreibung während der Schwungphase ändern. Die großen individuellen Unterschiede der wirkenden Reibung werden evtl. durch die individuellen Schmiereigenschaften der Synovia verursacht.

„Loading of total hip joint replacements –

In vivo measurements with instrumented hip implants“

by Dipl.-Ing. Philipp Damm

Abstract

Total hip joint replacements are one of the most successful operations in joint arthroplasty. However, patients have become younger and more active in recent years. Thus the requirements for implants in terms of load–carrying ability and lifetime have increased. Increased loads and resulting friction-induced wear of the joint partners still pose a significant problem. In order to optimize gliding partners of the implant, realistic *in vivo* friction parameters are needed in order to minimize wear and moments acting at the cup and subsequent loosening of the implant. Representative *in vivo* joint load data during rehabilitation and everyday activity such as walking is also needed in order to improve the patient's postoperative care.

As part of this work, an instrumented hip prosthesis with a ceramic-polyethylene pairing was developed, creating the unique opportunity to measure contact forces and friction moments *in vivo* for the first time. Ten osteoarthritis patients were provided with such instrumented implants as part of this study.

When walking, the joint is loaded on average with a contact force of 248% BW. Using crutches reduced the joint contact force during walking by 17% during 3-point, 12% during 4-point and 13 % during 2-point gait.

The unique dataset of *in vivo* friction during walking has shown that friction torque increases continuously during the entire stance phase to an average maximum of 0.22%BWm. However, great inter-individual variability was observed.

The changes of the coefficient of friction during every step indicated that the lubrication conditions of the fluid film changed from mixed to dry during the swing phase. The large individual friction differences may be caused by different lubrication properties of the synovial fluid.

1. Introduction

Total hip joint replacements are one of the most successful procedures in joint arthroplasty. However, in recent years, candidates for such a joint replacement have been getting younger and more athletic [1-2]. Thus, the requirements of implants in terms of stability and lifetime have increased. This leads to increased friction-induced wear, higher moments at the cup and subsequently to higher loosening risks [3]. In order to extend implant life spans, knowledge of realistic *in vivo* joint loads and friction conditions is essential for preclinical testing and optimization of hip implants.

Such *in vivo* data on friction and load magnitudes can provide more realistic parameters for implant testing. The *in vivo* measured torsion moment around the femoral shaft can be used to optimize fixation of the implant stem. Data on the bending moments in the femoral neck may feasible more stable implants used for fractures of the femoral neck. Data on the joint loads acting during different activities will allow to improve the physiotherapy following joint replacement and give advice to patients with Osteoarthritis.

Davy et al., Kotzar et al. and Bergmann et al. [5-7] report *in vivo* load measurements in total hip joint replacements. However, contact forces were measured only in a group of very old and inactive patients. Furthermore they were not able to measure the *in vivo* friction in the joint.

The main scope of this work was to access for the first time ever the *in vivo* hip joint loads in a group of relatively young and athletic patients by measuring joint contact forces and friction using instrumented implants.

2. Objectives

The first objective of this work was to develop an instrumented hip implant to simultaneously measure the *in vivo* acting friction moment and the contact forces at the hip joint. As part of a clinical study, the newly developed instrumented prostheses were implanted in ten active osteoarthritis hip patients to help answer the following questions:

- How is the hip joint loaded during postoperative physiotherapy?
- How effective are forearm crutches to reduce hip joint loading?
- What are the *in vivo* friction conditions in artificial hip joints during walking?

The second objective of the study was to develop a hip implant capable of measuring *in vivo* the friction-induced joint temperatures. Using such implants, it is planned to record the temperatures during long lasting activities in patient with implants which have different material combinations of head and cup.

3. Methods

3.1. Instrumented hip implant – HipIII

In order to simultaneously measure *in vivo* contact forces and friction moments in the hip joint an instrumented hip implant with inductive power supply was developed [8]. Measurement signals were transmitted at radio frequency to an external device and processed in a computer. Following extensive mechanical and biological testing, the implant was certified and approved for clinical trials in compliance with the "Medizinproduktegesetz" (MPG) and "Richtlinie 90/385/EWC".

Ten instrumented implants with the stem size 10 and 12 were manufactured and combined with an Al_2O_3 ceramic head. Each implant was individually calibrated [9] and a measurement accuracy of 2% for the contact forces and 1.5% for the moments was ascertained.

See also publication: *Total hip joint prosthesis for in vivo measurement of forces and moments* DOI: 10.1016/j.medengphy.2009.10.003

3.2. Instrumented hip implant – T-Implant

In vivo friction in the hip implant depends on both the gliding motion and lubricant conditions. We hypothesized that high friction can result in increased joint temperatures and possibly in implant loosening. In order to measure the joint temperatures, a second instrumented implant was developed. Five prototypes were manufactured with a measurement accuracy of 0.01°C. The power supply and data transmission are inductive and the implant can be combined with all common head/cup pairings. The instrumented implant was certified in compliance with the "Medizinproduktegesetz" (MPG) and "Richtlinie 90/385/EWC" and approved for a clinical trial.

See also publication: *High-tech hip implant for wireless temperature measurements in vivo* DOI:10.1371/journal.pone.0043489

3.3. Instrumented forearm crutches

Two instrumented forearm crutches were manufactured to measure the longitudinal crutch force synchronously to the *in vivo* joint load, depending on the type of crutch support. Two load transducers (KM30z-2kN, ME-Meßsystem GmbH, Germany) were integrated in the lower part of the crutches. The transducers were connected to the external equipment by cables. A physiotherapist adjusted the crutch lengths according to the patients needs.

3.4. Patients

Ten patients were selected to take part in the clinical trial; study scope, risk and procedures were explained and written consent was obtained from all patients to take part in the clinical trial (Table 1). Implantations of the instrumented implants (HipIII) were performed at the „Klinik für Endoprothetik“ of the “Sana Kliniken” in Sommerfeld/Kremmen, Germany.

Table1: Patients of the clinical trial

Patient	Age at implantation [years]	Sex [m/f]	Implantation	Bodyweight [kg]	Body height [cm]
H1L	55	m	Apr. 2010	73	178
H2R	62	m	Aug. 2010	75	172
H3L	59	m	Nov. 2010	92	168
H4L	51	m	Jan. 2011	83	178
H5L	62	f	Apr. 2011	87	168
H6R	67	m	Nov. 2011	85	176
H7R	52	m	Nov. 2011	90	179
H8L	55	m	Apr. 2012	90	178
H9L	54	m	Sep. 2012	118	181
H10R	53	f	Jan. 2013	100	164

3.5. Measurement values

Contact forces and friction moments

The 3D joint contact forces and friction moments were measured in a implant-based coordinate system, which is located at the center of the implant head. These loads were converted into the femur-based coordinate system with its origin at the center of the femoral head [10]. The fixed reference points for the x/y/z coordinate system are lateral/anterior/superior. The resultant contact force (F_{res}) acting onto the joint center is calculated from its three components. Similar to the contact force the friction moments were measured around the x/y/z axes of the femur based coordinate system (flexion-extension/abduction-adduction/internal-external rotation) and the resultant friction moment (M_{res}) was calculated there from the three components.

See also publication: *Friction in Total Hip Joint Prosthesis Measured In Vivo during Walking* DOI:10.1371/journal.pone.0078373

In vivo hip joint loads during three methods of walking with forearm crutches DOI: 10.1016/j.clinbiomech.2012.12.003

In vivo hip joint loading during post-operative physiotherapeutic exercises DOI:10.1371/journal.pone.0077807

Torsion and bending moments

In addition to the acting forces and moments at the joint, the torque M_{tors} around the bone/shaft interface can have a significant influence on the primary stability of the joint replacement. M_{tors} depends on the joint contact forces, the individual implant geometry and the implant position in the femur.

After femoral neck fractures the bending moment M_{bend} in the neck can be a critical factor for the healing process. M_{bend} is determined by the contact forces acting onto the joint and its 3D lever arm relative to the fracture.

See also publication: *In vivo hip joint loading during post-operative physiotherapeutic exercises* DOI:10.1371/journal.pone.0077807

In vivo hip joint loads during three methods of walking with forearm crutches DOI: 10.1016/j.clinbiomech.2012.12.003

Coefficient of friction and friction-induced power

Friction in total hip joint replacements mainly depends on the lubrication properties of the synovia, the materials of the gliding partners and their surface roughness, and on the gliding speed. To characterize the friction coefficient μ *in vivo* and compare it with data from *in vitro* simulator studies, the Coulomb friction model was used. During walking, the hip joint rotates around all three axes of movement. Thus the model of Coloumb was transformed into a three-dimensional approach. With the input of F_{res} and M_{res} the coefficient μ was then calculated the first time ever *in vivo* over the entire gait cycle of walking.

Friction results in a temperature increase in the implant, which is proportional to the friction-induced power loss in the joint. This power is determined by the product of the friction force between the gliding surfaces and the gliding speed. Average values of this power loss were calculated during the walking cycle, for extension and flexion separately.

See also publication: *Friction in Total Hip Joint Prosthesis Measured In Vivo during Walking* DOI:10.1371/journal.pone.0078373

3.6. Investigated activities

Hip joint loads during level walking

Level walking is one of the activities that every patient should be able to perform even shortly after total hip joint replacement surgery. However, up to now there was no data available about the friction during this activity.

The *in vivo* measurements were performed three months post surgery during level walking. The patients were asked to walk several times on level ground over a distance of 10m at a self-selected speed. The *in vivo* hip joint contact forces and friction moments were measured and analysed.

See also publication: *Friction in Total Hip Joint Prosthesis Measured In Vivo during Walking* DOI:10.1371/journal.pone.0078373

Hip joint loads during physiotherapeutic exercises

Following total joint arthroplasty, physiotherapeutic exercises are the first kind of activities the patient has to perform post surgery. However, during the first weeks after joint replacement bone ingrowths at the implant interface is still susceptible to micro movement which can jeopardise the implant stability. Therefore protecting the implant from high forces and high torque around the implant stem is crucial during the early stages after surgery.

However, up to today there exists no realistic data on *in vivo* hip joint loading during post-operative physiotherapy. As part of this study, *in vivo* hip joint loads were therefore measured during 13 typical physiotherapeutic exercises.

See publication: *In vivo hip joint loading during post-operative physiotherapeutic exercises* DOI:10.1371/journal.pone.0077807

Hip joint loading during walking with crutches

Patients with osteoarthritis, with joint implants or osteosynthesis use crutches in order to reduce lower limb loading. However, insufficient information exists about the really achieved reductions. In this study, the load reduction in the hip joint while walking with crutches was investigated *in vivo* during 3-, 4- and 2-point gait. Furthermore, synchronously to the *in vivo* joint loads, the crutch loads were measured using instrumented crutches.

The first part of the study compared the joint loads while walking with crutches to the joint loads without crutches. These measurements were taken three months after implantation. The second part of the study looks at the postoperative changes of the joint load reductions during 4-point gait.

See publication: *In vivo hip joint loads during three methods of walking with forearm crutches* DOI: 10.1016/j.clinbiomech.2012.12.003

3.7. Data evaluation

Each patient was requested to repeat each activity at least six times in order to access the intra-individual variability of the joint loads. The patient's activities were measured and recorded continuously; load data and patient movements were simultaneously videotaped. All forces are reported in percent of the bodyweight (%BW) and the moments in %BWm. The load-time patterns during single trials were individually averaged by using a 'time warping' method [11]. The average load patterns of all investigated patients were combined by the same method. They represent the joint loads of an average subject.

"First the period times of all included load cycles are normalized. The single time scales were then distorted in such a way that the squared differences between all deformed curves, summed over the whole cycle time, were smallest. Finally, an arithmetically averaged load-time pattern was calculated from all the deformed curves. Using these algorithms, an average time course was first calculated from the time patterns of the resultant joint forces. The obtained time deformations of the single trials were then transferred to the corresponding force and moment components before averaging them, too." [12]

Peak values of the load cycles were additionally numerically averaged. Changes of the peak values as a function of post operatively time or differences between the investigated activities were determined statistically for the individual patients separately by using 'Man-Whitney-U Test' and changes for the average subject by using the 'Wilcoxon Test'.

Published in Medical Engineering & Physics 32; 2010: p. 95-100;

DOI: 10.1016/j.medengphy.2009.10.003

4. Total hip joint prosthesis for *in vivo* measurement of forces and moments

P. Damm, F. Graichen, A. Rohlmann, A. Bender, G. Bergmann

Abstract

A new instrumented hip joint prosthesis was developed which allows the *in vivo* measurement of the complete contact loads in the joint, i.e. 3 force and 3 moment components. A clinically proven standard implant was modified. Inside the hollow neck, 6 semiconductor strain gauges are applied to measure the deformation of the neck. Also integrated are a small coil for the inductive power supply and a 9-channel telemetry transmitter. The neck cavity is closed by a titanium plate and hermetically sealed by electron beam welding. The sensor signals are pulse interval modulated (PIM) with a sampling rate of about 120 Hz. The pulses are transmitted at radio frequencies via a small antenna loop inside the ceramic head, which is connected to the electronic circuit by a two pin feed through. Inductive power supply, calculation of the loads from the measured deformations and real time load display are carried out by the external equipment. The maximum error of the load components is 2% including cross talk. The instrumented hip joint prostheses are to be implanted into 10 young and sportive patients.

Introduction

Knowledge of the forces and moments acting *in vivo* in total hip joint prostheses is necessary in order to develop and test new implants, especially for optimizing their friction properties [1, 2, 3]. It is also essential to optimize postoperative rehabilitation, assess the severity of load conditions during sportive activities, and optimize musculoskeletal models used in combination with gait analyses to calculate the internal joint loads [4, 5, 6, 7]. Especially the effect of muscular co-contractions on the joint loads can accurately be accessed by direct measurements only.

Research work has previously been performed on the contact forces acting in total hip joint prostheses during walking, stair climbing and additional activities, both by other authors [8, 9, 10, 11, 12] and by our group [13, 14, 15, 16]. However, the patients were between 60 to 80 years old. With 26% and 48% of all cases, friction-induced polyethylene wear and wear-related aseptic loosening are the most frequent reason for revisions of hip joint prostheses [17]. Other bearing combinations as metal–metal or ceramic–ceramic have much lower wear rates but still retain the problem of aseptic loosening [18, 19, 20, 21, 22]. The friction in the joint and thus the wear of the implants can be determined from measured joint contact forces and moments, but this has, to our knowledge, never been undertaken before. Patients with total hip replacement become younger, more active and sportive [23, 24, 25, 26]. It is expected that their increased physical activities result in higher loads acting on the total hip joint.

The aim of the study was to design and calibrate a non-cemented, instrumented hip joint prosthesis which could be used to measure the 3 force components plus the 3 moment components acting between head and cup *in vivo*. Measured load data will offer realistic test conditions for friction and wear and serve as a ‘gold standard’ for optimizing analytical models.

Material and methods

Requirements for implant instrumentation

Instrumented hip joint prostheses must meet the following clinical and technical requirements:

- All materials in direct body contact must be biocompatible.
- All electronics inside the implant must be hermetically sealed.
- The power supply must allow long term measurements.
- The implant must have sufficient mechanical strength.
- A clinically proven type of prosthesis should be the basis of the instrumented implant, and its clinical function and fixation must remain unchanged.

Design

The ‘Cementless Tapered Wedge’ (CTW) prosthesis (Merete Medical GmbH, Berlin, Germany) was chosen as a basis for the instrumented implant. Its design is similar to the ‘Spotorno’ prosthesis, which is one of the clinically most successful types. Prosthesis stem and neck are made out of a titanium alloy and are combined with a ceramic head. The standard prostheses have a 12/14 mm conus. To provide enough space for the internal electronics (Figure 1), neck and conus diameters were both increased by 2 mm. The changed dimensions match the clinically successful standard used until some years ago.

The electronic components are arranged inside the implant neck, which is hermetically sealed with an electron beam-welded titanium plate. Integrated into this plate is a 2-pin feedthrough adapted from a pacemaker (Biotronik GmbH, Berlin, Germany). An antenna loop is formed by a niobium wire (NbZr1) and is laser-welded onto the feedthrough. This antenna is located inside the cavity of the 32 mm standard ceramic head, which protects antenna and feedthrough against mechanical damage. In addition, the antenna is isolated by medical-grade polysiloxane (Polytec PT GmbH, Waldbronn, Germany) against synovial fluid which could possibly infiltrate between implant neck and head. The instrumented prosthesis can be combined with standard polyethylene or ceramic sockets, with or without metal backing.

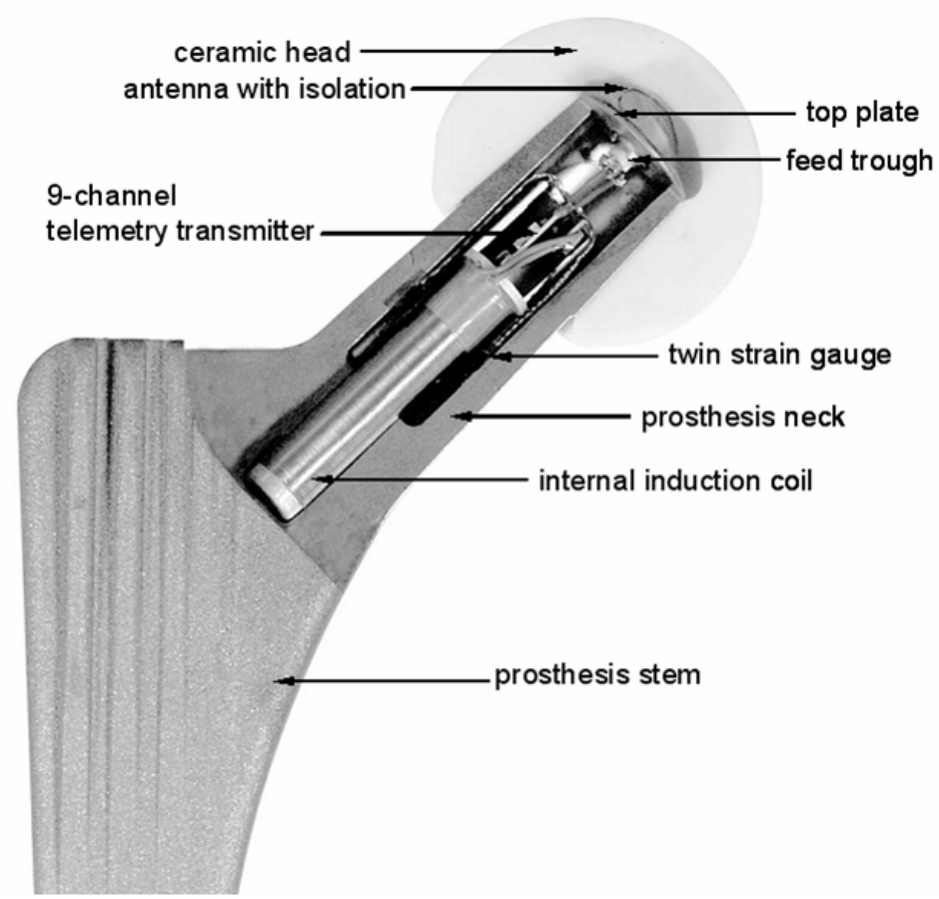

Figure 1: *Cut-model of the modified CTW prosthesis with internal electrical components*

Instrumentation

Three custom-made twin semiconductor strain gauges (ACAM Instrumentation Ltd., Northampton, UK) inside the hollow neck serve as sensors for measuring the 6 deformations required for calculating 6 load components (Figure 2). Each twin strain gauge is 5 by 4 mm in size and the 2 sensor elements are arranged at an angle of 45°. An NTC resistor on the telemetry circuit allows measurement of the implant temperature, which is used to compensate thermal influences. The internal induction coil delivers the power of 5 mW, required by the 9-channel telemetry circuit [27]. This is the only active element on the 9-channel telemetry transmitter (2.0 x 2.6 mm) custom-made chip. Strain gauges and the induction coil are connected to the telemetry. All signals are sampled at a rate of approximately 120Hz. They are multiplexed, converted to pulse interval modulated signals and transferred at a frequency of about 120 MHz. The transmission range is up to 50 cm. The telemetry

transmitter is powered inductively via the internal and external coil. The measuring time is therefore not limited.

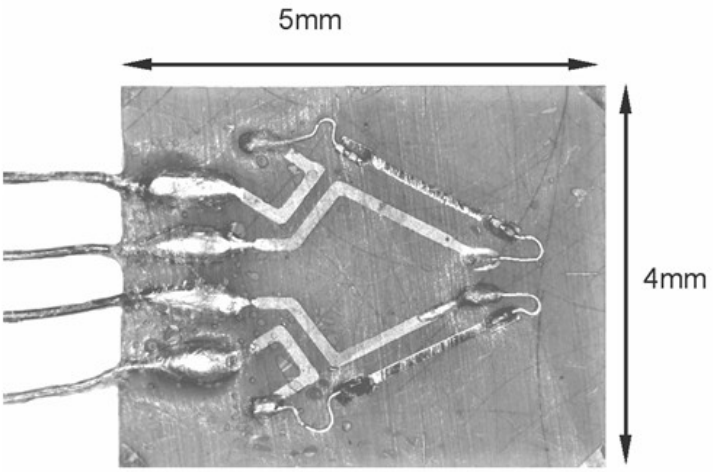

Figure 2: *Twin strain gauges*

The telemetry is shielded against the magnetic field by a metal cylinder with high magnetic permeability (MEGAPERM 40L, Vacuumschmelze GmbH, Hanau, Germany). The magnetic field is generated by the external induction coil, witch is placed around the thigh, below the hip joint. Further details of the measurement equipment have been described elsewhere [27, 28, 29, 30].

The external measurement system consists of the following components:

- A unit with regulated power supply, signal receiver and signal pre-processing.
- An induction coil placed around the thigh below the hip joint, and
- a receiving antenna close to hip joint.

The power generator regulates the magnetic field in the external induction coil at its resonance capacity. The telemetry signals, received by a single-loop antenna, are checked for transmission errors and sorted by a micro-processor system. A personal computer is connected via USB to this system. In the PC the 6 load components are calculated from the 6 strain signals, using the calibration data. All force and moment components can be observed in real time on a monitor. This is advantageous, for example when investigating physiotherapeutic exercises or for immediately modifying exercise conditions upon detecting unexpected load characteristics.

During the *in vivo* load measurements, the activities of the patients are to be recorded on a digital video tape. The video signal and the received signals from the implant are recorded synchronously on the same video tape. All data can be analysed in detail after the measurements have been taken. Further details of the measurement equipment are described elsewhere [27].

Calibration

During calibration the coordinate system of the instrumented implant is fixed in the middle of the implant neck. The X-axis points in the medial direction, the Y-axis posteriorly for a right implant and the Z-axis is aligned along the neck axis (Figure 3).

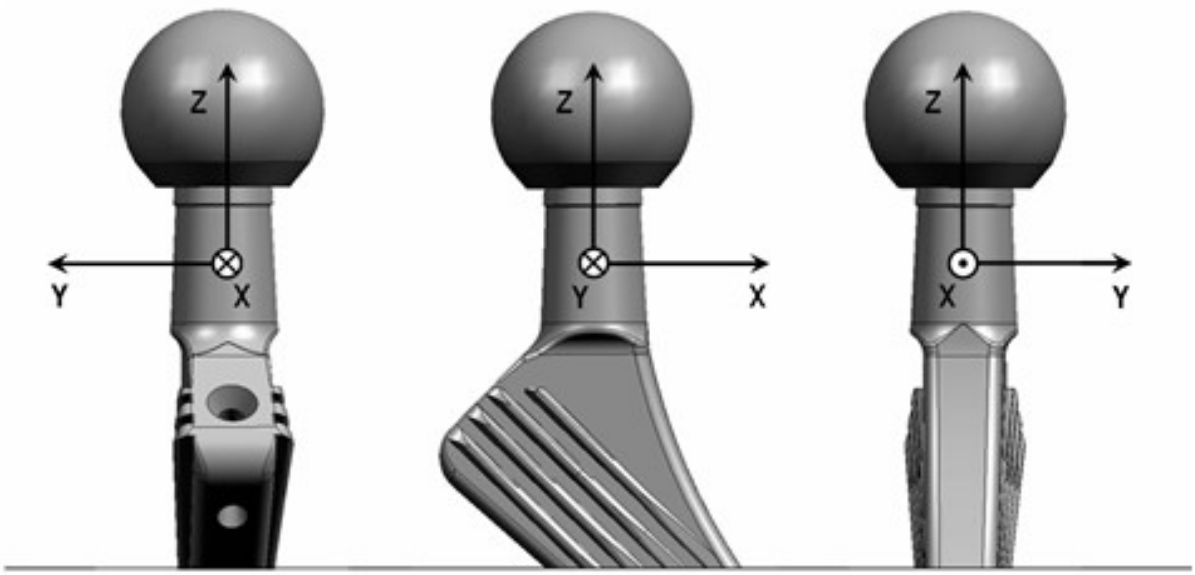

Figure 3: *Coordinate system during calibration*

The instrumented implant is calibrated using the matrix method [31, 32]. Details of the test setup can be found in reference [33]. Load application during calibration is performed in a custom-built uniaxial test rig. The calibration force is measured with an accuracy of 0.1% by an uniaxial force transducer (U2B, HBM, Germany).

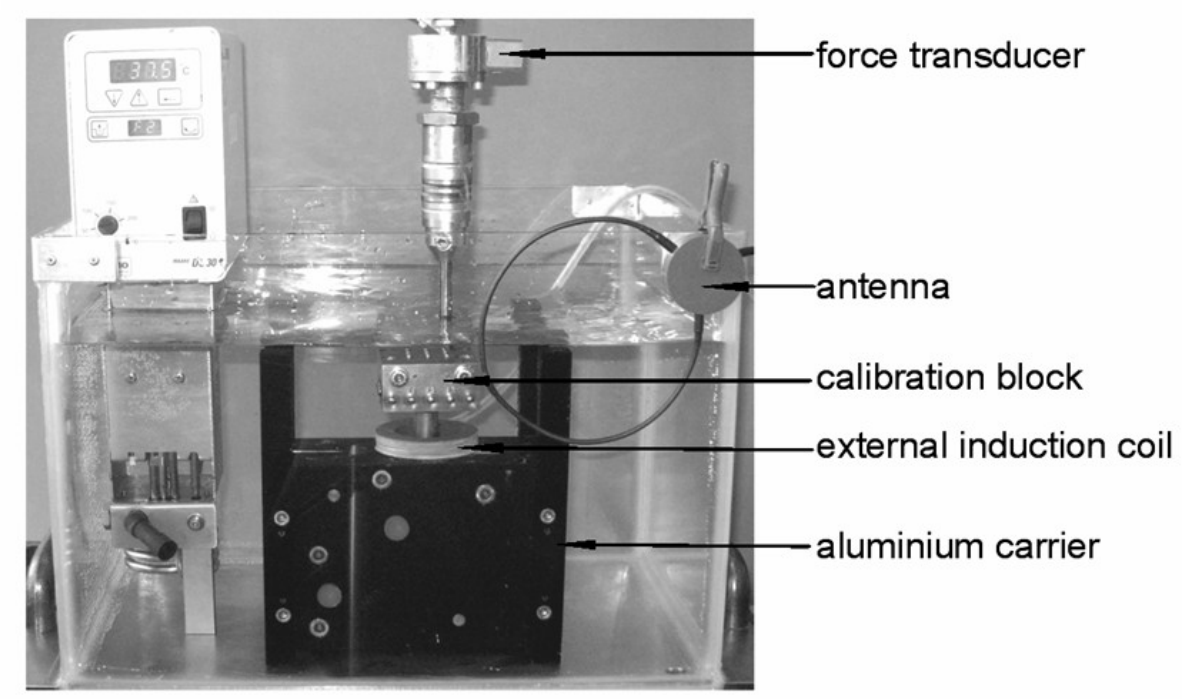

Figure 4: *Calibration setup; uniaxial force are applied at 21 different locations*

During calibration, the implant stem is fixed with bone cement in an aluminium carrier, and a calibration block is mounted on top of the implant (Figure 4). Twenty-one steel balls at the top and all side walls of this block serve as points of load application, with known xyz lever arms relative to the origin of the coordinate system. Load components $-F_z$, $\pm M_x$ and $\pm M_y$ are generated if the calibration force is acting on a top loading point, the other components produced if it is applied to a lateral point. When loading one of these points, a combination of up to 3 force and moment components acts simultaneously. This can be regarded as a load vector $\underline{L}$ with 6 components, of which 1 to 3 exist for the different loading points. The chosen calibration ranges of all 6 components are given in Table 1.

Table 1: *External loads and the measured errors of forces and moments*

Calibration range Forces		maximum measuring error	average measuring error	Calibration range Moments		maximum measuring error	average measuring error
[kN]		[%]	[%]	[Nm]		[%]	[%]
F_x	3.5	1.3	0.4	M_x	45.4	1.3	0.5
F_y	2	1.9	0.9	M_y	79.3	0.7	0.3
F_z	5	0.8	0.8	M_z	24	1.5	0.7

The calibration force is increased from zero to its maximum and back while 10,000 readings from the 6 strain gauges are taken. Any set of 6 signals can be regarded as a signal vector $\underline{S}$. Data from all 21 calibration points are used to calculate 36 components of the 6 x 6 calibration matrix $\underline{C}$ from the values of $\underline{L}$ and $\underline{S}$, as indicated by the following equation

$$\underline{S} = \underline{C} * \underline{L}.$$

The measuring matrix $\underline{M}$ is the inverse calibration matrix ($\underline{M} = \underline{C}^{-1}$) whereby

$$\underline{L} = \underline{M} * \underline{S}.$$

This is used to calculate the load vector $\underline{L}$ from the signal vector $\underline{S}$ during the measurements.

The implant temperature is measured by an NTC resistor inside the prostheses neck. To compensate the temperature sensitivity of the strain gauges, the implant is calibrated at three different temperatures (39°C ± 3°C).

Results

Accuracy

To examine the accuracies of measurements taken with the prostheses, defined forces and moments are applied consecutively at each of the calibration points and are compared to the measured load components. Measuring errors are calculated as percentages of the different calibration ranges of the 6 components and include the crosstalk between all components. Examples of the achieved accuracies of the 6

load components are shown in Figure 5. The applied loads versus measured loads are shown in the 6 different diagrams.

To check the accuracies of the load components, the relation between the applied and the measured load was calculated. The highest and average errors are given in Table 1. The maximum force error is 1.9 % for F_y. The average absolute error of all force components is 0.7 %. The highest error of the moments occurs for M_z and is 1.5 %, while the average error of all moments is 0.5 %. All these values included crosstalk between the components of the first prototype.

Implant safety and pre-clinical testing

The instrumented hip joint prostheses must fulfil the same safety criteria as a standard implant. The welds were checked for thickness and voids, using test specimens which were welded in the same way and at the same time as the implants. The welds of each implant were inspected in vacuum for the absence of leaks. The strengths of the implant stem and neck were tested according to the test standard for hip implants (ISO 7206 Part 4/6/8) at a certificated testing laboratory (EndoLab, Germany). Five million cycles with a maximum load of 2.3 kN were applied at the head to test the shaft and 10 million cycles with a maximum load of 5.4 kN were used to check the dynamic stability of the implant neck. After that the neck was additionally tested in-house under even more severe conditions, with loads increasing from 5.8 kN to 7.8 kN within 5 million cycles. Finally a static force of 14 kN was applied without implant failure. The safety of the implant and the external equipment was audited (90/385/EWG, §20 MPG) at BerlinCERT GmbH (Berlin, Germany). The instrumented implants are now approved by the ethical committee of our university.

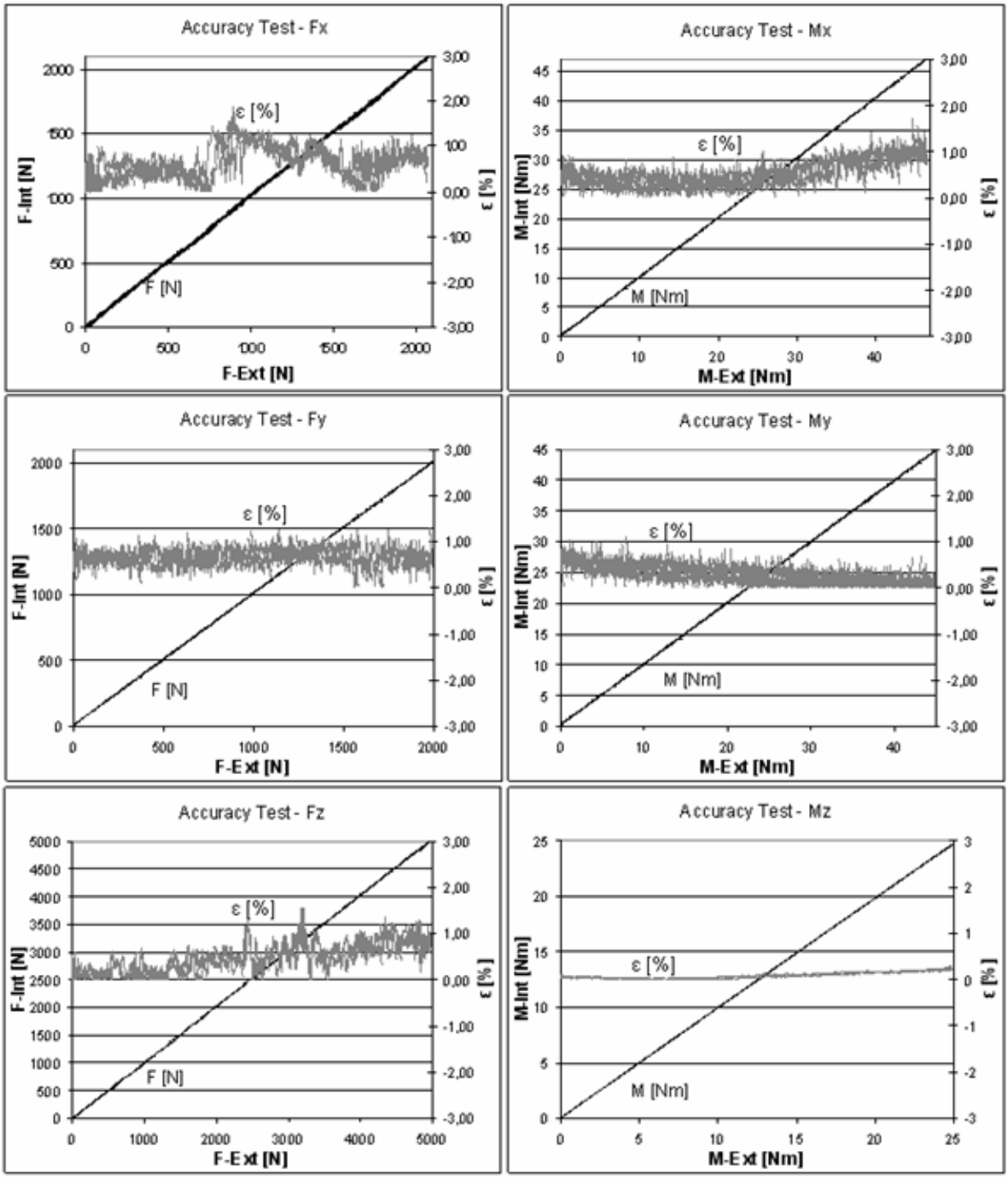

Figure 5: *Accuracy tests; measured load components versus applied loads. Left diagrams forces, right diagrams moments. Left scale absolute values, right scales relative error in percent.*

Discussion

One of the main reasons for revisions of total hip joint prostheses is wear rate [17, 18, 19]. Except for the mechanical risk of worn-out cups [34, 35], the frequent biological consequence of wear particles is aseptic loosening of stem or cup fixation [18, 19, 20]. Optimization of the bearing materials is therefore still required to improve the endurance of total hip joint prostheses.

At the moment, a great amount of literature exists concerning friction and wear of hip implants, tested in joint simulators [36, 37, 38, 39, 40, 41]. As the data of Bergmann et al. [42, 43] suggest, friction *in vivo* probably depends much on the individually strongly varying lubrication properties of the synovial fluid. This means that laboratory tests on the wear of hip implants were, until now, not performed under the worst conditions encountered in patients. This underlines the importance of measuring the real moments acting *in vivo*, which is now possible with the instrumented hip implant described. The measuring accuracy of 1.5 % for moments respectively 1.9 % for forces is in the same range as that of technical transducers of much more complex design, larger dimensions and with direct signal transmission.

Another important reason to measure the acting forces and moments *in vivo* is the decreasing age and increasing activity levels of patients. This not only requires an prolongation of implant lifetime by reducing wear but may also necessitate a rising of the loads applied in fatigue tests above the current level as given by ISO standards. Even the contact forces measured in elderly patients often exceed the current ISO limits [44, 45].

The described implant, with its ability to accurately measure forces and moments acting in the joint, will allow adapt the test conditions to the real situation when testing new implants. It will furthermore allow us to advise more sportive younger patients and their physiotherapists and orthopaedists as to which activities are preferable for condition training without endangering the implant stability.

Acknowledgements

This project was supported by the German Research Society (SFB760-C6). The modified implants were provided by Merete Medical GmbH, Berlin, Germany.

References

1. Maloney WJ, Galante JO, Anderson M, Goldberg V, Harris WH, Jacobs J, Kraay M, Lachiewicz P, Rubash HE, et al. Fixation, polyethylene wear, and pelvic osteolysis in primary total hip replacement. Clin Orthop Relat Res 1999: 157-64
2. Harris WH. Wear and periprosthetic osteolysis: the problem. Clin Orthop Relat Res 2001: 66-70
3. Schmalzried TP, Jasty M, Harris WH. Periprosthetic bone loss in total hip arthroplasty. Polyethylene wear debris and the concept of the effective joint space. J Bone Joint Surg Am 1992;74: 849-63
4. Heller MO, Bergmann G, Deuretzbacher G, Durselen L, Pohl M, Claes L, Haas NP, Duda GN. Musculo-skeletal loading conditions at the hip during walking and stair climbing. J Biomech 2001;34: 883-93
5. Heller MO, Bergmann G, Deuretzbacher G, Claes L, Haas NP, Duda GN. Influence of femoral anteversion on proximal femoral loading: measurement and simulation in four patients. Clin Biomech (Bristol, Avon) 2001;16: 644-9
6. Brand RA, Pedersen DR, Davy DT, Kotzar GM, Heiple KG, Goldberg VM. Comparison of hip force calculations and measurements in the same patient. J Arthroplasty 1994; 9: 45-51
7. Stansfield BW, Nicol AC, Paul JP, Kelly IG, Graichen F, Bergmann G. Direct comparison of calculated hip joint contact forces with those measured using instrumented implants. An evaluation of a three-dimensional mathematical model of the lower limb. J Biomech 2003; 36: 929-36
8. English TA, Kilvington M. In vivo records of hip loads using a femoral implant with telemetric output (a preliminary report). J Biomed Eng 1979; 1: 111-5
9. Hodge WA, Fijan RS, Carlson KL, Burgess RG, Harris WH, Mann RW. Contact pressures in the human hip joint measured in vivo. Proc Natl Acad Sci U S A 1986; 83: 2879-83
10. Davy DT, Kotzar GM, Brown RH, Heiple KG, Goldberg VM, Heiple KG, Jr., Berilla J, Burstein AH. Telemetric force measurements across the hip after total arthroplasty. J Bone Joint Surg Am 1988; 70: 45-50
11. Kotzar GM, Davy DT, Goldberg VM, Heiple KG, Berilla J, Heiple KG, Jr., Brown RH, Burstein AH. Telemeterized in vivo hip joint force data: a report on two patients after total hip surgery. J Orthop Res 1991; 9: 621-33

12. Taylor SJ, Perry JS, Meswania JM, Donaldson N, Walker PS, Cannon SR. Telemetry of forces from proximal femoral replacements and relevance to fixation. J Biomech 1997; 30: 225-34
13. Bergmann G, Graichen F, Rohlmann A. Hip joint contact forces during stumbling. Langenbecks Arch Surg 2004; 389: 53-9
14. Bergmann G, Deuretzbacher G, Heller M, Graichen F, Rohlmann A, Strauss J, Duda GN. Hip contact forces and gait patterns from routine activities. J Biomech 2001; 34: 859-71
15. Bergmann G, Graichen F, Rohlmann A. Is staircase walking a risk for the fixation of hip implants? J Biomech 1995; 28: 535-53
16. Bergmann G, Graichen F, Rohlmann A. Hip joint loading during walking and running, measured in two patients. J Biomech 1993; 26: 969-90
17. CJRR. 2007 CJRR Report: Total Hip and Total Knee Replacements in Canada: Canadian Institut for Healt Information, 2008
18. Heisel C, Silva M, Schmalzried TP. Bearing surface options for total hip replacement in young patients. Instr Course Lect 2004; 53: 49-65
19. Schmalzried TP, Callaghan JJ. Wear in total hip and knee replacements. J Bone Joint Surg Am 1999; 81: 115-36
20. Buechel FF, Drucker D, Jasty M, Jiranek W, Harris WH. Osteolysis around uncemented acetabular components of cobalt-chrome surface replacement hip arthroplasty. Clin Orthop Relat Res 1994: 202-11
21. Stewart TD, Tipper JL, Insley G, Streicher RM, Ingham E, Fisher J. Long-term wear of ceramic matrix composite materials for hip prostheses under severe swing phase microseparation. J Biomed Mater Res B Appl Biomater 2003; 66: 567-73
22. Santavirta S, Bohler M, Harris WH, Konttinen YT, Lappalainen R, Muratoglu O, Rieker C, Salzer M. Alternative materials to improve total hip replacement tribology. Acta Orthop Scand 2003; 74: 380-8
23. Chatterji U, Ashworth MJ, Lewis PL, Dobson PJ. Effect of total hip arthroplasty on recreational and sporting activity. ANZ J Surg 2004; 74: 446-9
24. Huch K, Muller KA, Sturmer T, Brenner H, Puhl W, Gunther KP. Sports activities 5 years after total knee or hip arthroplasty: the Ulm Osteoarthritis Study. Ann Rheum Dis 2005; 64: 1715-20

25. Naal FD, Maffiuletti NA, Munzinger U, Hersche O. Sports after hip resurfacing arthroplasty. Am J Sports Med 2007; 35: 705-11
26. Flugsrud GB, Nordsletten L, Espehaug B, Havelin LI, Meyer HE. The effect of middle-age body weight and physical activity on the risk of early revision hip arthroplasty: a cohort study of 1,535 individuals. Acta Orthop 2007; 78: 99-107
27. Graichen F, Arnold R, Rohlmann A, Bergmann G. Implantable 9-channel telemetry system for in vivo load measurements with orthopedic implants. IEEE Trans Biomed Eng 2007; 54: 253-61
28. Graichen F, Bergmann G. Four-channel telemetry system for in vivo measurement of hip joint forces. J Biomed Eng 1991; 13: 370-4
29. Graichen F, Bergmann G, Rohlmann A. [Telemetric transmission system for in vivo measurement of the stress load of an internal spinal fixator]. Biomed Tech (Berl) 1994; 39: 251-8
30. Bergmann G, Rohlmann A, Graichen F. Instrumentation of a hip joint prosthesis. Implantable telemetry in orthopaedics 1990: 35-60
31. Bergmann G, Siraky J, Rohlmann A, Koelbel R. Measurement of spatial forces by the "Matrix"-Method. Proc. V/VI 9th World Congr. IMEKO 1982: 395-404
32. Bergmann G, Graichen F, Siraky J, Jendrzynski H, Rohlmann A. Multichannel strain gauge telemetry for orthopaedic implants. J Biomech 1988; 21: 169-76
33. Bergmann G, Graichen F, Rohlmann A, Westerhoff P, Heinlein B, Bender A, Ehrig R. Design and calibration of load sensing orthopaedic implants. J Biomech Eng 2008; 130: 021009
34. Dowling JM, Atkinson JR, Dowson D, Charnley J. The characteristics of acetabular cups worn in the human body. J Bone Joint Surg Br 1978; 60-B: 375-82
35. Catelas I, Campbell PA, Bobyn JD, Medley JB, Huk OL. Wear particles from metal-on-metal total hip replacements: effects of implant design and implantation time. Proc Inst Mech Eng [H] 2006; 220: 195-208
36. McKellop HA, D'Lima D. How have wear testing and joint simulator studies helped to discriminate among materials and designs? J Am Acad Orthop Surg 2008; 16 Suppl 1: S111-9
37. Fialho JC, Fernandes PR, Eca L, Folgado J. Computational hip joint simulator for wear and heat generation. J Biomech 2007; 40: 2358-66

38. Estok DM, 2nd, Burroughs BR, Muratoglu OK, Harris WH. Comparison of hip simulator wear of 2 different highly cross-linked ultra high molecular weight polyethylene acetabular components using both 32- and 38-mm femoral heads. J Arthroplasty 2007; 22: 581-9
39. Affatato S, Spinelli M, Zavalloni M, Mazzega-Fabbro C, Viceconti M. Tribology and total hip joint replacement: current concepts in mechanical simulation. Med Eng Phys 2008; 30: 1305-17
40. Muller LP, Degreif J, Rudig L, Mehler D, Hely H, Rommens PM. Friction of ceramic and metal hip hemi-endoprostheses against cadaveric acetabula. Arch Orthop Trauma Surg 2004; 124: 681-7
41. Fruh HJ, Willmann G. Tribological investigations of the wear couple alumina-CFRP for total hip replacement. Biomaterials 1998; 19: 1145-50
42. Bergmann G, Graichen F, Rohlmann A, Verdonschot N, van Lenthe GH. Frictional heating of total hip implants. Part 2: finite element study. J Biomech 2001; 34: 429-35
43. Bergmann G, Graichen F, Rohlmann A, Verdonschot N, van Lenthe GH. Frictional heating of total hip implants. Part 1: measurements in patients. J Biomech 2001; 34: 421-8
44. Baleani M, Cristofolini L, Viceconti M. Endurance testing of hip prostheses: a comparison between the load fixed in ISO 7206 standard and the physiological loads. Clin Biomech (Bristol, Avon) 1999; 14: 339-45
45. Bergmann G. Realistic loads for testing hip implants. article in press 2009

Published in: PLoS ONE 7(8): e43489.

DOI:10.1371/journal.pone.0043489

5. High-tech hip implant for wireless temperature measurements *in vivo*

G. Bergmann, F. Graichen, J. Dymke, A. Rohlmann, G. N. Duda, P. Damm

Abstract

When walking long distances, hip prostheses heat up due to friction. The influence of articulating materials and lubricating properties of synovia on the final temperatures, as well as any potential biological consequences, are unknown. Such knowledge is essential for optimizing implant materials, identifying patients who are possibly at risk of implant loosening, and proving the concepts of current joint simulators. An instrumented hip implant with telemetric data transfer was developed to measure the implant temperatures *in vivo*. A clinical study with 100 patients is planned to measure the implant temperatures for different combinations of head and cup materials during walking. This study will answer the question of whether patients with synovia with poor lubricating properties may be at risk for thermally induced bone necrosis and subsequent implant failure. The study will also deliver the different friction properties of various implant materials and prove the significance of wear simulator tests.

A clinically successful titanium hip endoprosthesis was modified to house the electronics inside its hollow neck. The electronics are powered by an external induction coil fixed around the joint. A temperature sensor inside the implant triggers a timer circuit, which produces an inductive pulse train with temperature-dependent intervals. This signal is detected by a giant magnetoresistive sensor fixed near the external energy coil. The implant temperature is measured with an accuracy of 0.1°C in a range between 20°C and 58°C and at a sampling rate of 2 - 10 Hz. This rate could be considerably increased for measuring other data, such as implant strain or vibration. The employed technique of transmitting data from inside of a closed titanium implant by low frequency magnetic pulses eliminates the need to use an electrical feedthrough and an antenna outside of the implant. It enables the design of mechanically safe and simple instrumented implants.

Introduction

Friction of implant materials

High friction in joint implants and subsequent temperature rise during continuous activities, such as walking, may cause increased polyethylene wear, decreased polyethylene strength, or loosening of the cup in hip implants due to high frictional torque [1]. The natural cartilage has a coefficient of friction of 0.02 to 0.04 [2]. Articulating materials used for total joint replacement have higher friction. Coefficients reported in the literature are as follows: 0.04 to 0.05 for the combination Al_2O_3 - Al_2O_3, 0.05 to 0.055 for Al_2O_3 - UHMWPE, 0.06 to 0.07 for CoCrMo - UHMWPE, and 0.10 to 0.20 for CoCrMo - CoCrMo [3,4,5]. Moreover, a strong influence of the protein concentration in the synovia on friction was reported [5], especially for CoCrMo - CoCrMo.

Synovia properties

After joint replacement, a pseudo-synovial membrane is formed, which produces hyaluronic acid (HA), similar to the natural membrane. The synovia volume is small. In the hip joint, volumes of 2.7 ml in asymptomatic hips and 6.1 ml in fractured hips were reported [6].

The properties of synovia vary considerably, and synovia can lose its lubricating properties at high temperatures [7]. Synovia viscosity in natural joints depends on the type of joint disease [8]. Differences of at least a factor of 10 were determined between subjects and between healthy and osteoarthritic joints [9]. The most decisive factor for lubrication is the protein content in the synovia [10]. The lubrication ability of synovia from degenerative knee joints was worse than that of bovine serum [11], which may indicate that joint simulators do not actually mimic the real situation in hip or knee implants if a ‘standardized’ bovine serum is used [12,13], especially if the temperature is kept constant at 37°C.

The cited literature indicates that individually varying synovia properties may strongly influence wear and temperature increases in replaced hip and knee joints during long-lasting activities, such as walking.

Temperature in hip and knee joints

In vitro temperature measurements on two intact human hip joints delivered a temperature increase of 2.5 °C during simulated walking [14]. *In vivo* measurements of temperatures in the natural knee joint showed a 1°C increase in temperature after 20 minutes and 2°C after 40 minutes of walking [15]. Depending on the implant type and articulating materials, this increase was observed up to 7°C for a rotating hinge implant (CoCrMo - UHMWPE). In an analytical study, validated by simulator data, temperatures up to 51°C were found in CoCrMo - UHMWPE hip implants [16].

With instrumented implants, the forces and temperatures in Al_2O_3 - UHMWPE hip joints were measured in 5 subjects during 45 to 60 minutes of walking and bicycling [17]. After walking, the temperature rose up to 43.1°C in the patient with the lowest body weight. Another patient with a much higher body weight reached a joint temperature of only 40.0°C. In the only patient with bi-lateral implants, the temperature was 0.9°C lower with an Al_2O_3 cup than with a UHMWPE cup. After cycling, which caused 55% lower joint forces than walking, the temperatures were 1.5°C lower. We assume that the steady-state temperature after walking is closely correlated to the friction coefficient.

In a simulator, the surface temperature directly between a UHMWPE cup and an Al_2O_3 head was 45°C, but was 60°C with a CoCrMo head and 99°C with a zirconia ceramic [18]. These are temperatures at which synovia precipitates and loses its lubricating properties.

Bone necrosis

After heating rabbit thighs up to 42.5°C to 44.0°C using microwaves, strongly increased bone formation was observed [19]. After 4 minutes at 50°C, osteocytes were found to be irreversibly damaged [20]. Approximately 15 - 20% of the osteoblasts became necrotic after being exposed to 48°C for 10 minutes, while they withstood 45°C without damage [21]. After heating the superficial skull of rats to 48°C for 15 minutes, dead osteocyte areas were found, and the formation of new bone was delayed [22]. From the available literature on bone reactions to increases in temperature during drilling and sawing, it was concluded that 47°C is a critical temperature [23]. All of these studies investigated only the effect of non-recurrent

high temperatures. Repeatedly acting heat may even cause cell damage at lower temperatures.

Concepts of instrumented implants

Electronic components used for measurements with permanent implants, such as joint replacements, must be hermetically encapsulated. The optimal solution would be a complete enclosure by a metal [24] or ceramic [25] material. If an antenna or induction coil is placed outside the implant, only biocompatible materials are permitted [26,27]. Certified pacemaker feedthroughs are then favorably used for connections to the implant electronics. Our force measuring hip implants employed an internal power coil and an external niobium antenna [28,29,30,31]. Solutions using plastic-encapsulation for non-biocompatible electronic components [32,33,34] should only be used for non-permanent implants.

Power and signals could respectively be transferred to and from the implant by electro-magnetic fields. These fields are partly absorbed by a metal implant with the loss dependent on the alloy and frequency. Pure Ti, Al and V are paramagnetic with a relative magnetic permeability slightly greater than one. Implants made from such alloys only moderately weaken magnetic fields of low frequencies. However, ferromagnetic materials, such as Co or Ni, with a relative magnetic permeability of 80 to 600 almost completely shield the interior of an implant.

The loss caused by encapsulations made from Ti alloys is strongly frequency-dependent. A closed $TiAl_6V_4$ housing with a 2-mm wall thickness shields 23% of a magnetic field at 4 kHz but 53% at 10 kHz [30]. Any energy loss is accompanied by a temperature increase of the implant. Both the power consumption and the shielding loss must therefore be kept low. A titanium implant with an internal secondary power coil and transmitting antenna should use frequencies below 10 kHz for power as well as signal transfer. All transponder systems work at higher frequencies up to the GHz range and can therefore not be used inside a metallic implant. Locating transponder systems at the surface of a metallic implant [35] may cause problems for signal and energy transfer.

Goals of this work

The reported strong differences of friction coefficients, the individual variations of synovia properties, and the question of how well joint simulators mimic the *in vivo* loading conditions demonstrate the need to obtain *in vivo* information on the friction-induced temperature rise in joint implants.

The aim of the study was to design a temperature measuring hip implant with telemetric data transfer, which is completely safe for patients and can be used in a clinical study with a large number of patients. Furthermore, the technique described should be applicable for the instrumentation of other kinds of implants.

The following features were included: inductive power supply, inductive data transfer through the wall of the hermetically closed metallic implant, power consumption below 10 mW, measuring accuracy of 0.2°C, design based on a clinically well-proven implant type, and no requirement to change the surgical procedure.

Methods

Mechanical design

The non-cemented CTW™ Classic hip implant with a 12/14-mm cone (Merete Medical, Berlin, Germany) was used for instrumentation. It closely resembles implants of other manufacturers with very good clinical results [36]. The implant shape was only slightly modified between the neck and shaft to further increase its stability (Figure 1). A 6.2-mm-wide by 50-mm-long bore in the neck houses the temperature telemetry. At its top, a 5-mm-thick plate was welded using an electron beam (ENG Produktions-GmbH, Berlin, Germany) with a weld depth of 2.5 mm. The low required welding energy and the clamping of a massive copper block around the welding area facilitated temperature retention at the outside of the implant neck, at half of its length, below 80°C. The weld quality was checked for each produced batch by cutting samples, and the density of the welds was determined in a vacuum chamber. Fatigue strength of the implant stem and neck were tested according to [37, 38, 39] but with double the force levels in the neck test.

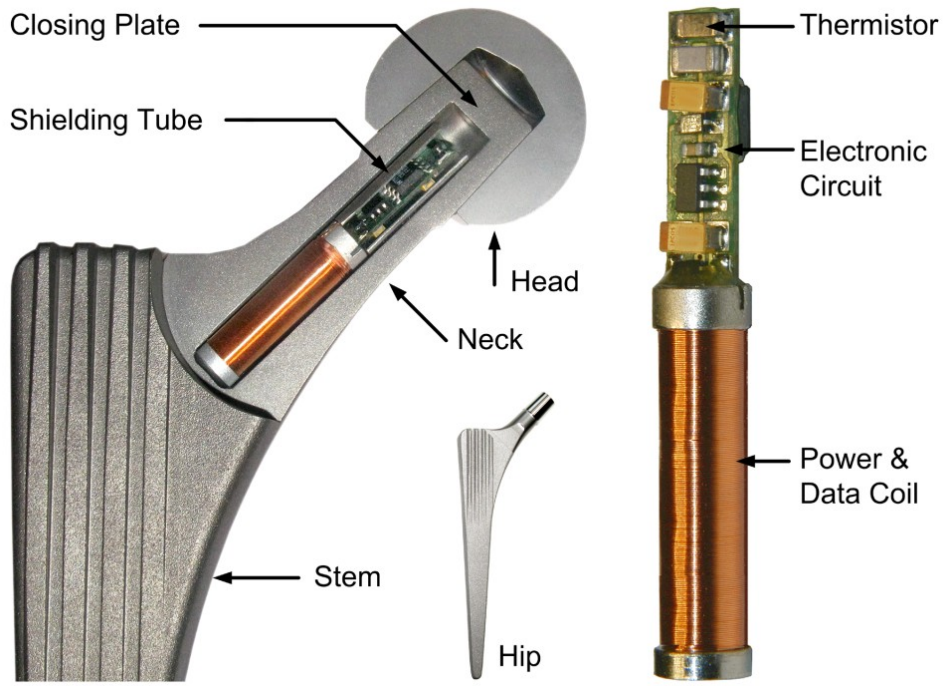

Figure 1: *Cross-section of a model of the modified hip implant with a metal head; The temperature telemetry with thermistor, electronic circuit and power/data coil are placed inside the neck of the implant.*

Telemetry

The telemetry (Figure 2) is powered inductively at 4 kHz, as in our previous implants [29]. The internal coil L consists of 2700 loops on a core of PERMENORM 5000 H2 (μ_r > 12000, Vacuumschmelze). The induced voltage U_L is limited to 12.3 V by the Zener diode ZD, rectified by D3 and regulated to 5 V DC (Max 8881, Maxim).

A NTC thermistor (Epcos) serves as a temperature sensor. The ceramic capacitor C_t (Kemet) with COG/NPO parameters has a high Q, low K, a temperature-compensated dielectric, and stable electrical properties at varying voltage, temperature, frequency and time. Together NTC and C_t set a time constant t_T, which triggers a timer (ICM 7242, Intersil). This timer produces the output signal S, a pulse train with temperature-dependent pulse intervals. The sampling rate is approximately 10 Hz at 60°C, 5 Hz at 37°C, and 2.1 Hz at 20°C.

Coil L is used not only for power transfer but also for signal transmission by superimposed magnetic pulses. The tantalum chip capacitor C is charged by L and the Schottky diodes D1, D2 to a maximum of U_C = 11.7 V DC. The electrical pulses

of signal S close the digital FET switches S1 and S2 (FDC 6303N, Fairchild Semiconductor). C is then discharged over L resulting in magnetic pulses. After each pulse, both FET open and C is charged again. The transmitted pulses have a duration of 3 ms, and this telemetry circuit has a power consumption of 7 mW.

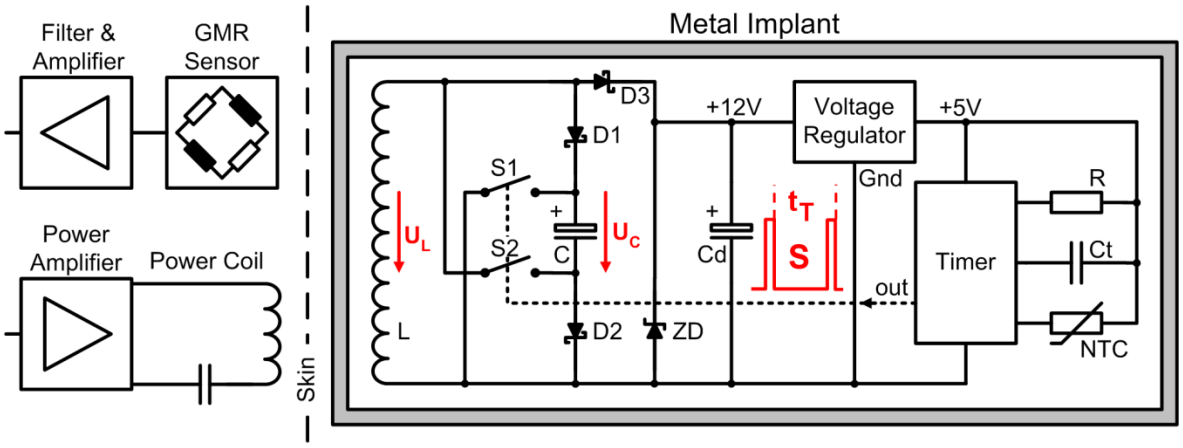

Figure 2: *Principle of the temperature telemetry; Energy and temperature data are transferred through the titanium implant by induction.*

All active and passive components are surface mount devices on both sides of an 18 x 5 mm wide substrate (Figure 1). The NTC is positioned near the center of the prosthetic head. To shield the electronic components against the magnetic field, a tube of PERMENORM 5000 H2 with a wall thickness of 0.25 mm is slipped over the whole circuit and fixed with epoxy structural adhesive DP190 (3M Scotch-Weld). The telemetry (40 mm long, 6.1 mm Ø) is fixed inside the prosthetic neck with DP190.

External measuring system

The specially developed unit ‘TELETEMP’ contains a power oscillator, amplifier and microcontroller (AVR-ATmega128, Atmel) with a USB interface and display. Because the transmitted magnetic pulses are low in power, a very sensitive sensor had to be chosen. This giant magnetoresistive (GMR) field sensor (AA002-02, NVE-Corporation) consists of a Wheatstone bridge and has an on-chip flux concentrator to increase its sensitivity along a specified axis.

Because the external powering field is much stronger than the field produced by the signal pulses, care must be taken that the GMR sensor measures as little as possible of the 4-kHz powering field. The spatial positions of GMR sensor and external induction coil (n = 210, D = 25 cm, L = 7.85 mH, C = 0.22 µF) are therefore fixed by a common, massive plastic housing (Figure 3). Within 5 cm from this housing the coil windings are furthermore inflexible. The sensor position is finally optimized by precisely adjusting the sensor board inside the housing.

The sensor signal is first high-pass-filtered (fc = 109 Hz, first-order) to remove the 50-Hz content. After a first amplification (AD8230, Analog Devices) a low-pass filter (1 kHz, 10^{th} order, LTC1569-6, Linear Technology Corp.) eliminates the remaining influence of the 4-kHz powering field. The gain of a second amplifier (AD8042, Analog Devices) can be set by a digital potentiometer (AD5282, Analog Devices). The pulses are converted to 12-bit digital values (MAX197, Maxim Integrated Products). The microcontroller checks the received signals S for missing pulses, amplifies their peak values to 3 ± 1 V, counts their temperature-dependent time intervals t_T and sends S and t_T to a Windows PC.

Power supply

During the measurements the power coil is placed around the hip joint (Figure 3). The power oscillator generates a sinusoidal output voltage at 4 ± 0.5 kHz. This frequency is permanently adapted to the resonance frequency of the coil. The oscillator output voltage and, thus, the magnetic field strength are controlled by the microcontroller. Primary and secondary power coils are fixed to the thigh and the femur, respectively. Except from soft tissue deformations they therefore move in the same way during walking and the induced supply voltage varies by not more than 5%. Using an induction frequency of 4 kHz with loose air-coupled coils a shift of the titanium implant is not detectable by the primary power coil.

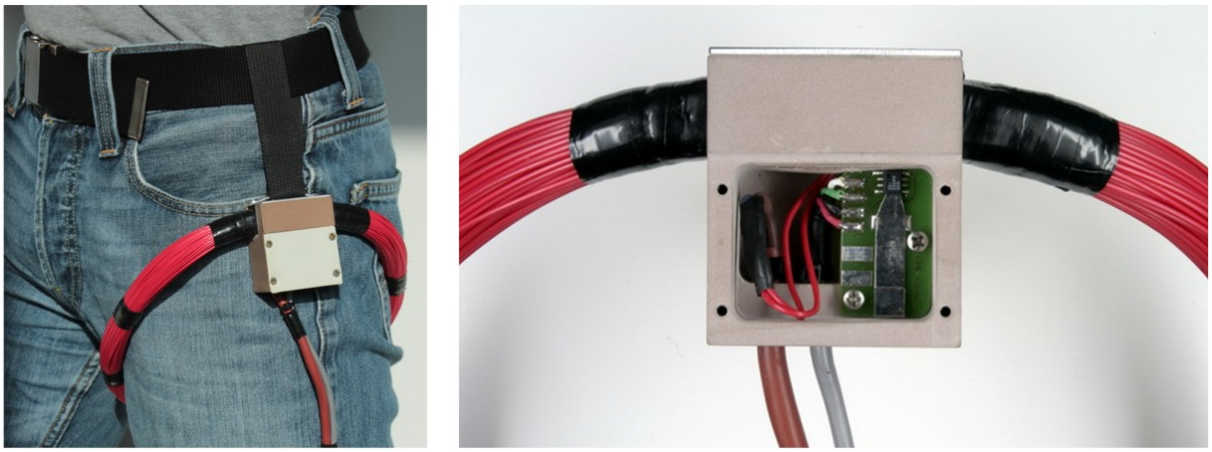

Figure 3: *External equipment; The power coil with GMR sensor are fixed near the patient's hip and connected to the external device TELETEMP.*

The voltage U_C and, thus, the strength of the transmitted signal pulse directly depend on the magnetic field strength. For U_C below 5 V, the circuit is unstable, and the pulses cease. Levels above 11.7 V are prevented using Zener diodes. The range of the internal voltage U_C is controlled by analyzing the amplitude of the received pulses. Beginning with a high amplification, the magnetic field strength is reduced until the pulse height begins to decrease; U_C is then at its upper limit of 11.7 V. When the pulses vanish, U_C has reached its lower limit of 5 V. Based on these two values, U_C is set to 7.5 V. The operating range of 6 V to 9 V is a compromise between sufficient signal strength and the minimal power dissipation. This range allows position changes between the signal source inside the implant and the power coil around the leg without endangering the power supply. If U_C nevertheless exceeds one of its borders, U_C is automatically re-adjusted.

Data processing

The evaluation program is written in Visual Basic (Figure 4). Signal S is displayed, and its peak values are marked as well as the times used for counting t_T. The temperature is calculated from previously obtained calibration data and charted for visual control.

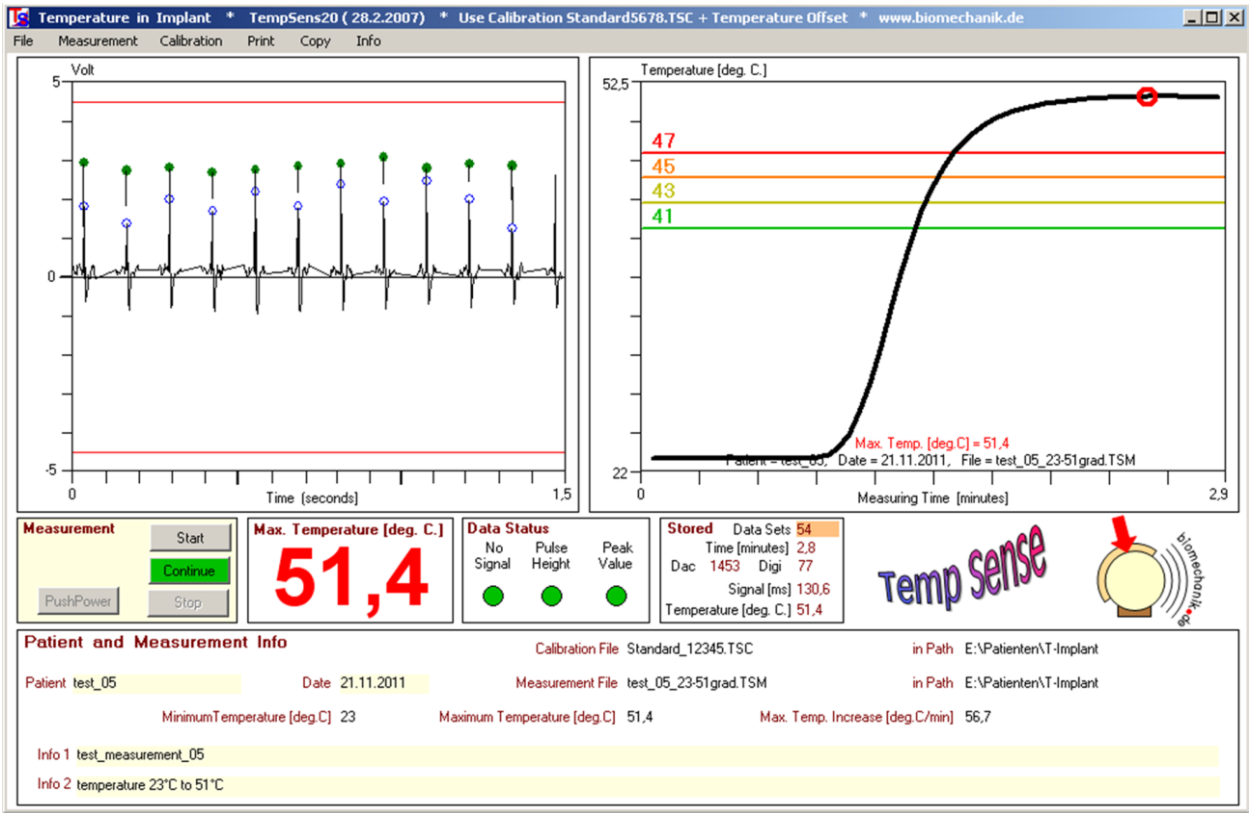

Figure 4: *Measuring program; Screen shot from test measurements.Left: pulse signal from implant. Marked peak values and time points for counting temperature dependent pulse intervals. Right: sudden temperature increase in a water bath.*

Calibration

For calibration, 5 prostheses were placed in a circulating water bath at 10 different temperatures between 23°C and 58°C (Figure 5). The temperature was adjusted with an accuracy of 0.1°C and measured close to the implant with an accuracy of 0.01°C (9540, Guildline Instruments). From this data, an average polynomial temperature curve, Temperature = $f(t_T)$, was calculated (Figure 6). Only an offset temperature at 37.5°C must later be determined for the implants used in patients.

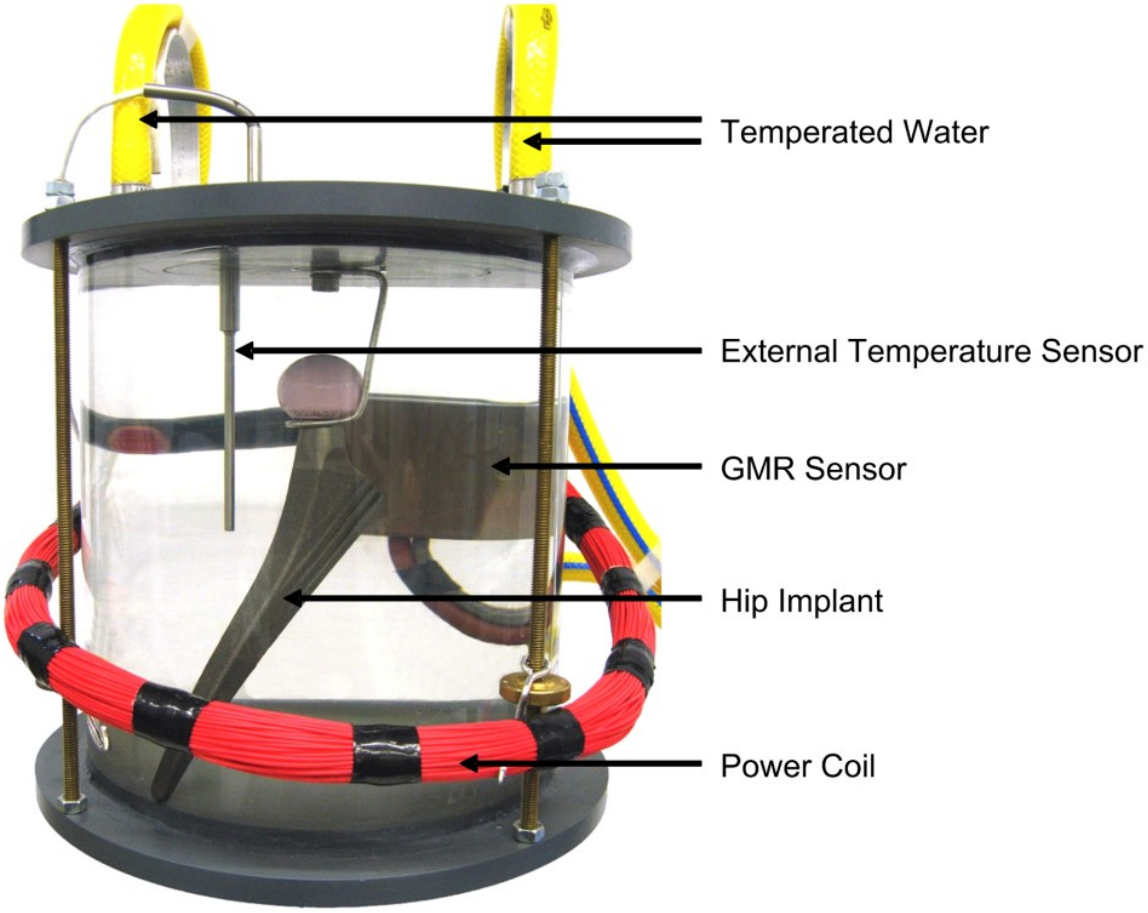

Figure 5: *Implant calibration; the implants were calibrated in a circulating water bath at temperatures between 23°C and 58°C.*

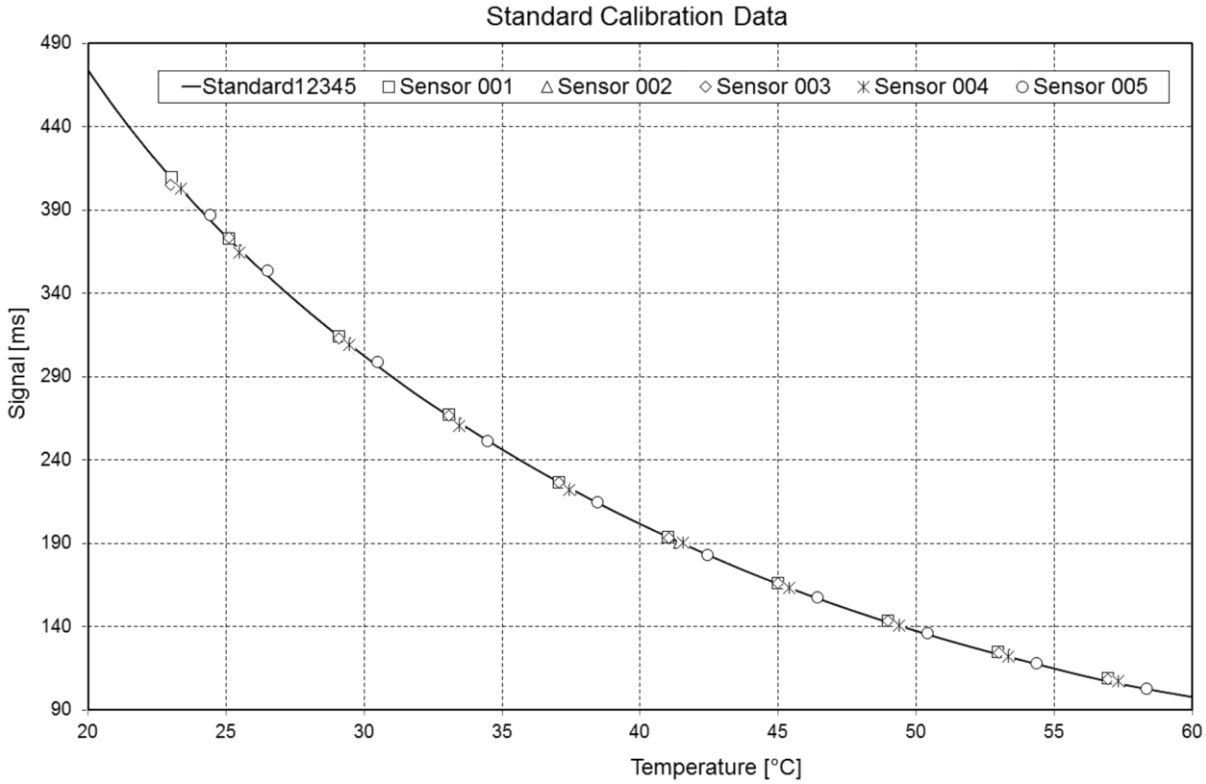

Figure 6: *Standard temperature curve; The temperature-dependent signals of 5 implants are plotted.*

Results

Implant safety

Only prostheses with neck lengths XS (extra-small), S (small), M (medium) and L (large) will be implanted. For fatigue tests, a longer neck length of XL (extra-large) was used. Under this more severe condition, the implant stem passed the fatigue tests [37]. Then, the neck was tested with a maximum load of 5.3 kN during 10 million cycles [38]. This load was further increased every 1 million cycles in steps of 1 kN, without failure, up to 13 kN. This load was more than 2 times higher than the standard force for testing implant necks. The mechanical tests were performed by EndoLab GmbH (Rosenheim, Germany), and the sterilization process was certified by Vanguard AG (Berlin, Germany).

The telemetry system described was approved by BerlinCERT (Berlin, Germany) using standards of both EU Directive 90/385/EWG (AIMDD, Active Implantable Medical Device Directive) and EU Directive 93/42/EWG (MDD, Medical Device Directive).

A planned clinical study with 100 patients will begin after receiving approval from our Ethics Committee.

Measuring accuracy

The measuring accuracies were determined at 37.5°C, 43°C, and 50°C. The measured temperatures were compared with readings from a thermometer with an accuracy of 0.01°C. The error of the calibrated implants was always below 0.1°C.

To determine how fast the instrumented implants are able to detect temperature changes, a prototype was placed in cold circulating water. Then, boiling water was quickly added such that the temperature rose from 23°C to approximately 51°C. This temperature increase was recorded by the implant within 70 s (Figure 4).

Discussion

The clinical study on temperature rise in hip implants is planned with 100 patients. The shape of the original implant was unchanged by the instrumentation, and thus, current surgical procedures can be used. Therefore, the same good clinical success, such as with other Spotorno-like implants, can be expected.

Investigations will be performed with 4 different combinations of head and cup materials and 2 different head sizes. This data will allow us to answer the following questions: a) Are certain material combinations producing such high temperatures that implant fixation of patients with badly lubricating synovia is endangered? b) How much do the lubrication properties of synovia differ individually? c) Can patients at risk be identified by intra-operative synovia tests? d) Do joint simulators deliver realistic results for friction and wear?

Our previous instrumented joint implants (www.OrthoLoad.com), with multi-channel telemetries for load measurements, required higher sampling rates and a signal transmission by radiofrequency. Because such signals are shielded by the metallic implant, electrical feedthroughs and an antenna outside of the implant were needed, which had to be biocompatible and protected mechanically. The low frequency magnetic pulses, now used for data transfer, are only marginally weakened by titanium implants and can therefore be transmitted through the metallic wall. This enables the design of mechanically safe and simple instrumented orthopedic

implants. In addition, the described technique is also well suited for measuring strains or detecting implant loosening by frequency analyses.

The low power consumption of 7 mW prevents a temperature increase by the inductive power supply. The transmission rate of 5 Hz is sufficiently high for measuring temperatures, and the measuring error of 0.1°C is lower than expected.

The transmission rate can be increased, for example, up to 50 Hz, with good accuracy. For measuring fast changing signals this rate may still be too low. Sampling can be accelerated, however, if the signals are not transmitted in real-time. Instead, they can be measured at a high rate, stored temporarily in the memory of a microcontroller and transmitted at a lower rate directly after the measurement. Transmitting signals at a rate that is ten times lower would allow sampling of 1 signal of at least 500 Hz or of several signals at a lower rate.

As described, the GMR sensor has to be adjusted carefully, and its signal is filtered not to measure the 4-kHz powering field but to measure only the magnetic pulses produced by the implant. Currently the signal-receiving circuit is changed such that the signal will only be received at time points when the powering field is close to the zero crossing, which will ensure that the quality of the signals is significantly less dependent on the exact adjustment of the power coil and the GMR sensor.

References

1. Streicher RM, Semlitsch M, Schon R, Weber H, Rieker C (1996) Metal-on-metal articulation for artificial hip joints: laboratory study and clinical results. Proc Inst Mech Eng H 210: 223-232.
2. Drewniak EI, Jay GD, Fleming BC, Crisco JJ (2009) Comparison of two methods for calculating the frictional properties of articular cartilage using a simple pendulum and intact mouse knee joints. J Biomech 42: 1996-1999.
3. Bergmann G, Graichen F, Rohlmann A, Verdonschot N, van Lenthe GH (2001) Frictional heating of total hip implants. Part 1: measurements in patients. J Biomech 34: 421-428.
4. Fialho JC, Fernandes PR, Eca L, Folgado J (2007) Computational hip joint simulator for wear and heat generation. J Biomech 40: 2358-2366.
5. Brockett C, Williams S, Jin Z, Isaac G, Fisher J (2007) Friction of total hip replacements with different bearings and loading conditions. J Biomed Mater Res B Appl Biomater 81: 508-515.
6. Moss SG, Schweitzer ME, Jacobson JA, Brossmann J, Lombardi JV, et al. (1998) Hip joint fluid: detection and distribution at MR imaging and US with cadaveric correlation. Radiology 208: 43-48.
7. Liao YS, Benya PD, McKellop HA (1999) Effect of protein lubrication on the wear properties of materials for prosthetic joints. J Biomed Mater Res 48: 465-473.
8. Rainer F, Ribitsch V, Ulreich A (1980) Viscosity of synovial fluid and possible artificial lubricants (author's transl). Acta Med Austriaca 7: 92-95.
9. Fam H, Bryant JT, Kontopoulou M (2007) Rheological properties of synovial fluids. Biorheology 44: 59-74.
10. Chikama H (1985) [The role of protein and hyaluronic acid in the synovial fluid in animal joint lubrication]. Nippon Seikeigeka Gakkai Zasshi 59: 559-572.
11. Swann DA, Bloch KJ, Swindell D, Shore E (1984) The lubricating activity of human synovial fluids. Arthritis Rheum 27: 552-556.
12. Williams S, Leslie I, Isaac G, Jin Z, Ingham E, et al. (2008) Tribology and wear of metal-on-metal hip prostheses: influence of cup angle and head position. J Bone Joint Surg Am 90 Suppl 3: 111-117.
13. Smith SL, Unsworth A (2001) A five-station hip joint simulator. Proc Inst Mech Eng H 215: 61-64.

14. Tepic S, Macirowski T, Mann RW (1985) Experimental temperature rise in human hip joint in vitro in simulated walking. Journal of Orthopaedic Research 3: 516-520.
15. Pritchett JW (2006) Heat generated by knee prostheses. Clin Orthop Relat Res 442: 195-198.
16. Rocchi M, Affatato S, Falasca G, Viceconti M (2007) Thermomechanical analysis of ultra-high molecular weight polyethylene-metal hip prostheses. Proc Inst Mech Eng H 221: 561-568.
17. Bergmann G, Graichen F, Rohlmann A, Verdonschot N, van Lenthe GH (2001) Frictional heating of total hip implants. Part 2: finite element study. J Biomech 34: 429-435.
18. Lu Z, McKellop H (1997) Frictional heating of bearing materials tested in a hip joint wear simulator. Proc Inst Mech Eng H 211: 101-108.
19. Leon SA, Asbell SO, Arastu HH, Edelstein G, Packel AJ, et al. (1993) Effects of hyperthermia on bone. II. Heating of bone *in vivo* and stimulation of bone growth. Int J Hyperthermia 9: 77-87.
20. Moritz AR, Henriques FC (1947) Studies of Thermal Injury: II. The Relative Importance of Time and Surface Temperature in the Causation of Cutaneous Burns. Am J Pathol 23: 695-720.
21. Li S, Chien S, Branemark PI (1999) Heat shock-induced necrosis and apoptosis in osteoblasts. J Orthop Res 17: 891-899.
22. Yoshida K, Uoshima K, Oda K, Maeda T (2009) Influence of heat stress to matrix on bone formation. Clin Oral Implants Res 20: 782-790.
23. Gronkiewicz K, Majewski P, Wisniewska G, Pihut M, Loster BW, et al. (2009) Experimental research on the possibilities of maintaining thermal conditions within the limits of the physiological conditions during intraoral preparation of dental implants. J Physiol Pharmacol 60 Suppl 8: 123-127.
24. Schneider E, Michel MC, Genge M, Zuber K, Ganz R, et al. (2001) Loads acting in an intramedullary nail during fracture healing in the human femur. J Biomech 34: 849-857.
25. Holland HJ, Grätz H, Braunschweig M, Kuntz M (2012) INHUEPRO: sensorsystem for use in implants. Proc MikroSytemTechnik Kongress 2011 Darmstadt, VDE-Verlag: 437-440.

26. Taylor SJ, Perry JS, Meswania JM, Donaldson N, Walker PS, et al. (1997) Telemetry of forces from proximal femoral replacements and relevance to fixation. J Biomech 30: 225-234.
27. Puers R, Catrysse M, Vandevoorde G, Collier RJ, Louridas E, et al. (2000) A telemetry system for the detection of hip prosthesis loosening by vibration analysis. Sensors and Actuators A 85: 42-47.
28. Bergmann G, Graichen F, Siraky J, Jendrzynski H, Rohlmann A (1988) Multichannel strain gauge telemetry for orthopaedic implants. J Biomech 21: 169-176.
29. Graichen F, Arnold R, Rohlmann A, Bergmann G (2007) Implantable 9-channel telemetry system for *in vivo* load measurements with orthopedic implants. IEEE Trans Biomed Eng 54: 253-261.
30. Graichen F, Bergmann G (1991) Four-channel telemetry system for *in vivo* measurement of hip joint forces. J Biomed Eng 13: 370-374.
31. Graichen F, Bergmann G, Rohlmann A (1999) Hip endoprosthesis for *in vivo* measurement of joint force and temperature. J Biomech 32: 1113-1117.
32. Moss C, Weinrich N, Sass W, Mueller J (2010) Integration of a telemetric system within an intramedullary nail for monitoring of the fracture healing progress. Proc 3rd Int Symp on Applied Sciences in Biomedical and Communication Technologies: 1-5
33. Marschner U, Grätz H, Jettkan B, Ruwisch D, Woldt G, et al. (2009) Integration of a wireless lock-in measurement of hip prosthesis vibrations for loosening detection. Sensors and Actuators A 156 145–154.
34. Moss Ch, Sass W, Weinrich N, Seide K, Müller J (2009) Low Frequency RFID – Strain Measurement on Passive Implants. Proc SOMSED ‘09 1: 97-100.
35. Brown RH, Burstein AH, Frankel VH (1982) Telemetering *in vivo* loads from nail plate implants. J Biomech 15: 815-823.
36. Karrholm J (2010) The Swedish Hip Arthroplasty Register (www.shpr.se). Acta Orthop 81: 3-4.
37. ISO7206-4 (2010) Implants for surgery -- Partial and total hip joint prostheses -- Part 4: Determination of endurance properties and performance of stemmed femoral components.

38. ISO7206-6 (1992) Implants for surgery -- Partial and total hip joint prostheses -- Part 6: Determination of endurance properties of head and neck region of stemmed femoral components.
39. ISO7206-8 (1995) Implants for surgery -- Partial and total hip joint prostheses -- Part 8: Endurance performance of stemmed femoral components with application of torsion.

Published in: PLoS ONE 8(11): e78373.

DOI:10.1371/journal.pone.0078373

6. Friction in total hip joint prosthesis measured *in vivo* during walking

P. Damm, J. Dymke, R. Ackermann, A. Bender, F. Graichen, A. Halder, A. Beier, G. Bergmann

Abstract

Friction-induced moments and subsequent cup loosening can be the reason for total hip joint replacement failure. The aim of this study was to measure the *in vivo* contact forces and friction moments during walking. Instrumented hip implants with Al_2O_3 ceramic head and an XPE inlay were used. *In vivo* measurements were taken 3 months post operatively in 8 subjects. The coefficient of friction was calculated in 3D throughout the whole gait cycle, and average values of the friction-induced power dissipation in the joint were determined.

On average, peak contact forces of 248% of the bodyweight and peak friction moments of 0.26% bodyweight times meter were determined. However, contact forces and friction moments varied greatly between individuals. The friction moment increased during the extension phase of the joint. The average coefficient of friction also increased during this period, from 0.04 (0.03 to 0.06) at contralateral toe off to 0.06 (0.04 to 0.08) at contralateral heel strike. During the flexion phase, the coefficient of friction increased further to 0.14 (0.09 to 0.23) at toe off. The average friction-induced power throughout the whole gait cycle was 2.3 W (1.4 W to 3.8 W).

Although more parameters than only the synovia determine the friction, the wide ranges of friction coefficients and power dissipation indicate that the lubricating properties of synovia are individually very different. However, such differences may also exist in natural joints and may influence the progression of arthrosis. Furthermore, subjects with very high power dissipation may be at risk of thermally induced implant loosening. The large increase of the friction coefficient during each step could be caused by the synovia being squeezed out under load.

Introduction

In 20% to 40% of all cases [1], polyethylene wear and aseptic loosening are the most frequent reasons for revisions of total hip joint replacements (THR). Both factors are related to friction in the joint. Cup loosening has been reported to be the only cause in 30% to 62% of revisions [2, 3]. Subjects, who obtained a THR are becoming increasingly younger and are, therefore, more active and athletic [4, 5]. However, higher activity levels produce more wear and more strenuous activities cause higher friction moments. This will increase the risk of implant loosening [6,7]. These facts indicate that reduction of friction between head and cup is critical for further improvement of THR.

Several *in vivo* studies have been performed to investigate the loads acting in hip implants during different activities [8, 9]. These studies have shown that the contact force during normal walking falls in a range between 240 and 480% of the bodyweight (BW). However, *in vivo* measurements of friction in hip endoprostheses have not been reported previously.

One *in vivo* study *indirectly* assessed friction in the joint by measuring the implant temperature during an hour of walking [10,11]. Its increase is mainly related to the friction-induced power generated in the implant. A peak temperature of 43.1°C was measured in 1 subject, a level at which bone tissue may already be impaired [12], especially when this temperature occurs repeatedly. Therefore, it cannot be excluded that friction and increased implant temperatures may be underestimated risk factors for the long-term stability of THR.

To determine the friction in total hip joint prosthesis, *in vitro* simulator studies were performed [13, 14]. To evaluate the friction between two sliding partners, the coefficient of friction μ was used. For the tribological pairing Al_2O_3/UHMWPE μ ranges depended on the lubricant [13], ranging from 0.044 (distilled water), to 0.054 (bovine serum), and 0.089 (saline). The coefficient increased dramatically up to values of 0.14 when the conditions changed from lubricated to dry [15].

However, most of the simulator tests load the joint only in the flexion-extension plane and use load patterns which may not be realistic [16]. Newer studies investigated friction under more realistic conditions, simulating *in vivo* measured gait data [17]. Varying parameters for friction were investigated, for example, different material combinations for implant head and cup [18], and various lubricant regimes [17, 19–

22]. These simulator studies were performed under very different test conditions, such as deviating patterns of joint loading and movement or by using different lubricants. Nevertheless, it was shown that friction in THR is mainly influenced by the material of the sliding partners and the lubrication regime.

The aim of our study was to determine the *in vivo* contact forces in hip implants during walking, plus the moments caused by friction, and derive the coefficient of friction from these data. These data will help to understand the *in vivo* lubrication conditions and allow validating, potentially improving the conditions applied in joint simulators.

Methods

Ethic statement

The study was approved by the Charité Ethics committee (EA2/057/09) and registered at the 'German Clinical Trials Register' (DRKS00000563). All patients gave written informed consent prior to participating in this study.

Subjects and measurements

Eight subjects with instrumented hip joint prostheses (Table 1) participate in this study. Measurements were taken 3 months postoperatively (pOP) during level walking at a self-selected walking speed. Selected trials of each investigated subject are also shown and can be downloaded at the public data base www.OrthoLoad.com.

Table 1: *Patients investigated*

Patient	Age [years]	Gender	Body weight [N]	Gait Velocity [m/s]	Mean Gliding Speed Extension | Flexion [m/s]
H1	56	m	754	1.0	0.02 | 0.04
H2	62	m	755	1.0	0.03 | 0.05
H3	60	m	880	0.8	0.02 | 0.06
H4	50	m	783	1.0	0.03 | 0.06
H5	62	f	853	0.9	0.02 | 0.08
H6	69	m	832	1.1	0.03 | 0.05
H7	53	m	899	1.1	0.03 | 0.06
H8	56	m	779	1.1	0.03 | 0.06
Average	*59*	-	*821*	*1.0*	*0.03* | *0.06*

Measuring equipment

Joint forces and friction moments were measured *in vivo* with instrumented hip implants. The prosthesis (CTW, Merete Medical, Berlin, Germany) has a titanium stem, a 32 mm Al_2O_3 ceramic head (BIOLOX forte, CeramTec GmbH, Plochingen, Germany) and an XPE inlay (Durasul, Zimmer GmbH, Winterthur, Switzerland). A telemetry circuit, 6 strain gauges, and a secondary induction coil are placed in the hollow neck, which is closed by welding. A detailed description of the instrumented implant was published previously [23]. A coil around the hip joint inductively powers the inner electronics. The strain gauge signals are transferred via an antenna in the implant head to the external receiver. These signals and the subject's movements are recorded simultaneously on videotape. The external measurement system has previously been described in detail [24, 25].

From the 6 strain gauge signals, the 3 force and 3 moment components acting on the implant head are calculated [26] with an accuracy of 1-2%. The femur-based

coordinate system [27] is fixed in the center of the head of a right sided implant, but is defined relative to the bone. Data from left implants were mirrored to the right side. The positive force components F_x, F_y, and F_z act in lateral, anterior, and superior directions, respectively (Figure 1A). From the 3 force components the resultant contact force F_{res} is calculated. The measured friction moments M_x, M_y, and M_z, act clockwise around the positive axes. The 3 moment components deliver the resultant friction moment M_{res}. Positive/negative moments M_x are caused by extension/flexion of the joint. Positive/negative moments M_y act during abduction/adduction. Positive/negative moments M_z are caused by external/internal rotation.

Data evaluation

All forces are reported as percent of bodyweight (% BW) and the friction moments as % BWm. Average force-time patterns from 32-96 steps were calculated for each subject. The employed 'time warping' method [28] weighted the congruency of high forces more than that of lower ones. First the period times of all the included steps are normalized. The single time scales were then distorted in such a way that the squared differences between all deformed curves, summed over the whole cycle time, were smallest. Finally, an arithmetically averaged load-time pattern was calculated from all the deformed curves. Using these algorithms, an average time course was first calculated from the time patterns of the resultant joint forces F_{res}. The obtained time deformations of the single trials were then transferred to the corresponding force and moment components before averaging them, too. The resultant friction moment M_{res} was calculated from an average of its components.

This procedure was first applied on all trials of the single subjects, leading to 'individual' averages. These averages from all subjects were then combined to a 'general' average, which describes the loads acting in an 'average' subject.

In some cases, peak values were not taken from the averaged time courses, but instead, the numerical peak values of the *single* trials were averaged, first individually and then inter-individually. Extreme values of the averaged load-time patterns can slightly deviate from these numerically averaged numbers. These values of the average subject were statistically analysed ($p \leq 0.05$; Wilcoxon).

Coefficient of friction

The coefficient of friction μ between the head and the cup was calculated by a 3D approach (Figure 1B). Joint movement takes place in a plane perpendicular to the axis of the vector $\underline{M}_{res}$. This axis is not perpendicular to the axis of vector $\underline{F}_{res}$. The vector of the friction force $\underline{F}_{friction}$ acts perpendicular to $\underline{F}_{res}$ at point P on the head. $\underline{H}$ is the vector of the lever arm between $\underline{F}_{Friction}$ and the axis of $\underline{M}_{res}$ and is perpendicular to both. $\underline{D}$ is a vector in direction of $\underline{M}_{res}$. $\underline{R}$ = 16 mm is the radius vector to point P.

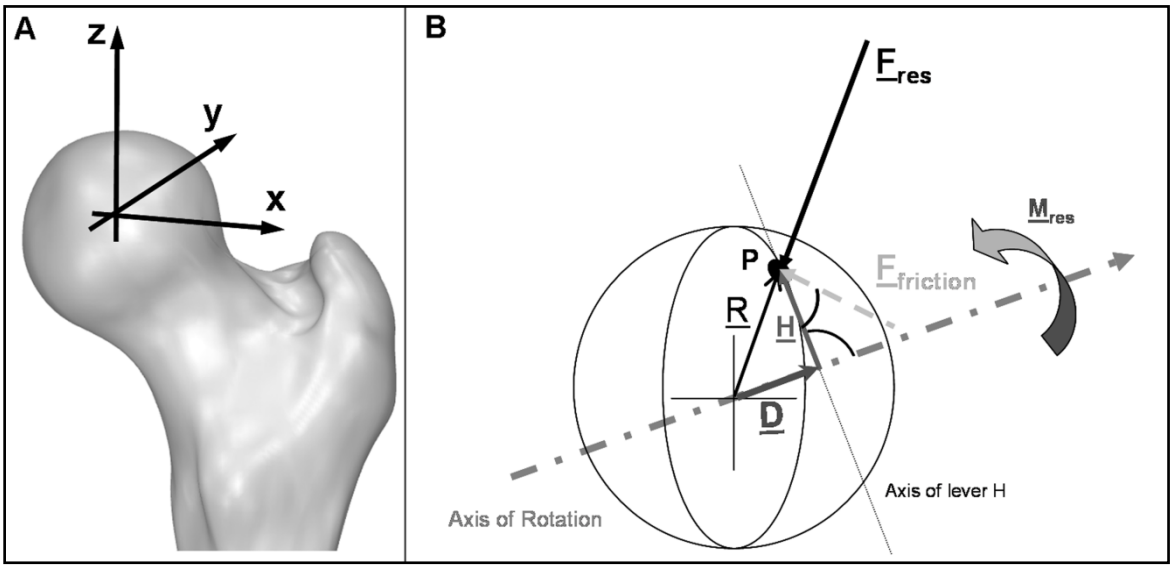

Figure 1: *Coordinate system and vectors for calculation of the coefficient of friction μ; Right joint, posterior view.*

Assuming a Coulomb friction between the head and the cup, the friction force acting on the head is

$$F_{friction} = \mu * F_{res} \qquad (1)$$

The moment determined by the force $\underline{F}_{friction}$ and its lever arm $\underline{H}$ has to counteract $\underline{M}_{res}$. Because $\underline{F}_{friction}$ and $\underline{H}$ are perpendicular to each other, this delivers the scalar equation

$$H * F_{friction} = M_{res} \qquad (2)$$

From the combination of (1) and (2), the following equation can be derived:

$$\mu = M_{res} / (H * F_{res}) \qquad (3)$$

R is the radius of the head. R points to P and has the direction opposite to F_{res}:

$$\underline{R} = -R * \underline{F}_{res} / F_{res}$$

$\underline{H}$ can be substituted by

$$\underline{H} = \underline{R} - \underline{D} \qquad (5)$$

With $\underline{D}$ being the orthogonal projection of $\underline{R}$ on $\underline{M}_{res}$:

$$\underline{D} = R * \cos(\underline{R}, \underline{M}_{res}) * \underline{M}_{res} / M_{res} \qquad (6)$$

The angle between $\underline{R}$ and $\underline{M}_{res}$ can be derived from their scalar product:

$$\cos(\underline{R}, \underline{M}_{res}) = (\underline{R} * \underline{M}_{res}) / (R * M_{res}) \qquad (7)$$

Applying (4), (6), (7), equation (5) becomes

$$\underline{H} = R * (\underline{F}_{res} / F_{res}) * [(\underline{M}_{res} / M_{res})^2 - 1] \qquad (8)$$

The friction coefficient μ is determined from (3), using the measured load vectors $\underline{F}_{res}$ and $\underline{M}_{res}$, the known head radius R, and the lever arm H, which is calculated by (8). Due to measuring errors, μ will be inaccurate if $\underline{F}_{res}$ or $\underline{M}_{res}$ is very small. Therefore, μ was only determined for $F_{res} \geq 20\%$ BW *and* $M_{res} \geq 0.02\%$ BWm.

In previous simulator tests, μ has mostly been determined in the sagittal plane. To compare our 3D-derived values with this data, we additionally calculated μ from the forces and moments measured in the sagittal, frontal, and horizontal planes as follows:

$$\mu_x = M_x / (F_{yz} * R) \qquad (9a)$$

$$\mu_y = M_y / (F_{xz} * R) \qquad (9b)$$

$$\mu_z = M_z / (F_{xy} * R) \qquad (9c)$$

F_{yz}, F_{xz} and F_{xy} are the forces in the sagittal, frontal, and horizontal planes, respectively.

Friction-induced power

In addition to the measured joint loads and the calculated friction coefficient μ, we determined the friction-induced power Q in the joint, which is caused by the friction

force $F_{friction}$. With v being the gliding speed between head and cup, Q is given by the simplified equation

$$Q = F_{friction} * v = F_{res} * \mu * v \quad (10)$$

Average values of Q were calculated separately for the extension and flexion phases of the gait cycle:

$$Q_{ext} = F_{ext} * \mu_{ext} * v_{ext} \quad (11a)$$

$$Q_{flex} = F_{flex} * \mu_{flex} * v_{flex} \quad (11b)$$

The average power Q_{aver} over the *whole* gait cycle was then determined from

$$Q_{aver} = (Q_{ext} * T_{ext} + Q_{flex} * T_{flex}) / (T_{ext} + T_{flex}) \quad (11c)$$

Calculations were based on the intra-individually averaged load-time patterns of the single subjects. Before F_{ext}, μ_{ext}, F_{flex}, and μ_{flex} were inserted in (11a, b), their time-dependent values were averaged arithmetically over the corresponding time periods T_{ext} and T_{flex}. The speed v was determined from the flexion/extension range of the shank in the sagittal plane, the times of flexion and extension, and the radius of the prosthetic head. The data of 4-7 steps per subject were averaged. Because no gait analyses had been performed, the shank movement had to be determined from the patient videos**.** The Intra-observer variation of v and therefore Q was on average 1%, the inter-observer variability of four investigators was on average 2%.

Results

Unless stated otherwise, the values reported here were taken from the time patterns of the average subject. The notation “X|Y” indicates a value of X at the instant of the first peak F_{res1} of the resultant force and a value of Y at the second peak F_{res2}.

Joint contact forces

Figure 2A shows the time patterns of F_{res} and its components for the average subject during one walking cycle. F_{res} was nearly identical with $-F_z$; the latter acts distally along the z-axis of the femur and compresses the hip joint. F_{res} had 2 peak values $F_{res1}|F_{res2}$. F_{res1} acted at about the time of contralateral toe off (CTO) and F_{res2} close to contralateral heel strike (CHS).

Figure 3A contains individual numerical averages of the 8 subjects. For $F_{res1}|F_{res2}$ peak values of 248|233% BW at 31|57% of the gait cycle were determined. However, these peak forces varied widely inter-individually. F_{res1} ranged from 210% BW (subject H3) to 301% BW (H8), and F_{res2} from 218% BW (H3) to 287% BW (H8). In 6 subjects F_{res1} was higher than $F_{res2,}$ but in H2 and H3 F_{res1} was lower than F_{res2}. The peak forces during the repeated trials of the same subject had standard deviations in the ranges of 7-14%BW (F_{res1}) and 5-14%BW (F_{res2}).

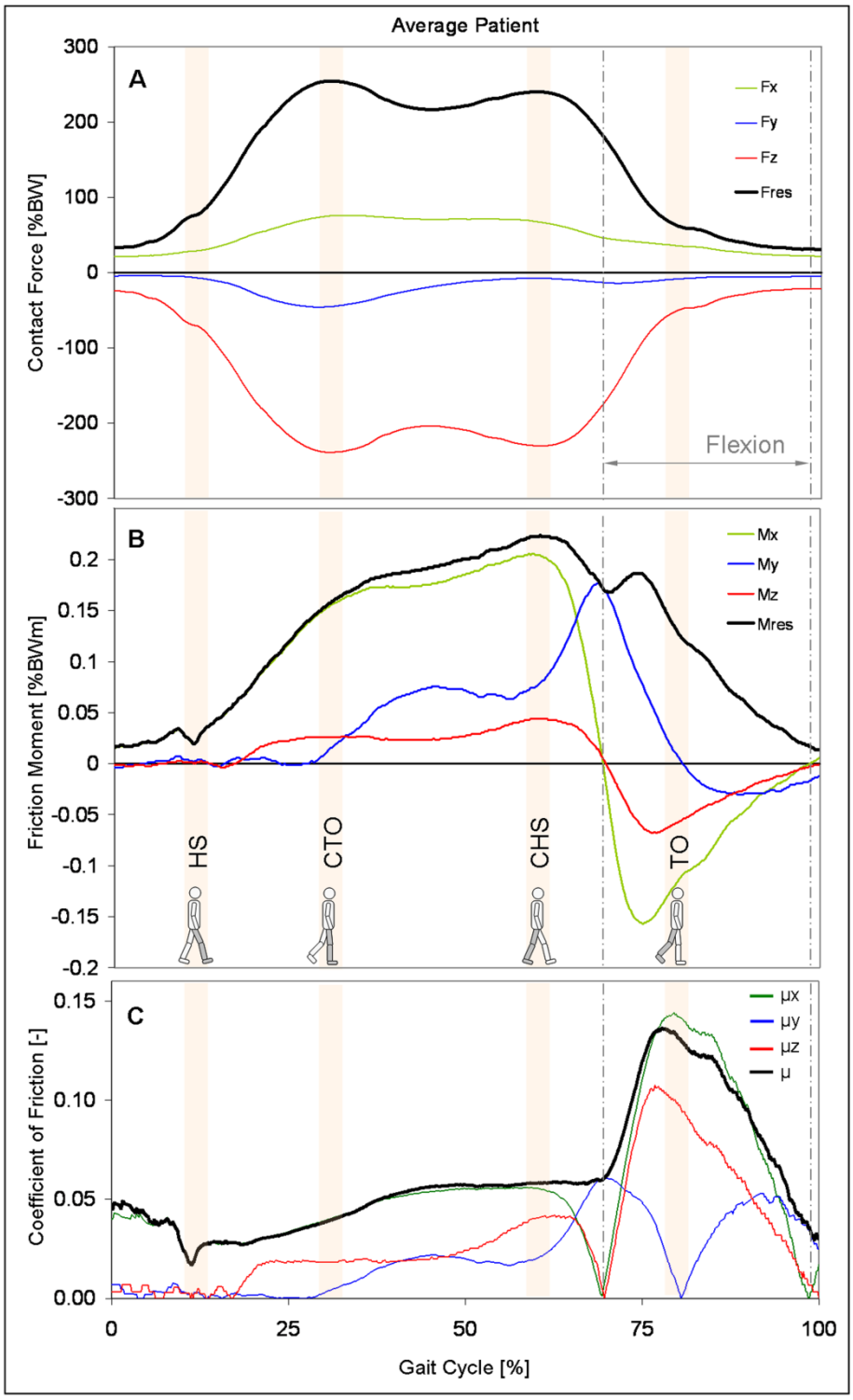

Figure 2: *Time courses of contact force, friction moment, and coefficient of friction; Top: contact force F_{res} and its components. Middle: friction moment M_{res} and its components. Bottom: coefficients of friction.μ from 3D calculation; μ_x (sagittal plane), μ_y (frontal plane), and μ_z (horizontal plane) from simplified 2D calculations. The data presented are for an average subject during level walking at approximately 1 m/s. Vertical lines: borders of the flexion phase. The diagram starts before heel strike.*

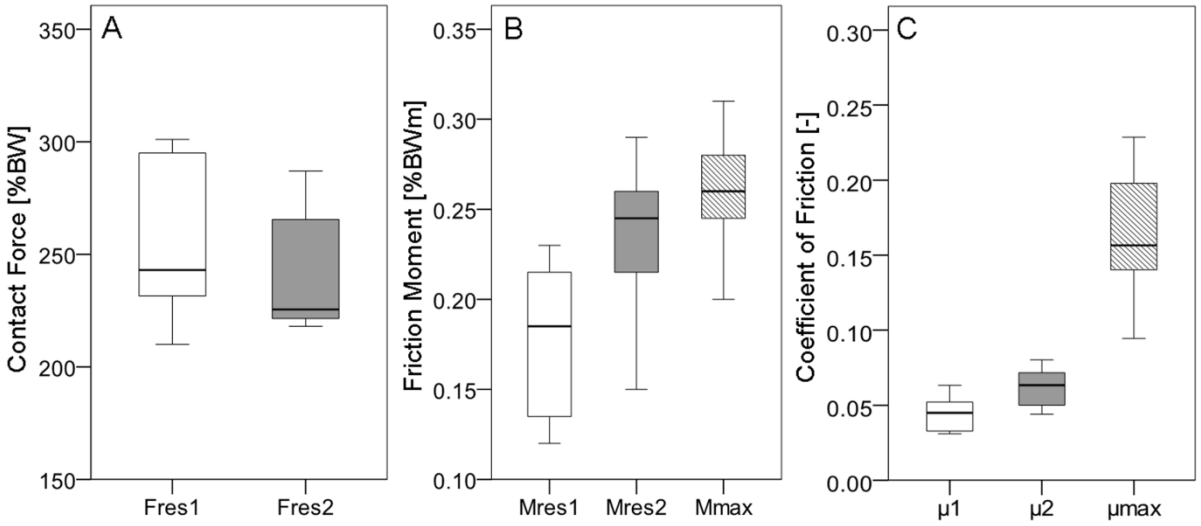

Figure 3: *Peak values of contact force, friction moment and coefficient of friction; A: contact force F_{res}, B: friction moment M_{res}, C: coefficient of friction μ. Individual numerical mean values and ranges from 8 subjects. $M_{res1}|M_{res2}$, $\mu_1|\mu_2$ = values at the instant of the force maxima $F_{res1}|F_{res2}$ (see Figure 2). M_{max}, μ_{max} = absolute maxima during a whole walking cycle.*

Friction moments

Figure 2B shows the time courses of M_{res} and its components. M_{res} increased from heel strike (HS) to CHS and reached values of $M_{res1}|M_{res2}$ = 0.16|0.21% BWm. The maximum M_{max} = 0.22% BWm acted slightly later than the force maximum F_{res2}. M_{res} climbed to a second, smaller peak of 0.19% BWm, which acted 15% of the cycle time after CHS, but before toe off of the ipsilateral leg (TO). During the intermediate minimum between CHS and TO, the joint rotation changed from extension to flexion. From HS to CHS, M_{res} was predominantly determined by component M_x, which acts in the sagittal plane of movement. After that and until the end of the stance phase the absolute values of M_y in the frontal plane exceeded those of M_x.

The patterns and magnitudes of M_x were relatively uniform for all 8 subjects (Figure 4A). On average the maximum of M_y had nearly the same magnitude as that of M_x (Figure 4B). The individual maxima of M_y (second peak value in subject H7) acted at very similar times. However, the variation of the individual maxima was much larger compared to M_x. Especially during the first half of the stance phase the time courses of M_y individually varied greatly. On average the peak value of the moment M_z was

about ¼ of that of M_x or M_y (Figure 4C). The individual time courses of M_z were similar, but the magnitudes varied considerably.

Figure 3B shows the averages and ranges of the peak values of M_{res} at the times of $F_{res1}|F_{res2}$. $M_{res1}|M_{res2}$ individually varied extremely with inter-trial standard deviations of 0.01 to 0.03%BW for both peak moments M_{res1} and M_{res2}. M_{res1} ranged from 0.12% BWm (H2) to 0.23% BWm (H1), while M_{res2} lay between 0.15% BWm (H3) and 0.29% BWm (H7). In 7 subjects M_{res} increased between the times of F_{res1} and F_{res2} (Figure 4D), with peak values of M_{max} between 0.2% BWm (H8) and 0.32% BWm (H4); it decreased only in H3, but increased again after the time of F_{res2}. In 5 subjects M_{max} occurred with a time delay after F_{res2} between 6% (H4) and 16% (H2) of the gait cycle; in 1 patient M_{max} occurred 2% before F_{res2} (H7), and in 2 subjects, no time delay was observed (H5 and H8). The individual inter-trial standard deviations of M_{max} lay between 0.01 and 0.03%BWm.

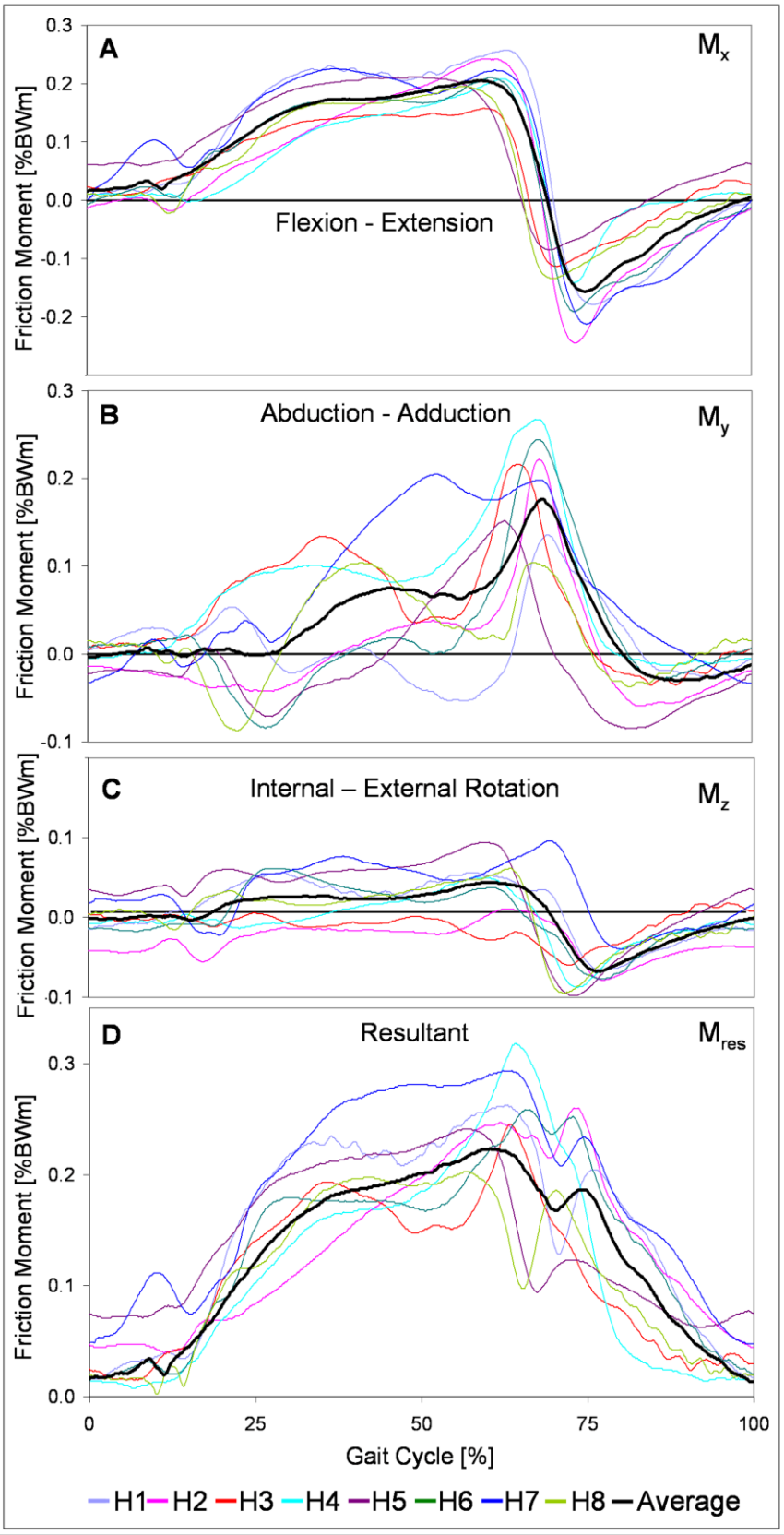

Figure 4: *Components of friction moment; Components M_x, M_y, M_z around x, y, z axes (see Figure 1). Individually averaged patterns of subjects H1 to H8 (color), and average patterns of all subjects (black)*

Friction coefficients

At HS μ was the lowest with an average value of μ = 0.02 (Figure 2C) and then increased nearly linearly. The values at the times of $F_{res1}|F_{res2}$ were $\mu_1|\mu_2$ = 0.04|0.06. After the instant when the joint rotation changed from extension to flexion, μ rose dramatically and reached its maximum μ_{max} = 0.14, shortly before TO.

The individual numerical values of μ at the instants of $F_{res1}|F_{res2}$ varied by a factor of 2 (Figure 3B); μ_1 had values between 0.03 (lowest in H2, H4, H8) and 0.06 (highest in H3); μ_2 varied between 0.04 (H3, H8) and 0.08 (H7). The maxima μ_{max}, which occurred shortly before TO, varied more, with values between 0.09 (H8) and 0.23 (H2).

The average patterns of the coefficients μ_x, μ_y, μ_z, calculated by the two-dimensional approaches, changed throughout the whole gait cycle (Figure 2C). μ_x in the main plane of movement corresponded well to μ (3D) throughout most of the loading cycle. However, shortly before and after joint rotation changed from extension to flexion, μ_x fell to zero. During the flexion phase, especially at its end, μ_x also deviated from μ. A temporary decline similar to μ_x was also observed for μ_z in the plane of femur rotation, when joint movement changed from extension to flexion. At the same time μ_y in the abduction-adduction plane reached a maximum.

Friction-induced power

With Q_{flex} = 5.0 W, the highest friction-induced power was observed in subjects H5 and H7 during the flexion phase (Figure 5), although F_{res} and M_{res} were very small (Figure 2A) during most of this period. In 7 of the 8 subjects, Q_{flex} was higher than Q_{ext}, which was mainly due to the higher values of μ and v during flexion (equation 11a, b). The individual differences between Q_{flex} and Q_{ext} varied considerably (Figure 5). The greatest difference was calculated for H5, in which Q_{Flex} was 2.9 times higher than Q_{ext}. The smallest difference was 4%, observed in H4. In H8, Q_{flex} was 21% lower than Q_{ext}. The inter-individual average power throughout the whole cycle was Q_{aver} = 2.3 W, with a range between 1.4 W (H1) and 3.8 W (H7). The average sliding speed during flexion was 2.2 times higher than during extension (Table 1), with individual values between 1.5 (H8) and 4.5 (H5).

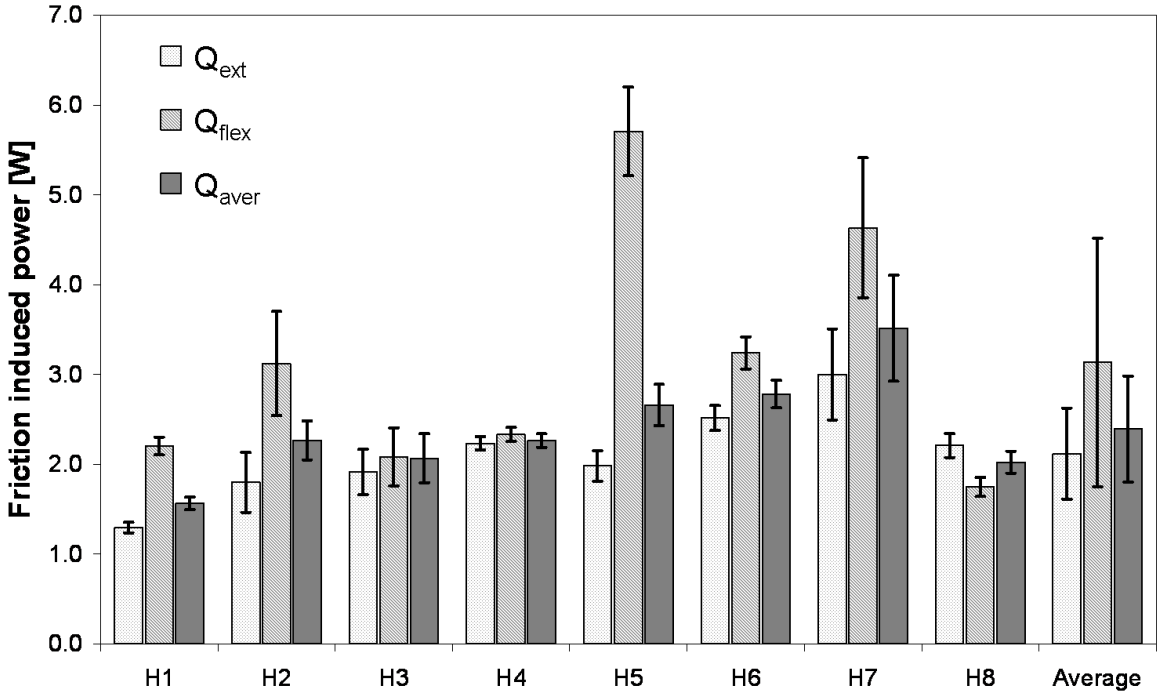

Figure 5: *Average friction-induced power Q during flexion and extension phases and whole walking cycle; Q_{ext} = Q during extension phase; Q_{flex} = Q during flexion phase; Q_{aver} = Q during whole step; Individual values of subjects H1 to H8 and averages (right columns)*

Discussion

This study reports for the first time on the assessment of *in vivo* friction in artificial hip joints during walking. The *in vivo* measured friction moment, at 3 month post-operative, increased during every gait cycle and as a consequence the coefficient of friction.

Forces and friction moments

Different *in vitro* test conditions were applied by others when investigating friction in hip joint prostheses. Several studies investigated friction by moving the joint in one plane like a pendulum [18, 19, 29, 30], simulating flexion/extension, and neglected movement around the other 2 axes. Our results show that these test conditions may be much too simplified. In reality the abduction-adduction moment M_y rises to nearly the same peak value (0.18% BWm) as the flexion-extension moment M_x (0.2%

BWm). Additionally, the joint contact force is not sinusoidal. It may affect the re-formation of a lubricating film during the swing phase when applying a sinus-load.

The resultant moment M_{res} shows a different time-course than the resultant force F_{res} (Figure 2A, B). Although the second force maximum is slightly lower than the first one, the moment is much higher at the instant of the second force peak. This is because friction continuously increases during the extension phase of walking (Figure 2C). The additional peak in the moment curve, shortly before TO, is caused by the sharp increase of the moments M_x and M_z when the hip begins to flex (see below). This finding stands in contrast to *in vitro* findings [18, 30], which are based on movements in only one plane. In these studies, the moment showed a plateau phase.

Micro-separation during the swing phase, as reported by others [31, 32], can alter the lubrication conditions in the joint. This effect was never observed in our subjects, investigated now and in the past. Otherwise fast changes in the directions of F_{res} or one of its components would have been observed.

Coefficient of friction

The coefficient μ increases by 46% from HS to the instant when the joint starts to flex (Figure 2C). Directly after the change of joint movement from extension to flexion, μ rose sharply in all subjects and reached its maximum at about TO, when the resultant force has markedly been fallen already. This effect has not been described previously in such detail.

It must be assumed that the synovia is squeezed out by the high forces during the extension. *In vitro* studies reported that μ increases when the sliding properties change from lubricated to dry [17, 21, 22, 35]. Furthermore numerical studies with hard/hard pairings have shown that the thickness of the fluid film changes in relation to the joint loading during the gait cycle [30, 34]. It was shown that the fluid film thickness decreases at the end of the swing phase, and therefore μ and wear rise, if the swing phase load is increased [30]. A higher swing phase load prevents or restrains the re-formation of the lubrication film, required for good lubrication during the subsequent stance phase. If this explanation also holds true for the investigated ceramic/polyethylene combination of head/cup, a higher swing phase load would let

μ decrease less sharply after TO and thus raise the level at which μ starts at the next HS.

Moreover, the strong increase of μ when the joint starts to flex could possibly be caused by a breakdown of the fluid film at the temporary stop of the relative joint movement, similar to the *in vitro* observation during the first step after a rest [33].

Another factor influencing the time pattern of μ may be a changing size of the load bearing area between head and cup, perpendicular to the resultant force vector. This could be especially true if μ were dependent on the pressure magnitude. Both factors could not be investigated in this study.

In contrast to previous *in vitro* studies, the *in vivo* coefficient of friction was now determined for the 3D case. The obtained pattern of μ differs from the pattern of μ_x in the main movement plane of the femur. Both coefficients are nearly identical from HS to CHS and deviate by no more than 5%. However, during the flexion phase, the difference between both coefficients increased up to 9% at TO.

Studies with a simple pendulum test determined values of μ_x between 0.04 and 0.09 for a lubricated regime [18,36,37]. This compares well with our finding of μ_1=0.04 and μ_2=0.06 during the extension phase. However, μ_{max} = 0.14 at the instant of toe off was much higher in our study.

The peak values of F_{res} individually varied by 39%, but the peak values of μ differed by 246% (Figure 3C). The variance of μ is most likely due to individually different lubrication properties of the synovia fluid.

Friction-induced power

The friction-induced temperature rise in ceramic/PE implants has been measured *in vivo* previously [10]. An estimated average friction-induced power of 0.79 W during walking was reported, which is much less than the average of 2.3 W determined in the current study. It may be that heat convection by the blood flow has been underestimated in the previous study. Other reasons for this discrepancy may be differences between the subjects investigated, and the small sizes of both cohorts. This assumption is supported by another result of the cited study, namely that the temperature increase, measured after 1 hour of walking, individually varied by a factor of nearly 3 after the body weight of all subjects had been standardized. A

similarly large factor of 2.7 was observed for the friction-induced power Q_{aver}, which decreased to 2.3 after normalizing the body weight.

The large individual differences of Q_{aver} are most likely caused by varying synovia properties, as already indicated by the variations of μ. Additionally, different running-in effects of the gliding partners may affect the friction-induced power. This running-in effect and the expected decrease of μ and Q_{aver} with increased postoperative time will be investigated in a future study.

In conclusion it was shown: The friction moment in the hip joint mainly occurred in the frontal and sagittal plane during walking. The resultant coefficient of friction increased nearly linearly during extension and increased drastically in the beginning of flexion with the maximum value approximately the ipsilateral toe off. This suggests that the synovia is squeezed out of the intra-articular joint space. Furthermore, the peak values of the coefficient of friction were always determined during the flexion phase. This indicates that the lubrication regime certainly changed into a dry phase at every step.

Limitations of the study

There are some limitations to this study: the number of investigated subjects was small; they were younger than the majority of hip-replacement patients; and only one implant type was investigated at only one speed of walking and one time after implantation. However, the large individual variations of friction coefficient and generated power, as well as the changes of the friction coefficient throughout the gait cycle will probably not be much influenced qualitatively by age or materials. The effects of walking speed and postoperative time is currently investigated an additional study.

Acknowledgements

The authors gratefully acknowledge the voluntary collaboration of all subjects.

References

1. CJRR (2013) CJRR annual report: Hip and knee replacements in Canada. Canadian Institute for Health Information.
2. Havelin LI, Fenstad AM, Salomonsson R, Mehnert F, Furnes O, et al. (2009) The Nordic Arthroplasty Register Association: a unique collaboration between 3 national hip arthroplasty registries with 280,201 THRs. Acta orthopaedica 80: 393–401. doi:10.3109/17453670903039544.
3. AOA (2007) Australian Orthopaedic Association National Joint Replacement Registry. Annual Report 2007.
4. Huch K, Müller KAC, Stürmer T, Brenner H, Puhl W, et al. (2005) Sports activities 5 years after total knee or hip arthroplasty: the Ulm Osteoarthritis Study. Annals of the Rheumatic Diseases 64: 1715–1720. doi:10.1136/ard.2004.033266.
5. Chatterji U, Ashworth MJ, Lewis PL, Dobson PJ (2004) Effect of total hip arthroplasty on recreational and sporting activity. ANZ journal of surgery 74: 446–449.
6. Flugsrud GB, Nordsletten L, Espehaug B, Havelin LI, Meyer HE (2007) The effect of middle-age body weight and physical activity on the risk of early revision hip arthroplasty. Acta Orthopaedica 78: 99–107. doi:10.1080/17453670610013493.
7. Malchau H, Herberts P, Söderman P, Odén A (2000) Prognosis of Total Hip Replacement. The swedish national hip arthroplasty registry.
8. Bergmann G, Deuretzbacher G, Heller M, Graichen F, Rohlmann A, et al. (2001) Hip contact forces and gait patterns from routine activities. Journal of biomechanics 34: 859–871.
9. Bergmann G, Graichen F, Rohlmann A (1993) Hip joint loading during walking and running, measured in two patients. Journal of biomechanics 26: 969–990.
10. Bergmann G, Graichen F, Rohlmann A, Verdonschot N, Van Lenthe GH (2001) Frictional heating of total hip implants. Part 2: finite element study. Journal of biomechanics 34: 429–435.
11. Bergmann G, Graichen F, Rohlmann A, Verdonschot N, Van Lenthe GH (2001) Frictional heating of total hip implants. Part 2: finite element study. Journal of biomechanics 34: 429–435.

12. Li S, Chien S, Branemark P-I (1999) Heat shock-induced necrosis and apoptosis in osteoblasts. Journal of orthopaedic research 17: 891–899. doi:10.1002/jor.1100170614.
13. Hall RM, Unsworth A (1997) Review Friction in hip prostheses. Biomaterials 18: 1017–1026.
14. Mattei L, Di Puccio F, Piccigallo B, Ciulli E (2011) Lubrication and wear modelling of artificial hip joints: A review. Tribology International 44: 532–549. doi:10.1016/j.triboint.2010.06.010.
15. Xiong D, Ge S (2001) Friction and wear properties of UHMWPE/Al2O3 ceramic under different lubricating conditions. 250: 242–245.
16. Bergmann G, Graichen F, Rohlmann A, Bender A, Heinlein B, et al. (2010) Realistic loads for testing hip implants. Bio-medical materials and engineering 20: 65–75. doi:10.3233/BME-2010-0616.
17. Bishop NE, Hothan A, Morlock MM (2012) High Friction Moments in Large Hard-on-Hard Hip Replacement Bearings in Conditions of Poor Lubrication. Journal of Orthopaedic Research: 1–7. doi:10.1002/jor.22255.
18. Brockett C, Williams S, Jin Z, Isaac G, Fisher J (2006) Friction of Total Hip Replacements With Different Bearings and Loading Conditions. Journal of Biomedical Materials Research: 508–515. doi:10.1002/jbmb.
19. Scholes SC, Unsworth A, Goldsmith AAJ (2000) A frictional study of total hip joint replacements. Physics in medicine and biology 45: 3721–3735.
20. Scholes SC, Unsworth A, Hall RM, Scott R (2000) The effects of material combination and lubricant on the friction of total hip prostheses. Wear 241: 209–213. doi:10.1016/S0043-1648(00)00377-X.
21. Unsworth A (1978) The effects of lubrication in hip joint prostheses. Physics in medicine and biology 23: 253–268.
22. Scholes SC, Unsworth A (2000) Comparison of friction and lubrication of different hip prostheses. Proceedings of the Institution of Mechanical Engineers Part H Journal of engineering in medicine 214: 49–57.
23. Damm P, Graichen F, Rohlmann, Bender A, Bergmann G (2010) Total hip joint prosthesis for in vivo measurement of forces and moments. Medical Engineering & Physics 32: 95–100.
24. Graichen F, Arnold R, Rohlmann, Bergmann G (2007) Implantable 9-channel telemetry system for in vivo load measurements with orthopedic implants. IEEE

transactions on bio-medical engineering 54: 253–261. doi:10.1109/TBME.2006.886857.

25. Graichen F, Bergmann G, Rohlmann (1994) Telemetric transmission system for in vivo measurement of the stress load of an internal spinal fixator. Biomedizinische Technik Biomedical engineering 39: 251–258.
26. Bergmann G, Graichen F, Rohlmann A, Westerhoff P, Heinlein B, et al. (2008) Design and calibration of load sensing orthopaedic implants. Journal of biomechanical engineering 130: 021009. doi:10.1115/1.2898831.
27. Wu G, Siegler S, Allard P, Kirtley C, Leardini A, et al. (2002) ISB recommendation on definitions of joint coordinate system of various joints for the reporting of human motion - part I: ankle, hip, and spine. Journal of Biomechanics 35: 543–548. doi:10.1016/j.pathophys.2011.08.001.
28. Bender A, Bergmann G (2011) Determination of Typical Patterns from Strongly Varying Signals. Computer Methods in Biomechanics and Biomedical Engineering iFirst: 1–9. doi:10.1080/10255842.2011.560841.
29. Saikko V (1992) A simulator study of friction in total replacement hip joints. Proceedings of the Institution of Mechanical Engineers Part H Journal of engineering in medicine 206: 201–211.
30. Williams S, Jalali-Vahid D, Brockett C, Jin Z, Stone MH, et al. (2006) Effect of swing phase load on metal-on-metal hip lubrication, friction and wear. Journal of biomechanics 39: 2274–2281. doi:10.1016/j.jbiomech.2005.07.011.
31. Blumenfeld TJ, Glaser DA, Bargar WL, Langston GD, Mahfouz MR, et al. (2011) In vivo assessment of total hip femoral head seperation from the acetabular cup during 4 common daily activities. Orthopedics 34: e127–e132. doi:10.3928/014774477-20110427-06.
32. Dennis D a, Komistek RD, Northcut EJ, Ochoa J a, Ritchie A (2001) In vivo determination of hip joint separation and the forces generated due to impact loading conditions. Journal of biomechanics 34: 623–629.
33. Morlock M, Nassutt R, Wimmer M, Schneider E (2000) Influence of Resting Periods on Friction in Artificial Hip Joint Articulations. Bone: 6–16.
34. Meyer DM, Tichy JA (2003) 3-D Model of a Total Hip Replacement In Vivo Providing Hydrodynamic Pressure and Film Thickness for Walking and Bicycling. Journal of Biomechanical Engineering 125: 777. doi:10.1115/1.1631585.

35. Hall RM, Unsworth A, Wroblewski BM, Siney P, Powell NJ (1997) The friction of explanted hip prostheses. British journal of rheumatology 36: 20–26.
36. Hall RM, Unsworth A (1997) Friction in hip prostheses. Biomaterials 18: 1017–1026.
37. Jin Z, Stone M, Ingham E, Fisher J (2006) (v) Biotribology. Current Orthopaedics 20: 32–40. doi:10.1016/j.cuor.2005.09.005.

Published in: PLoS ONE 8(10): e77807.

DOI:10.1371/journal.pone.0077807

7. *In vivo* hip joint loading during post-operative physiotherapeutic exercises

V. Schwachmeyer, P. Damm, A. Bender, J. Dymke, F. Graichen, G. Bergmann

Abstract

Introduction

After hip surgery, it is the orthopedist's decision to allow full weight bearing to prevent complications or to prescribe partial weight bearing for bone ingrowth or fracture consolidation. While most loading conditions in the hip joint during activities of daily living are known, it remains unclear how demanding physiotherapeutic exercises are. Recommendations for clinical rehabilitation have been established, but these guidelines vary and have not been scientifically confirmed. The aim of this study was to provide a basis for practical recommendations by determining the hip joint contact forces and moments that act during physiotherapeutic activities.

Methods: Joint contact loads were telemetrically measured in 6 patients using instrumented hip endoprostheses. The resultant hip contact force, the torque around the implant stem, and the bending moment in the neck were determined for 13 common physiotherapeutic exercises, classified as weight bearing, isometric, long lever arm, or dynamic exercises, and compared to the loads during walking.

Results: With peak values up to 441%BW, weight bearing exercises caused the highest forces among all exercises; in some patients they exceeded those during walking. During voluntary isometric contractions, the peak loads ranged widely and potentially reached high levels, depending on the intensity of the contraction. Long lever arms and dynamic exercises caused loads that were distributed around 50% of those during walking.

Conclusion: Weight bearing exercises should be avoided or handled cautiously within the early post-operative period. The hip joint loads during isometric exercises depend strongly on the contraction intensity. Nonetheless, most physiotherapeutic exercises seem to be non-hazardous when considering the load magnitudes, even though the

loads were much higher than expected. When deciding between partial and full weight bearing, physicians should consider the loads relative to those caused by activities of daily living.

Introduction

After hip surgery, such as total hip arthroplasty (THA), osteotomies or osteosynthesis of proximal femoral fractures, physiotherapy and mobilization usually begin on the first post-operative day. Early mobilization leads to faster recovery and reduces complications due to bed rest, such as thrombosis or pneumonia [1,2]. Concurrently, many elderly patients are unable to walk with partial weight bearing due to insufficient arm strength or poor body control [3,4]; therefore, many surgeons allow early full weight bearing.

The question has been addressed if immediate full weight bearing is detrimental for bone ingrowth in THA surfaces. When uncemented implant stems lack primary stability, micromotions at the bone-stem-interface may occur with high loads [5] and impair long-term fixation. Studies demonstrated that bone ingrowth into porous surfaces decreases with increasing micromotion: the larger the motion between the bone and the implant, the more the implant fixation is dominated by fibrous tissues instead of cancellous bone [6,7]. As a result, on one hand, a lack of primary stability requires partial weight bearing for up to 12 weeks to ensure proper bone ingrowth. On the other hand, implant design, coating materials and implantation techniques have substantially improved over the last decades, increasing the primary stability of uncemented stems [8–11], thus indicating that partial weight bearing is not essential for bone ingrowth. Due to the controversial arguments, there is no consensus among orthopedic surgeons whether to allow early full weight bearing, and recommendations vary in clinical practice from immediate unrestricted weight bearing to partial or even toe-touch weight bearing for several weeks [4,12–14].

For osteotomies or surgically stabilized femoral neck fractures, primary stability of the osteosynthesis is decisive for fracture consolidation. Depending on the location and complexity of the fracture, shear and bending forces or moments may delay or even hinder bone union [15,16]. For inter- and pertrochanteric femoral fractures, failure rates of 10 and 40% have been reported [17]. The aim of any surgical intervention is therefore to provide a stable fixation to allow full weight bearing during activities of

daily living. In some cases, this cannot be achieved or the weight bearing capacity of the fixation is questionable.

However, avoiding high loads at the fracture site or bone-stem-interface throughout the first post-operative weeks appears to be beneficial for optimal bone healing. A justified classification for ‘high’ or ‘low’ load levels depends on the investigated implant, the fracture situation, the disease, and several other factors; therefore it cannot be generalized. However, it is impossible to provide *general* exact thresholds for forces or moments which are detrimental for osteoarthritis or the outcome of surgical interventions. Most studies that tested the primary stability of implants used force magnitudes based on Bergmann’s findings [18,19]. As the primary stability depends on several factors, the tolerable load levels would have to be individually defined. Here, high loads are considered those that overload the surrounding musculoskeletal structures and thereby result in possible damage. Particularly during the most frequent activities of daily living (ADL), which include walking, standing and going up or down stairs, cyclic or permanent high loads may be detrimental. Previous *in vivo* investigations have measured peak hip contact forces of approximately 250% of the patient’s bodyweight (BW) during level walking and torsional moments of 1.6%BWm around the implant axis [18]. During stumbling, forces of nearly 900%BW were measured [20]. Whereas the loading conditions during most ADL are known, it remains unclear how demanding physiotherapeutic exercises are. Only one study investigated the hip contact forces during physiotherapy [21], which were measured telemetrically using an instrumented joint implant. The data were collected in only one patient and the loading situations were not precisely defined.

The aim of this study was to augment this knowledge by systematically measuring the hip contact loads during physiotherapeutic exercises *in vivo* in a cohort of 6 patients. This study focuses on the resultant joint contact force, the bending moments in the femoral neck and the torque around the implant stem axis, as these are the three most important mechanical factors for THA, osteotomies, femoral neck fractures, and coxarthrosis [19].

Materials and Methods

Subjects

Six patients (5 male, 1 female, mean age 58±7 years, body mass 86±6 kg, height 174±5 cm) with instrumented hip endoprostheses were investigated. In every patient, advanced hip osteoarthritis was confirmed and indications for total hip replacement were given. The study was approved by the Charité Ethics committee under the registry number EA2/057/09 and registered with the 'German Clinical Trials Register' (DRKS00000563). All patients gave written informed consent prior to participating in this study.

Physiotherapeutic exercises

Prior to the evaluations conducted for this study, we repeatedly measured peak forces during the exercises within the first post-operative year to investigate possible changes over time. Such changes were not observed, as shown by sample measurements provided in the data base www.OrthoLoad.com. Therefore, we present data from time points when the patients were able to perform the exercises without pain. Subject #4 reported pain in the contralateral hip during exercise #4; it was therefore excluded from the analysis for this patient. The finally selected and evaluated measurements were taken between the 5^{th} and 12^{th} post-operative month, except from exercise #11 with data taken from the 4^{th} postoperative week.

All patients followed an investigation protocol that included 13 common physiotherapeutic exercises (Table 1) which were performed on a therapy table. The selection included weight bearing exercises with closed kinetic chains (exercises #1-#4), isometric exercises in which the patient was instructed to actively contract his/her muscles (#5 - #7), exercises with the force acting at a long lever arm (#8, #9), and simple dynamic exercises in the supine position (#10 - #13). Instructions were given by an experienced physiotherapist who also ensured that all exercises were performed correctly without compensational movements that could influence the acting loads.

Every patient repeated the physiotherapeutic exercises 8 times. The first and last repetitions were excluded from the evaluation; the first one because verbal instructions slowed the movement down and the last one because the patients

tended to perform it faster. As a result, 6 repetitions were included in the analysis. Each subject additionally walked 5 times along a 10 m walkway on level ground and the data from 10 walking cycles were analyzed.

Table 1: *Description of 13 physiotherapeutic exercises*

Number	Exercise	Description
1	Lifting pelvis (Bridging) maximally	Supine position: knees flexed, feet standing on therapy table, arms at rest on table surface beside trunk. Pelvis lifted maximally.
2	Lifting pelvis (Bridging) slightly	Supine position: knees flexed, feet standing on therapy table, arms at rest on table surface beside trunk. Pelvis lifted slightly.
3	Lifting pelvis (Bridging) one legged standing on ipsilateral leg	Supine position: knees flexed, feet standing on therapy table, arms rest on table surface beside trunk. Pelvis and the contralateral leg lifted.
4	Lifting pelvis (Bridging) one legged standing on contralateral leg	Supine position: knees flexed, feet standing on therapy table, arms rest on table surface beside trunk. Pelvis and the ipsilateral leg lifted.
5	Isometric contraction; flexed knees	Supine position: feet standing on surface. Dorsiflexion, heels push into surface, gluteus maximus contracted, pelvis tilted posteriorly.
6	Isometric contraction; straight knees	Supine position: dorsiflexion, knee hollows push onto the therapy table surface (active knee extension), gluteus maximus contracted.
7	Isometric hip abduction	Supine position: Straight leg, patient pushes isometrically against external force transducer as strong as possible without pain.
8	Hip abduction with straight knee	Lateral position: hip abduction with dorsiflexion, extended knee, slight hip internal rotation. Strict supervision to prevent abdominal musculature, hip flexors or quadratus lumborum muscle being used for compensating possible weakness of abductor muscles.
9	Hip flexion with straight knee	Supine position: straight leg, hip flexed to about 30° and held for 4 seconds.
10	Dynamic hip abduction	Supine position: leg abducted and adducted dynamically back to original position while heel drags over surface, limb is only slightly lifted.
11	Hip and knee flexion/extension; heel on bench	Supine position: hip and knee flexed, heel drags over surface, limb is not lifted entirely.
12	Pelvis tilt	Supine position: feet standing on surface, pelvis tilted anteriorly (Hyperlordosis).
13	Pelvis tilt	Supine position: feet standing on surface, pelvis tilted posteriorly (Hypolordosis).

Instrumented implants

The *in vivo* forces and moments were measured using instrumented hip implants with an inductive power supply and telemetric data transmission. Clinically proven, standard implants (type CTW, Merete Medical GmbH, Berlin, Germany) with a titanium stem and 32-mm Al_2O_3 ceramic head were equipped with 6 internal strain gauges to measure the deformations in the implant neck. By applying complex calibration loads and procedures, 3 force and 3 moment components were calculated from the deformations with an accuracy of 1-2%. All forces and moments were normalized to the patient's body weight and are reported as %BW and %BM*m, respectively. The data from implants on the left side were mirrored to the right side. Further details have been described previously [22].

Coordinate systems

The forces and moments were measured in the implant system x', y', z', centered in the middle of the head (Figure 1). The plane x'/z' is formed by the implant neck and the long axis of the femur. The force component $F_{x'}$ acts laterally, $F_{y'}$ anteriorly, and $-F_{z'}$ distally along the femur axis. F_{res} is the resultant force, consisting of all 3 components. The moment components $M_{x'}$, $M_{y'}$, and $M_{z'}$ turn right around the x', y', and z' axes.

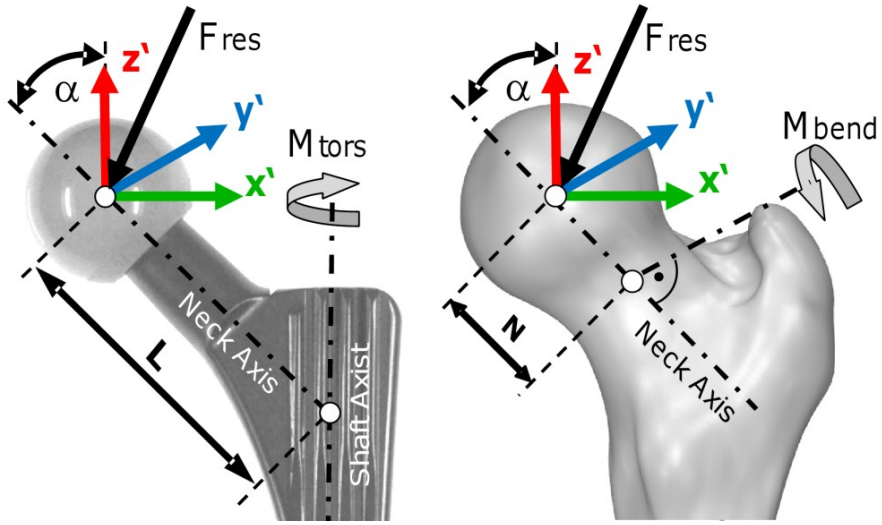

Figure 1: *Resultant force, torsional moment around the implant stem and bending moment in the femoral neck; View from posterior. The torsional moment M_{tors} rotates the implant backwards around its stem axis. The bending moment M_{bend} acts in the middle of the femoral neck. α = CCD angle.*

Evaluated loads

Three types of loads were evaluated (Figure 1):

1. The resultant contact force F_{res} consists of its 3 components:

$$F_{res} = \sqrt{(F_{x'}{}^2 + F_{y'}{}^2 + F_{z'}{}^2)} \qquad \text{(Equ. 1)}$$

2. The torsional moment M_{tors} acts around the implant's stem axis and rotates the implant inwards when positive. With α = 45° being the angle between the implant's stem and neck axes, and L being the length of the implant neck, given by the distance between the center of the implant head and the point of intersection of the neck axis and the implant shaft axis, M_{tors} is calculated by the following equation:

$$M_{tors} = M_{z'} - F_{y'} \cdot L \cdot \sin\alpha \qquad \text{(Equ. 2)}$$

3. The bending moment M_{bend} acts in the middle of the femoral neck, perpendicular to the neck axis:

$$M_{bend} = \sqrt{M_{bend1}{}^2 + M_{bend2}{}^2} \qquad \text{(Equ. 3)}$$

with $M_{bend1} = M_{x'} \cdot \cos\alpha + M_{z'} \cdot \sin\alpha - F_{y'} \cdot N$

$$M_{bend2} = F_{x'} \cdot |N\cos\alpha| + F_{z'} \cdot |N \cdot sin\alpha| + M_{y'}$$

N is the distance between the head center and the middle of the femoral neck and equals L/2. The direction of M_{bend} is not reported here.

Analysis of time-load patterns

The time-load patterns of F_{res}, M_{tors} and M_{bend} were averaged throughout the entire exercise. A dynamic time warping algorithm [23] was used to deform the time scales of the 6 repetitions, so that the summed squared errors between the 6 F_{res} patterns became a minimum. These time-deformed forces were then averaged arithmetically and delivered the 'patient-specific' time course of F_{res} for this exercise. The 'patient-specific' curves from all 6 patients were averaged again, using the same algorithms, which finally delivered the 'activity-specific' time pattern of F_{res}. The time deformations obtained when averaging F_{res} were then applied to the M_{tors} and M_{bend} patterns before averaging their time patterns, too.

Analysis of load maxima

The absolute maxima of F_{res}, M_{tors} and M_{bend}, acting within each single trial, were determined for the 6 repetitions of each of the 6 patients, resulting in 36 peak values for every exercise (30 for #4). An exploratory data analysis was performed on the 3 load maxima and depicted as box plots in Figure 2. The same procedure was performed for the 10 walking cycles of each patient.

For defining high and low loads and enabling an interpretation of the measured data, we used the peak load values during walking as references. The median peaks of F_{res}, M_{tors} and M_{bend} during walking with full weight bearing were set to 100% and exercise loads higher than these limits were classified to be 'high'. Loads were named 'medium' if their peak values lay between 50% and 100% of these limits, and 'low' if they were lower than 50%. These classifications are based on clinical considerations: If a surgeon allows the patient to walk without support, physiotherapeutic exercised causing medium and even high loads should also be tolerated. If only walking with half body weight is permitted, physiotherapeutic exercises which cause medium or even high loads should consequently be avoided.

Separately for each exercise, the individual median peak values of F_{res}, M_{tors} and M_{bend} were compared to the 100% and 50% levels of the *same* subject, using a Student's-*t*-Test for unpaired samples with a significance level of $p = 0.05$. The numbers of patients having high and medium loads were indicated in Figure 2.

Analysis of load dependency on muscular strength

Due to observations from previous measurements and theoretical considerations, we expected that the patient's muscular strength influences the maximum loads during the exercises, assuming that strong patients would produce high loads during isometric exercises (#5, 6, and 7). When exercising against gravity (e.g. #8, 9), however, the loads were expected to remain at the lowest possible limits, determined by the patient's anthropometric data as segment masses and lever arms of masses and muscles.

Patients were grouped into those being physically active or passive. The 'active' group consisted of patients 1, 3, and 5, who frequently practiced sports like biking, hiking, or swimming. Patients 2, 4, and 6, who didn't practice any sports, were

assigned to the ‘passive’ group. The forces during exercises # 5, 6, 7, 8, and 9 were analyzed and compared between groups using a Student’s-*t*-test to test the assumptions.

Results

Time-load patterns

Figure 3 shows the activity-specific time-load patterns for each exercise. The pattern of level walking showed two peaks for F_{res}, M_{tors}, as well as M_{bend}: the first peaks were F_{res} = 263%BW, M_{tors} = 2.2%BWm, and M_{bend} = 3.9%BWm on average. The second peaks were lower with F_{res} = 242%BW, M_{tors} = 0.8%BWm and M_{bend} = 3.7%BWm. The average loads during the two-legged stance were F_{res} = 93%BW, M_{tors} = 0.2%BWm, and M_{bend} = 1.3%BWm.

Throughout all activities, the time-load patterns of M_{bend} closely resembled those of F_{res}. The same was found for M_{tors} with the exception of exercises #1 (lifting pelvis maximally), #2 (lifting pelvis slightly), #8 (hip abduction lateral position), and #13 (tilting the pelvis posteriorly), in which the activity-specific M_{tors} moment remained close to zero.

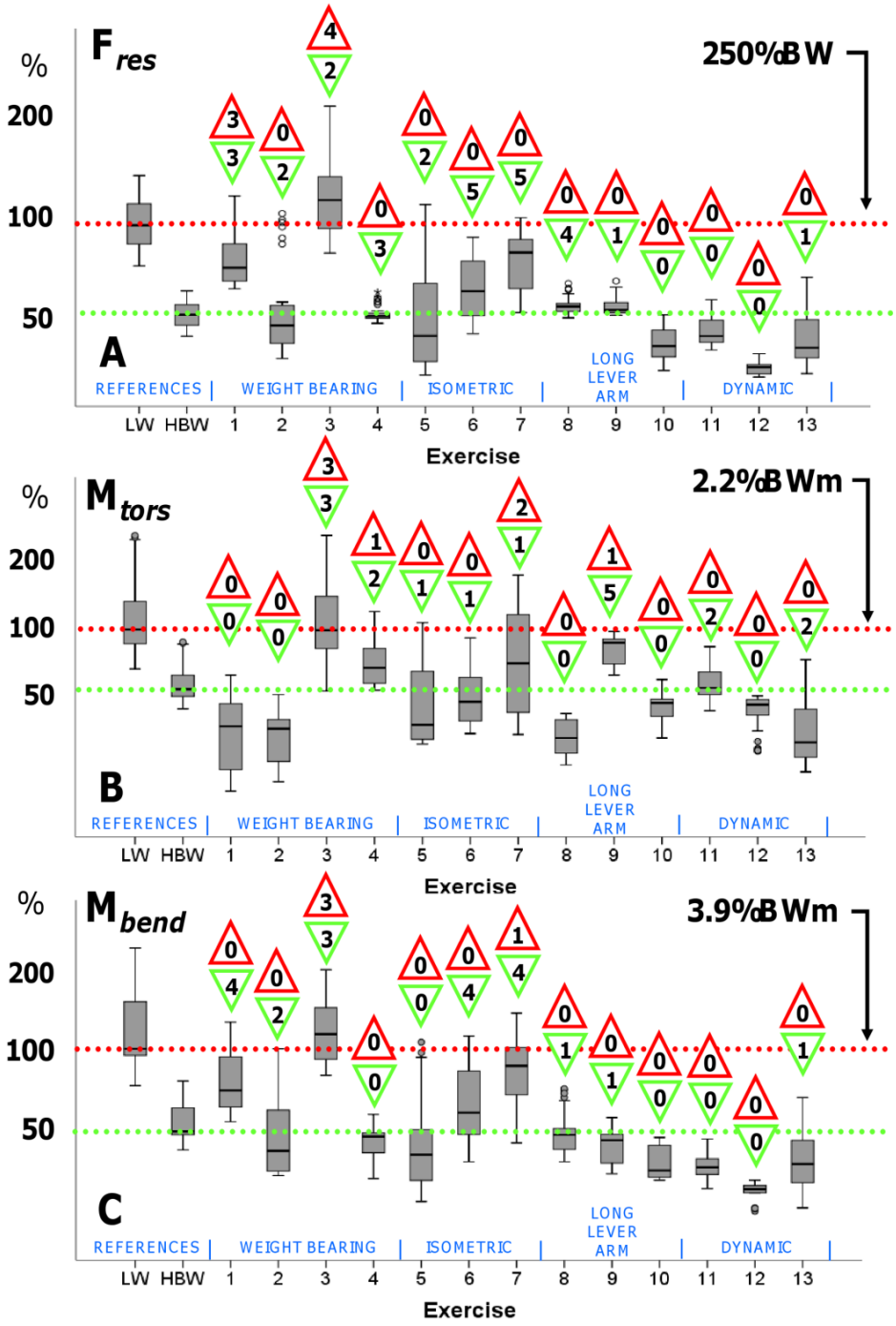

Figure 2: *Median peak loads; Median Peak values of F_{res} (A), M_{tors} (B), and M_{bend} (C) and their ranges for the reference activities Level Walking (LW) with full (=100%) and half (=50%) weight bearing as well as the 13 physiotherapeutic exercises. Horizontal lines mark the activity-specific median peak value from walking. See Table 1 for exercise numbers descriptions. Walking at 100% level (with full weight bearing) and 50% level serve as reference for comparison. The numbers in the upper triangles indicate the number of patients having high loads, the number in the triangles below indicate the number of patient, in which medium loads were found.*

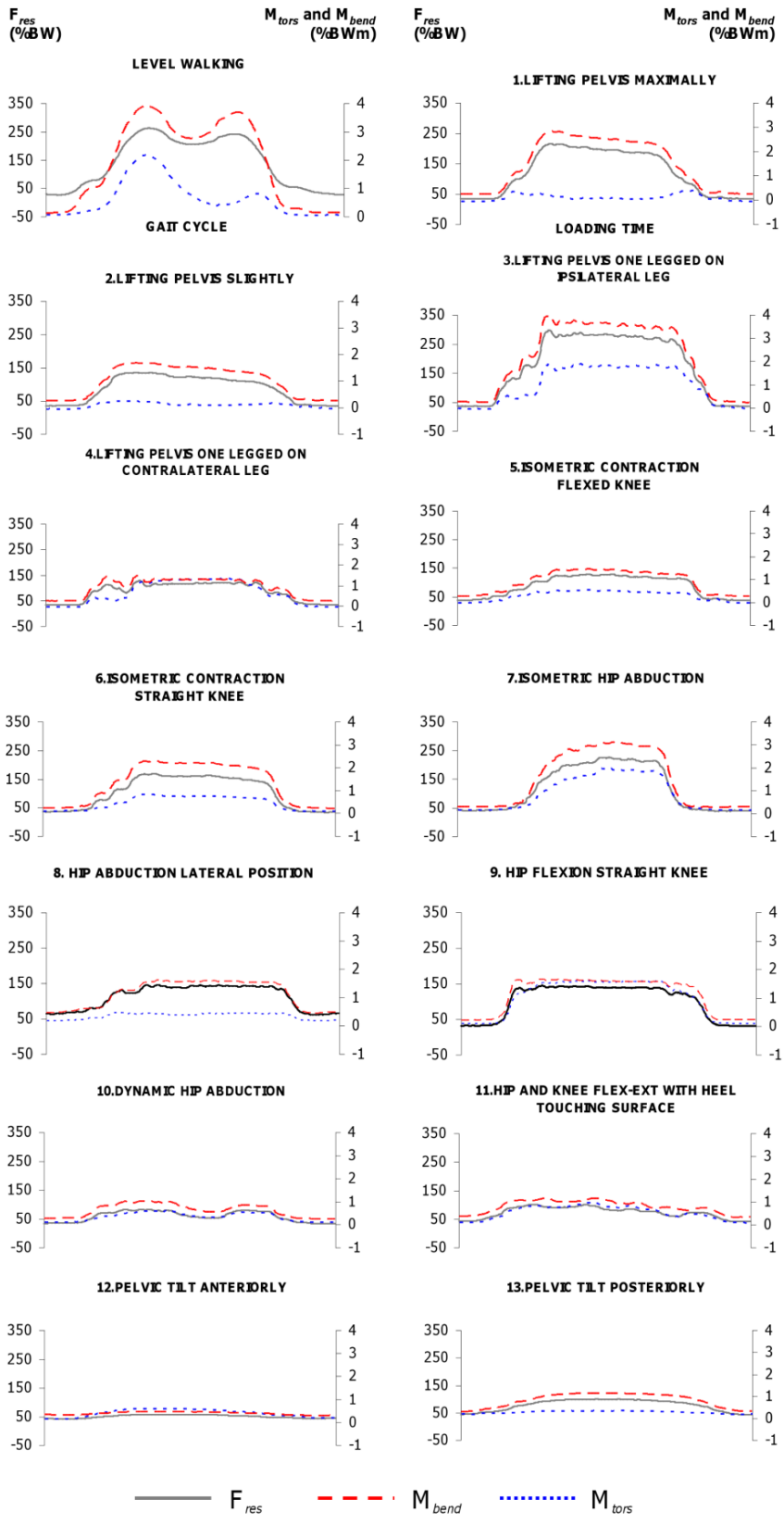

Figure 3: *Hip joint loading during reference activities and exercises 1 – 13; Resultant contact force F_{res} (black line, left axis), torque M_{tors} around implant shaft (dotted blue line, right axis) and bending moment M_{bend} in femoral neck (dashed red line, right axis). The x-axis indicates the loading time.*

Load maxima

Figures 2A - C depict the numerically determined medians and ranges of the peak values for F_{res}, M_{tors} and M_{bend}, obtained from the 36 trials (30 for exercise #4) of all subjects. Level walking at 100% (full weight bearing) and 50% (half body weight = partial weight bearing) served as individual references. The *median* 50% levels of all 3 evaluated loads *from all subjects* were with 130%BW lightly higher than the median levels during a one-legged stance (approximately 100%BW). The numbers in the upper triangles indicate the number of subjects for which an exercise caused *individual* median peak loads which were significantly higher than the *individual* median peak loads during walking ('high loads'). The lower triangles indicate the number of patients whose loads were significantly higher than the individual 50% levels but lower than the 100% levels and therefore graded as 'medium' loads.

Resultant force F_{res}: The median peak value of F_{res} during walking, i.e. the 100% level, was 266%BW. The weight bearing exercise #3 (one-legged bridging, standing on the operated leg) was the only exercise for which the median peak force *of all subjects* exceeded 100%, i. e. the reference during walking (median 303 %BW, range 225-441 %BW). Although the median peaks of exercises #1, #5, #6, and #7 (weight bearing or isometric exercises) were lower than during walking, the 99th percentiles exceeded the 100% level or came close to it. Only during exercise #1 did 3 patients have high loads. In the remaining exercises, the 99^{th} percentiles were lower than the 1^{st} percentile for level walking and in none of the patients high forces were found.

Torsional moment M_{tors}: The median peak value during walking was 2.2%BWm. Similarly to the observations for the force, the median peak torque during weight bearing exercise #3 was close to 100% (2.0 %BWm, 1.0 to 3.6 %BWm). In three of the subjects, high moments were found. The 99^{th} percentiles of exercises #4, #5, and #7 (weight bearing or isometric exercises) exceeded the 100% level. During exercise #4, one patient had high values of M_{tors} and 2 patients during exercise #7. The 99^{th} percentiles of exercises #6, #9, #11, and #13 did not reach 100%, but approached it closely, with one patient having high values. For exercises #1, 2, 8, and 13, the peak values ranged from negative values of -0.7%BWm to positive 1.5%BWm, i.e., the medians were distributed around zero.

Bending moment M_{bend}: The median peak value during walking was 3.9%BWm. As for force and torque, exercise #3 also caused the highest bending moment of all the exercises. The median was higher than 100% (4.0 BWm , 3.2 to 5.4 %BWm). Three of the patients had high values of M_{bend}. During other weight bearing and isometric exercises (#1, #2, #5, #6, and #7), the 99th percentiles exceeded the reference value; 1 subject had high values. During the exercises #4, #8, #9, #10#, #11, #12, and #13, the 99th percentiles remained below 100%.

Load dependency on muscular strength

From the isometric exercises, #7 revealed a statistically significant difference between the active and the passive group (#7: active 241%BW, passive 180%BW, $p < 0.01$). During exercise #5 and #6, the median peak forces showed small differences (#5: active 120%BW, passive 144%BW, $p = 0.35$; #6: active 177%BW, passive 171%BW, $p = 0.69$), but no trend towards higher loads in the active group. For the exercises with long lever arms, a significant difference between groups was observed when flexing the hip in supine position by raising the leg (#9: active 140%BW, passive 154%BW, $p < 0.01$) but abducting the leg in lateral position did not show any notable differences (#8: active 146%BW, passive 149%BW, $p = 0.51$).

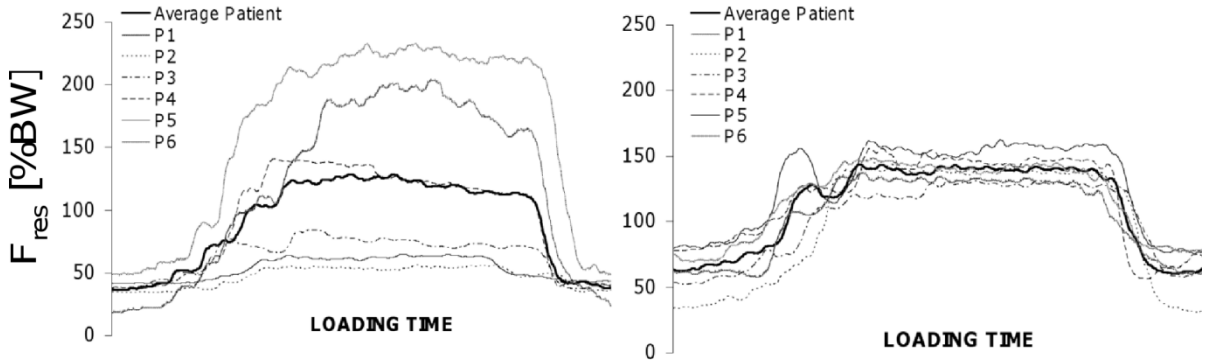

Figure 4: *Patient- and activity-specific time courses of resultant force F_{res}; Left: Exercise #5 = isometric contraction with flexed knees. Right: Exercise #7 = hip abduction in lateral position. Data from 6 patients. The curves of the isometric contraction reveal a broad scattering of the peak values, ranging from 56 to 232%BW. This range is due to different voluntary muscular contraction intensities and depends strongly upon the patient's motivation and the instructions given by the physiotherapist. When abducting the straight leg in the lateral position, peak loads*

range only slightly between 130 and 162%BW. This is a result of biomechanical factors such as similar leg lengths, segment masses and lever arms of the gluteal musculature.

Discussion

This study addressed the question of how demanding post-operative physiotherapeutic hip exercises are by determining the acting hip joint forces and moments with instrumented implants.

After hip surgery, physiotherapy is important to mobilize the patient and restore his function. The physiotherapist's aim is thereby to increase muscle strength, improve joint mobility and train activities, enabling the patient to live as independently as possible. To ensure optimal initial bone ingrowth around the implant, load-dependent micromotions at the bone-stem-interface must be minimized as they may otherwise prevent implant stabilization and cause loosening. Similarly, high loads acting at fracture implants may cause non-union or pseudarthrosis. Orthopedic surgeons are confronted with the conflict between permitting unrestricted weight bearing for fast recovery and avoiding high mechanical loading that may cause complications and hinder fracture consolidation. Additionally, walking with partial weight bearing or only floor contact requires a considerable amount of muscle strength in the upper extremities and trunk, so it is hardly achievable for many elderly patients [3,4]. These may be reasons why rehabilitation protocols vary between clinics. One study found large diversity in rehabilitation protocols [12]: out of 53 surveyed surgeons, 38 allowed full weight bearing for uncemented implants, yet 10 prescribed partial weight bearing with half body weight and 3 allowed only toe-touch weight bearing. Only 9 surgeons reported that their protocols were evidenced-based, but no detailed information was provided.

Among all exercises, the highest median peak loads were observed for the Lifting Pelvis weight bearing exercises (#1-4). When Lifting Pelvis was performed with support only by the operated leg (#3), the median peak forces and moments exceeded 100%, i.e. the values during walking, in 3 to 4 patients. In one trial, F_{res} rose up to even 441%BW equaling 166% of walking with full weight bearing. When the pelvis was lifted only slightly (#2), the median peak of F_{res} reached 82% and were therefore in the medium range. Some physicians disapprove Lifting Pelvis as a bed

exercise in the early post-operative period, but it should be taken into account that the same activity is necessary when using a bedpan. Fleischhauer (2006) recommends exercise #4 (Lifting Pelvis standing only on the contralateral leg while the operated leg is lifted with extended knee) to be practiced directly after pelvic osteotomies [24] because it is commonly believed that a non-weight bearing joint is unloaded. In our study, this exercise caused a medium hip contact force above 50%. The torsional moment reached values close to 100% in some trials. Such load levels in a non-weight bearing joint can be explained by co-contraction of the muscles crossing the hip joint as any muscular co-contraction unavoidably increases the joint contact force.

The force-increasing effect of co-contractions can also be observed during isometric exercises. Fundamental biomechanical reasons suggest that the theoretically achievable ultimate levels depend on the intensity of the muscle contraction and therefore on the muscle strength. We did not find notable differences between active and passive patients. The assignment to the two cohorts was based on subjective observations, however, and the maximum voluntary muscle strength had not been quantified. Nevertheless, our data suggest that the contraction intensity depends on multiple factors such as the patient's motivation and/or the instructions given by the physiotherapist rather than the maximum strength. Still, according to our observations, high intensive contractions may lead to high joint loads during isometric exercises. If fractures with uncertain stability prohibit high loads at the fracture site, the physiotherapist should therefore avoid high intensity muscle contractions by checking the contraction by palpation and controlling it by verbal instructions.

In contrast to the widely varying forces during isometric co-contractions, the loads when exercising against gravity can be predicted relatively precisely from our data (Figure 4). The individual forces during flexion or abduction of the straight leg, for example, remained in a close range between 49 and 68%BW for #8 and 50 and 69%BW for #9. The individual bending moments were also similar during flexion and abduction. The torsional moment, however, was 7-times higher during flexion than during abduction. This is due to the high anteroposterior force component $F_{y'}$ when flexing the hip joint. During exercises #1, #2, #8, and #13 M_{tors} was distributed around zero when the data from all subjects were averaged, which was a result of individually different signs of $F_{y'}$ and therefore of M_{tors}. These varying force directions may be a result of different hip joint anatomy, particularly the implant anteversion.

When the pelvis was tilted anteriorly and posteriorly (#12 & 13), M_{tors} even changed its sign within the movement in 4 patients, a factor that may increase the risk of delayed bone formation at the implant's interface.

Dynamic exercises with an open kinetic chain (non-weight bearing conditions) and short lever arms (#10-13) caused low peak forces of approximately 38%, torque between 23% and 45% and bending moments between 13% and 26%. These are values classified as low, but even much lower loads had been expected, because the moved body parts were supported by the therapy table and had therefore not to be lifted against gravity. This again demonstrates the decisive impact of the muscles on the internal loads.

It remains unclear whether the load magnitudes during walking (= 100%) are the critical upper loading limits. Furthermore, the primary stability varies from case to case and was not focus of this study so that statements about primary stability cannot be given. However, orthopedic surgeons should take the following into account when deciding on partial (or even toe-touch) weight bearing: unavoidable activities such as using a bed pan and even some bed exercises cause medium to high loads. If reduced weight bearing is nevertheless demanded by the surgeon, the physiotherapeutic exercises shown here to produce medium or high loads should consequently be omitted from physiotherapeutic treatment. Vice versa, the patient should be allowed to walk with full weight bearing if these exercises are thought to be tolerable. As muscle strengthening is a major aim of physiotherapeutic treatment and necessary for recovery, it should be discussed whether strengthening exercises with intensive muscle contraction shall be avoided.

This study has some limitations. We investigated only 6 subjects so that reliable and generally representative conclusions are difficult to be drawn. Additionally, the assignment to the active and passive group was only based on the sports activities reported by the patients. The muscular strength had not been quantified.

Furthermore, position changes between the single physiotherapeutic exercises could possibly lead to high loads. We did not evaluate these movements but instead collected the exercise data in a systematic manner for best averaging accuracy and intra-individual comparison. This method enabled us to note tendencies and provide unique data that have not been previously obtained. The findings of this study give important scientific information about *in vivo* loading during physiotherapeutic

exercises and will support orthopedic surgeons, therapists and patients in their decision making and help to develop effective and individual rehabilitation protocols.

Conclusions

Weight bearing activities caused the highest loads among all exercises. Movements against resistance or loads acting at long lever arms seem to be non-hazardous regarding the force magnitudes, but may cause high torsional moments. The forces during isometric contractions depend on the contraction intensity which is rather influenced by the motivation than by the maximal muscle strength. Generally, the joint contact forces are increased by muscle co-contractions, which press the joint partners against each other, an effect that is observed when exercising the contralateral limb while the ipsilateral limb is passive. When deciding between partial and full weight bearing, physicians should consider the loads relative to those observed during walking.

Acknowledgements

The authors would like to thank Prof. Dr. Andreas M. Halder and Dr. Alexander Beier from the Hellmuth-Ulrici-Klinik Sommerfeld and the patients for their engaged cooperation.

References

1. Kamel HK, Iqbal MA, Mogallapu R, Maas D, Hoffmann RG (2003) Time to Ambulation After Hip Fracture Surgery: Relation to Hospitalization Outcomes. The Journals of Gerontology Series A: Biological Sciences and Medical Sciences 58: M1042–M1045.
2. Oldmeadow LB, Edwards ER, Kimmel LA, Kipen E, Robertson VJ, et al. (2006) No rest for the wounded: early ambulation after hip surgery accelerates recovery. ANZ Journal of Surgery 76: 607–611.
3. Vasarhelyi A, Baumert T, Fritsch C, Hopfenmüller W, Gradl G, et al. (2006) Partial weight bearing after surgery for fractures of the lower extremity--is it achievable? Gait & Posture 23: 99–105.
4. Jöllenbeck T (2005) Die Teilbelastung nach Knie- und Hüft-Totalendoprothesen: Unmöglichkeit ihrer Einhaltung, ihre Ursachen und Abhilfen. Z Orthop Ihre Grenzgeb 143: 124–128.
5. Burke DW, O'Connor DO, Zalenski EB, Jasty M, Harris WH (1991) Micromotion of cemented and uncemented femoral components. The Journal of Bone and Joint Surgery British Volume 73: 33–37.
6. Piliar R (1986) Observation on the Effect of Movement on Bone Ingrowth into Porous-Surfaced Implants. Clin Orthop Relat Res 208: 108–113.
7. Bragdon CR, Burke D, Lowenstein JD, Connor DOO, Ramamurti B, et al. (1996) Differences in Stiffness Between a Cementless and Cancellous Bone into Varying Amounts of of the Interface Porous Implant vivo in Dogs Due Implant Motion. Clin Orthop 11: 945–951.
8. Claes L, Fiedler S, Ohnmacht M, Duda GN (2000) Initial stability of fully and partially cemented femoral stems. Clinical Biomechanics (Bristol, Avon) 15: 750–755.
9. Bieger R, Ignatius A, Decking R, Claes L, Reichel H, et al. (2011) Primary stability and strain distribution of cementless hip stems as a function of implant design. Clinical Biomechanics 27: 158–164.
10. Heller M, Kassi J-P, Perka C, Duda G (2005) Cementless stem fixation and primary stability under physiological-like loads in vitro. Biomed Tech (Berl) 50: 394–399.

11. Zwartelé RE, Witjes S, Doets HC, Stijnen T, Pöll RG (2012) Cementless total hip arthroplasty in rheumatoid arthritis: a systematic review of the literature. Archives of Orthopaedic and Trauma Surgery 132: 535–546.
12. Hol A, Van Grinsven S, Rijnberg Wj, Susante J, Van Loon C (2006) Varatie in nabehandeling can de primaire totaleheupprothese via de posterolaterale benadering. Nederlands Tijschrift voor Orthopaedie 13e: 105–113.
13. Thomas S, Mackintosh S, Halbert J (2011) Determining current physical management of hip fractrue in acute care hospital and physical therapists' rationale for this management. Phys Ther 91: 1490–1502.
14. Yang H, Zhou F, Tian Y, Ji H, Zhang Z (2011) Analysis of the failure reason of internal fixation in periptrochanteric fractures. Journal of Peking Inversity (Helath Sciences) 43: 699–702.
15. Lorich DG, Geller DS, Nielson JH (2004) Osteoporotic Pertrochanteric Hip Fractures. Management and Current Controversies. The Journal of Bone and Joint Surgery 86-A: 398–410.
16. Van Vugt AB (2007) Femoral neck non-unions: How do I do it? Injury, Int J Care Injured 38S: 51–54.
17. Knobe M, Münker R, Sellei R, Schmidt-Rohlfing B, Erli H, et al. (2009) Die instabile pertrochantäre Femurfraktur. Komplikationen, Fraktursinterung und Funktion nach extra- und intramedullärer Versorgung (PCCP^{TM}, DHS und PFN). Zeitschrift für Orthopädie und Unfallchirurgie 147: 306–313.
18. Bergmann G, Deuretzbacher G, Heller M, Graichen F, Rohlmann A, et al. (2001) Hip contact forces and gait patterns from routine activities. Journal of Biomechanics 34: 859–871.
19. Bergmann G, Graichen F, Rohlmann A (1995) Is staircase walking a risk for the fixation of hip implants? Journal of Biomechanics 28: 535–553.
20. Bergmann G, Graichen F, Rohlmann A (2004) Hip joint contact forces during stumbling. Langenbeck's Archives of Surgery / Deutsche Gesellschaft für Chirurgie 389: 53–59.
21. Bergmann G, Rohlmann A, Graichen F (1989) In vivo Messung der Hüftgelenkbelastung 1. Teil: Krankengymnastik. Z Orthop 127: 672–679.
22. Damm P, Graichen F, Rohlmann A, Bender A, Bergmann G (2010) Total hip joint prosthesis for in vivo measurement of forces and moments. Medical Engineering & Physics 32: 95–100.

23. Bender A, Bergmann G (2011) Determination of typical patterns from strongly varying signals. Computer Methods in Biomechanics and Biomedical Engineering: 37–41.
24. Fleischhauer M (2006) Leitfaden Physiotherapie in der Orthopädie und Traumatologie. 2. ed. Fleischhauer M, Heimann D, Hinkelmann U, editors Urban & Fischer München.

Published in Clinical Biomechanics 28; 2013; 530-535

DOI: 10.1016/j.clinbiomech.2012.12.003

8. *In vivo* hip joint loads during three methods of walking with forearm crutches

P. Damm, V. Schwachmeyer, J. Dymke, A. Bender, G. Bergmann

Abstract

Background

Patients with osteoarthritis, joint implants or fractures use crutches in order to reduce lower limb loading. However, insufficient information exists on how much the loading is then in fact reduced. This situation was studied by using seven patients who had instrumented hip implants.

Methods

Part I: To investigate the effectiveness of forearm crutches, crutch and hip joint contact forces were measured in seven patients with instrumented hip prostheses. Additionally, the bending moments in the implant neck and torsion around its stem were determined. Reductions of peak loads during 3, 4, and 2-point gaits were compared to loads present when walking without crutches.

Part II: This examines joint load reduction during a 4-point gait from one to 12 weeks post-operatively.

Findings

Part I: During a 3, 4, and 2-point gait, the joint force was 17, 12, and 13% lower than it was while walking without crutches. The corresponding reductions of the bending moment were 16, 11, and 12%, while the maximum torque decreased by 19, 21, and 10%.

Part II: The reductions of contact forces in comparison to walking without crutches were highest during the first 4 weeks after surgery. One and 4 weeks post-operatively, the force maximum was 21 and 8% lower than it was after three months.

When compared to the initial values of the 1st week, crutch forces decreased by 28% in the 4th week and by 38% in the 3rd month.

Interpretation

Average reductions of the joint load by more than 20% are only achieved during the first 4 post-operative weeks. Because fractures are in most cases relatively stable after 6 weeks, and bone ingrowth into implant interfaces is nearly finished after this time, a single crutch and a 2-point gait can be prescribed during the 5^{th} and 6^{th} post-operative week.

Introduction

Reduction of hip joint loading is of special interest in many clinical situations. Here are three important examples:

A) In the case of coxarthrosis, the resultant joint force F_{res} determines, in addition to the joint contact area, cartilage pressure and progress of the disease (Carter et al. 2004; Recnik et al. 2007). The pressure is also decisive in cases of cartilage repair and for determining the wear in total hip replacements (THRs) (Buford & Goswami 2004; Barbour et al. 1995).

B) For stable fixation of an uncemented THR, bony ingrowth at the stem interface and thus the torque M_{stem} around the implant stem is important. During the first weeks post-operatively (pOP), the torque can be critical (Mjöberg et al. 1984; Nunn et al. 1989).

C) Healing of femoral neck fractures often fails, especially in elderly patients (Iorio et al. 2004; Roberts & Goldacre 2003; Moran et al. 2005). One reason can be due to the high loads present during the first 6 to 12 weeks. Frequent consequences are non-union, avascular necrosis or even death (Grace et al. 1994). Most decisive for loading of the neck is the bending moment M_{neck} acting there.

Canes and crutches are frequently used to reduce the resultant hip contact force (F_{res}), the torque around the implant stem (M_{stem}) and the bending moment in the femoral neck (M_{neck}). After THR or femoral neck fractures, patients are often advised to use crutches for up to 3 months pOP. Commonly, it is recommended to start walking with a 3-point gait, when both crutches are moved parallel to the affected leg. After approximately 2 weeks, the crutches are in most cases used during an

alternating 4-point gait. Then, loading of the affected joint is only influenced by the force acting on the contralateral crutch. This type of walking is aimed at training more symmetric gait patterns than the 2-point gait does with only a contralateral crutch (McDonough & Razza-Doherty 1988).

The load-reducing effectiveness of crutches has already been discussed by several authors (Dabke et al. 2004; Hall & Jensen 2004; Hol et al. 2010). Reduced vertical ground reaction forces and muscle activities and more symmetrical gait patterns were observed in 19 patients with THR when walking 4 weeks pOP with a 4-point gait (Sonntag et al. 2000). It was concluded that contact loads in the hip joint can be reduced by up to 15% of the bodyweight (%BW). It was also reported that muscle activities changed when walking with canes, causing a decrease in joint contact forces of up to 35% (Neumann 1998; Neumann 1999;). Based on measurements of ground reaction and crutch forces, hip joint force reductions were reported to be 30 - 60%BW when applying 15 - 20%BW on the contralateral crutch (Brand & Crowninshield 1979; Bergmann et al. 1977). Joint forces during walking with a 2-point gait were measured using an instrumented implant in one subject (Bergmann et al. 1989). On the 6^{th} day, and also 6 weeks pOP, a maximum reduction of the joint force of 25% was measured.

The aim of this study was to determine whether or not – and to what extent – the use of crutches leads to load reductions in the hip joint when walking with a 3, 4, and 2-point gait. Based on the existing literature (Bergmann et al. 1989), we hypothesised that F_{res}, M_{stem} and M_{neck} are reduced by no more than 25%, even during a 3-point gait. Based on biomechanical considerations, we assumed that a 4 and 2-point gait are equally effective. Furthermore we hypothesised that an unloading of the hip joint depends on the post-operative time point as well.

Methods

Instrumented hip implant

Joint loads on instrumented hip implants were measured *in vivo*. The prosthesis (CTW, Merete Medical, Berlin; Germany) is based on a clinically successful implant with a titanium stem and a 32mm Al_2O_3 ceramic head. It has a CCD angle of 135° and a size-dependent neck length (Table 1). A telemetry circuit, 6 strain gauges and

an induction coil are arranged in the hollow neck. Detailed descriptions have been published previously (Damm et al. 2010). Power is provided inductively by a coil around the patient's hip joint. The strain gauge signals are transferred via an antenna in the implant head to an external receiver (Graichen et al. 2007). From the 6 strain gauge signals, the 3 force and 3 moment components acting on the implant head are calculated. After calibration, an accuracy of 1-2% was determined for each implant. The right-handed, femur-based coordinate system (Glaser & Bornkessel 2002) is located in the head centre of a right-sided implant. Positive forces F_x, F_y, and F_z act in the lateral, anterior, and superior directions (Figure 1). Data from the left implants are mirrored to the right side. From the 3 force components, the resultant contact force F_{res} is then calculated.

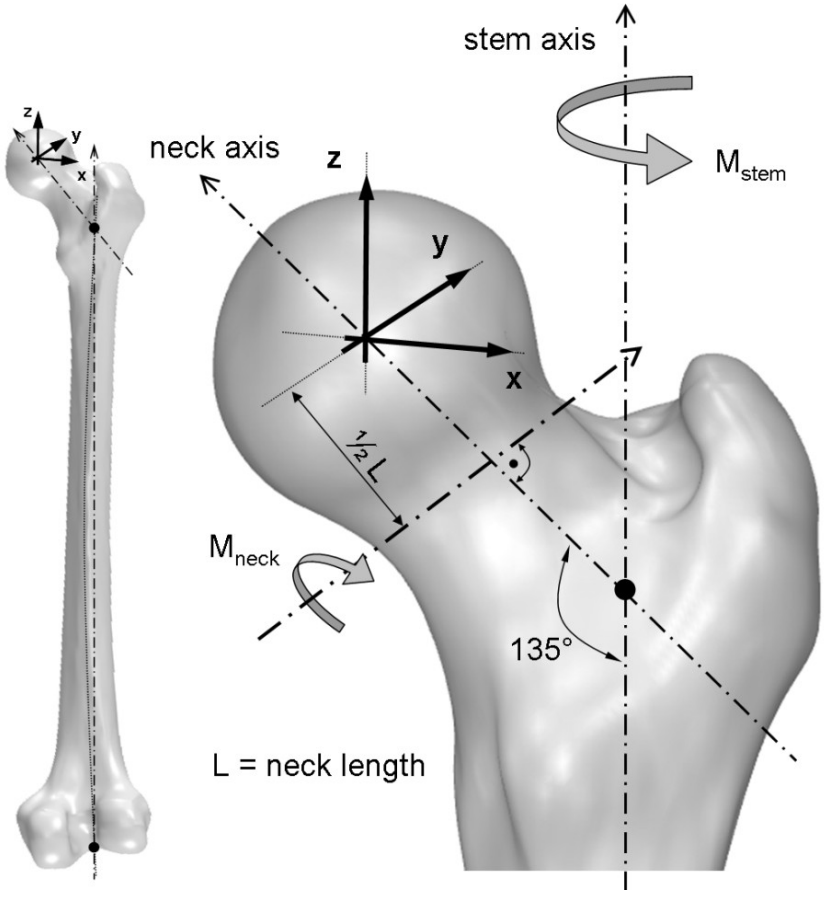

Figure 1: *Coordinate system for the right hip joint; M_{neck} = moment perpendicular to the neck axis, M_{stem} = moment around the stem axis*

External measurement system

The external measurement system has already been described (Graichen et al. 2007; Graichen et al. 1994). Patients are videotaped during the measurements. The telemetric load signals and the crutch forces are recorded simultaneously on video.

Load transducers (KM30z-2kN, ME-Meßsystem GmbH, Germany) were integrated into forearm crutches to measure the longitudinal force F_{crutch} in 1 or 2 crutches, depending on the type of crutch support. The transducers were connected to the external equipment by cables. The crutch length was adjusted to the patients by a physiotherapist.

Patients and measurements

The study was approved by the ethics committee (EA2/057/09) and registered at the 'German Clinical Trials Register' (DRKS00000563). Seven patients with hip osteoarthritis participated in the study (Table 1). They all gave informed written consent to participate in this study and have their images published. Selected trials of all patients are shown and can be downloaded at www.OrthoLaod.com. During rehabilitation, the patients had not been instructed to load the crutches in any given way. This was regarded as ineffective, because it had been shown that patients are unable to limit the ground reaction force at a given level, even after training on a bathroom scale (Bergmann et al. 1979). For the actual study we measured the acting crutch forces and the *in vivo* joint loads during a 4 point gait from one to 12 weeks pOP and further at 12 weeks pOP during a 3 and 2-point gait.

Part I of this study compares 3 types of walking with crutches in regard to the load reduction achieved in the joint. It comprises measurements taken 10 months pOP in patient H1L, 6 months pOP in H2R and 3 months pOP in the remaining 5 patients. The patients walked several times without crutches and with a 3, 4, and 2-point gait (except for H1L) at a self-selected speed over a distance of 10 m. They were instructed to load the crutches as they had done during their rehabilitation to observe typical loads under normal daily circumstances. The forces during walking with crutches were normalized to the joint forces during walking without crutches, as observed on the same day.

Table 1: *Patients investigated*

Patient	Age [years]	Sex	Body weight [N]	Neck Length [mm]
H1L	56	male	754	55.6
H2R	62	male	755	59.3
H3L	60	male	880	55.6
H4L	50	male	814	63.3
H5L	62	female	853	55.6
H6R	69	male	832	63.3
H7R	53	male	899	59.3

Part II reports on the changes in hip contact forces during a 4-point gait from the first week to the third month pOP. The joint loads were measured in 7 patients once a week during the first pOP month, and then monthly. Synchronously the crutch forces were measured. During the first four weeks, measurements were undertaken under the guidance of a physiotherapist.

Data evaluation

All forces were normalised and are given as a percent value of the patients' bodyweight (%BW). From the 3 force components, the torque M_{stem} around the stem axis, and the resultant bending moment M_{neck} in the middle of the femoral neck were calculated in % of the patients' body weight times meter (%BWm). The direction of M_{neck} is not reported here. Relative changes of M_{neck} in the middle of the neck are the same as the relative changes at other locations of the neck.

During all types of gait, F_{res} had 2 peak values (Fig. 2); labelled $F_{res1}|F_{res2}$ (notation "X|Y" generally indicates values at the instants of F_{res1} and F_{res2}). F_{res1} acted approximately at the instant of contralateral toe off (CTO), F_{res2} at contralateral heel strike (CHS). The loads $M_{stem1}|M_{stem2,}$ $M_{neck1}|M_{neck2}$ and $F_{crutch1}|F_{crutch2}$ were determined at the instants of $F_{res1}|$ F_{res2}.

In Part I, median values and standard deviations of the peak values from 20 – 70 steps were analysed from every subject for each kind of crutch use. The reductions

of these peak values, caused by the crutches, are stated in percent of the levels when walking without crutches. Separately and for each patient it was determined statistically whether F_{res} was significantly lower when walking with crutches than it was without crutches (Man-Whitney-U; $p<0.01$).

In addition, average force-time patterns from the 20 – 70 steps were calculated for F_{res}, M_{neck}, M_{stem} and F_{crutch} separately for each subject and kind of crutch use. The employed 'time-warping' method (Bender & Bergmann 2011) first normalises the period times of all included steps. Then, the single time scales are distorted in such a way that the squared differences between all deformed curves, summed over the period time, are minimised. Finally an arithmetic average curve is calculated from all deformed curves. This average curve was first calculated from the time patterns of F_{res}, and the time deformations obtained from the single trials were then transferred to M_{neck}, M_{stem} and F_{crutch} before these loads were averaged.

The averaging procedure was first performed on the data of the single subjects. Using the same method, the average force patterns of all 7 patients were combined. If not stated otherwise, all data presented refer to the obtained 'average' patient. Because the errors between the single trials were minimised over all loading cycles, the peak values of the average curves can deviate slightly from the averaged numerical values at the 1^{st} and 2^{nd} peak.

In Part II, the changes of $F_{res1}|F_{res2}$ in the 'average' patient and the additional average crutch forces were evaluated throughout the first 3 months pOP during a 4-point gait. The crutch-dependent reductions were related to the corresponding values 3 months pOP.

Results

Resultant joint force F_{res}

Figure 2 shows the average patterns of F_{res} during free walking without crutches and the 3 types of crutch use. Without crutches, $F_{res1}|F_{res2}$ were 240|237 %BW. During a 3-point gait, they changed by -17|-30%. During a 4-point gait, the changes were -12|-15%, which was the nearly the same as it was during a 2-point gait with -13|-14%.

The reductions of $F_{res1}|F_{res2}$ by crutches inter-individually varied considerably (Figure 3). During a 3-point gait, the changes of F_{res1} were in the range of +5% to -29%. In H1L, F_{res1} even increased. F_{res2} changed by -11% to -53%. When walking with a 4-point gait, F_{res1} changed from +11% to -21%, and F_{res2} changed from -2% to -25%. Again, F_{res1} increased in H1L, and in H7L F_{res2} remained unchanged. During a 2-point gait, F_{res1} changed by -13% to -20%, and F_{res2} changed by -4% to -38%.

In 5 patients, F_{res2} always decreased more than F_{res1} did. Only in H5L and H7R did the crutches reduce F_{res1} more than F_{res2}. In H3L, H4L, H5L and H7R, the reductions of F_{res1} and F_{res2} were similar during a 4 and 2-point gait. In H2R and H6R, walking with a 2-point gait was much more effective than walking with 4-point gait was.

The influence of the walking speed (Table 2) on the measured load reduction at $F_{res1}|F_{res2}$ was determined. The linear coefficients of determination (R^2) calculated were 0.18|0.52 for a 3-point gait, 0.51|0.01 for a 4-point gait and 0.04|0.17 for a 2-point gait.

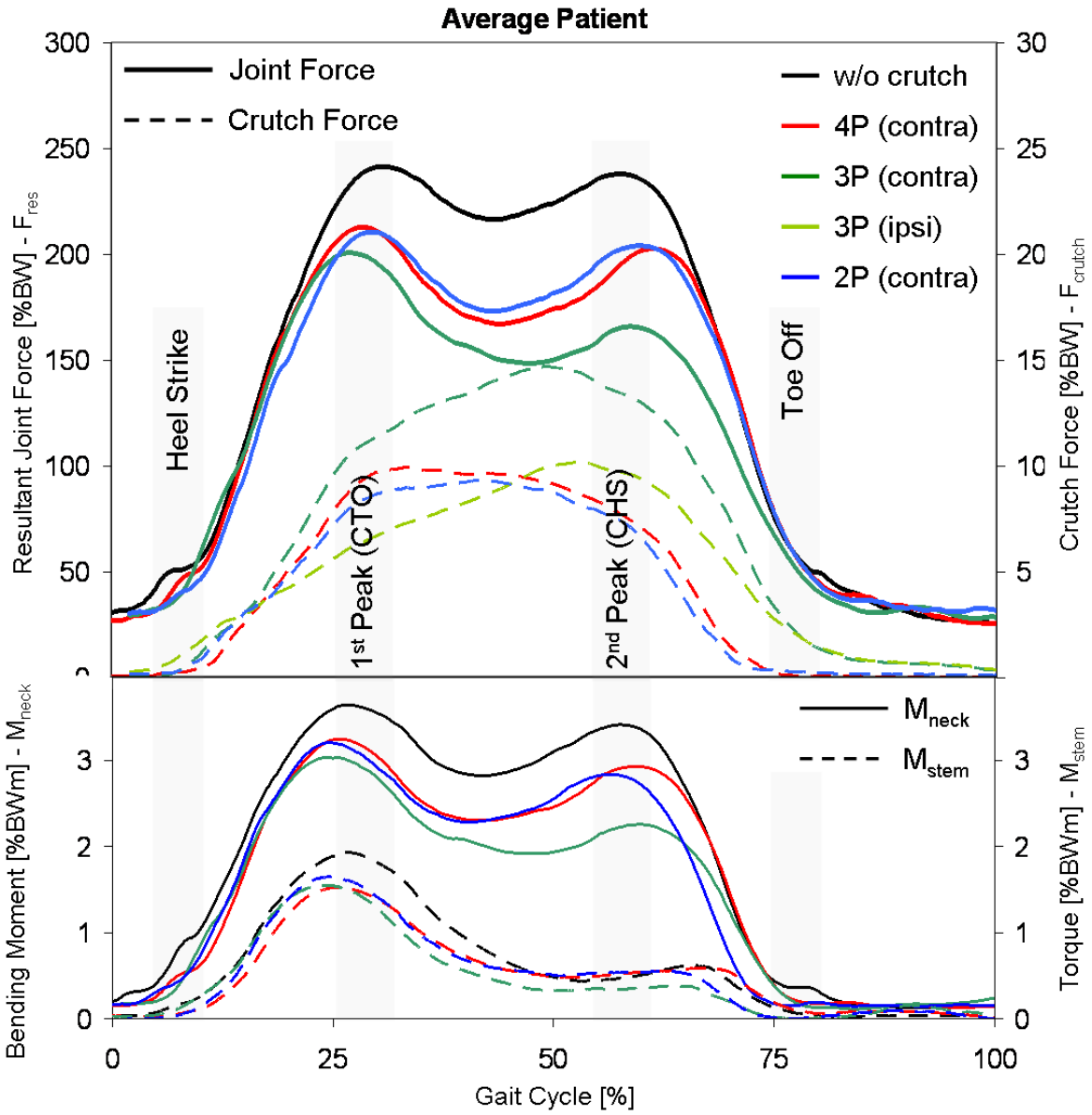

Figure 2: *Average changes of forces and moments during one load cycle; Walking without (w/o) and with crutches with a 3, 4, and 2-point gait. Averages of 7(6) subjects and 20 to 70 loading cycles per subject; Upper diagram: resultant joint contact force F_{res} and crutch forces F_{crutch}. Lower diagram: bending moment M_{neck} and torque M_{stem}; CTO = contralateral toe off, CHS = contralateral heel strike.*

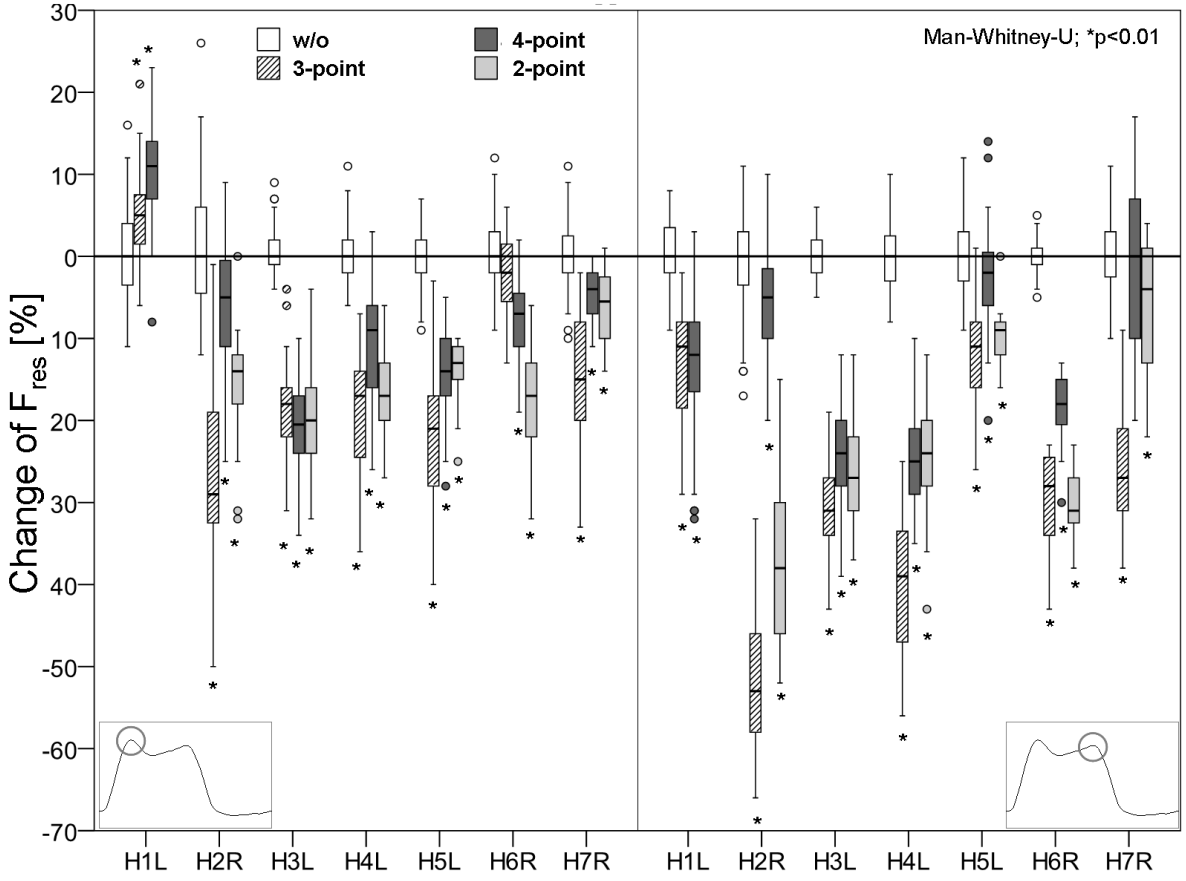

Figure 3: *Individual changes of peak force F_{res}; Walking without (w/o) and with crutches with a 3, 4 and 2-point gait. Changes in 7 subjects in percent of forces during free walking; Data from 20 to 70 loading cycles per subject, 3 to 10 months after THR; Left: peak value F_{res1}. Right: peak value F_{res2}. Asterisks *: Significant changes relative to free walking.*

Bending moment M_{neck} in the femoral neck

The 2 peak values $M_{neck1}|M_{neck2}$ acted at nearly the same times as did the peak forces $F_{res1}|F_{res2}$ (Figure 2). During free walking, $M_{neck1}|M_{neck2}$ values had the same average height of 3.5|3.5 %BWm. The following load changes were measured when walking with crutches: -16|-33% during a 3-point gait, -11|-14% during a 4-point gait, and -12|-14% during a 2-point gait. The reductions of M_{neck} during all types of crutch usage among the participants differed considerably (Table 2).

Torque M_{stem} around the stem axis

M_{stem2} was lower than M_{stem1} during free walking and all types of crutch-supported walking. When walking without crutches, $M_{stem1}|M_{stem2}$ had values of 1.7|0.5 %BWm (Figure 2). During a 3-point gait, changes of -19|-35% were observed. During a 4-point gait, $M_{stem1}|M_{stem2}$ changed by -21|0%. In a 2-point gait, the changes were -10|+15%. The changes of M_{stem} were also extremely dependent on the investigated subject for all types of crutch use (Table 2).

Crutch forces F_{crutch}

When walking with a 3-point gait, both *average* crutch forces reached their maxima at times between the peak forces F_{res1} and F_{res2} (Figure 2). Throughout the whole walking cycle, the average contralateral crutch force was higher than the ipsilateral force. On the average, the absolute maximum of F_{crutch} in the contralateral crutch was highest during a 3-point gait, followed by a 2 and a 4-point gait.

$F_{res1}|F_{res2}$ were both linearly dependent on the synchronous contralateral crutch force F_{crutch}. Coefficients of determination (R^2) of 0.65 | 0.75 were calculated for a 3-point gait, 0.74 | 0.62 for a 4-point gait and 0.84 | 0.75 for a 2-point gait. The regression lines revealed that F_{res1} was reduced by 6|9|13%BW during 3-|4-|2-point gait if the contralateral force F_{crutch} increased by 1%BW. For the 2nd peak of F_{res}, the reductions for each 1%BW of the crutch force were 6|11|12%BW.

Table 2: *Average gait velocity v, crutch forces F_{crutch} at the instants of the 2 peak forces F_{res} and changes of the bending moment M_{neck} and the torque M_{stem}; 7 subjects, 3 methods of crutch walking, 3 to 10 months after THR; arithmetic mean values (SD), contra = contralateral crutch, ipsilat. = ipsilateral crutch; changes in % of values during free walking*

Patient	**H1L**		**H2R**		**H3L**		**H4L**		**H5L**		**H6R**		**H7R**	
[m/s]	v		v		v		v		v		v		v	
w/o	1.0		1.0		0.8		1.0		0.9		1.1		1.1	
3-point gait	0.8		0.6		0.6		0.7		0.9		1.0		0.7	
4-point gait	0.7		0.8		0.7		0.8		0.9		1.0		0.8	
2-point gait	-		0.7		0.8		0.8		1.0		1.0		0.9	
[%BW]	$F_{crutch1}$	$F_{crutch2}$	$F_{crutch1}$	$F_{crutch2}$	$F_{crutch1}$	$F_{crutch2}$	$F_{crutch1}$	$F_{crutch2}$	$F_{crutch1}$	$F_{crutch2}$	$F_{crutch1}$	$F_{crutch2}$	$F_{crutch1}$	$F_{crutch2}$
3-point, contra	4 (1)	7 (3)	16 (5)	22 (4)	13 (2)	14 (2)	12 (4)	19 (5)	9 (3)	6 (2)	2 (1)	12 (2)	10 (5)	19 (2)
3-point, ipsilat.	2 (2)	5 (3)	14 (5)	18 (4)	5 (1)	7 (1)	6 (2)	12 (5)	5 (2)	6 (3)	2 (1)	10 (2)	6 (4)	18 (3)
4-point, contra	3 (2)	6 (3)	6 (3)	5 (2)	14 (2)	11 (2)	10 (3)	11 (3)	6 (2)	4 (1)	4 (1)	5 (2)	5 (2)	7 (4)
2-point, contra	---	---	12 (5)	18 (5)	12 (2)	11 (2)	7 (3)	10 (3)	6 (1)	4 (1)	8 (1)	9 (2)	5 (3)	8 (2)
Δ [%]	M_{neck1}	M_{neck2}	M_{neck1}	M_{neck2}	M_{neck1}	M_{neck2}	M_{neck1}	M_{neck2}	M_{neck1}	M_{neck2}	M_{neck1}	M_{neck2}	M_{neck1}	M_{neck2}
3-point gait	3	- 20	- 28	- 59	- 17	- 28	- 18	- 40	- 16	- 10	-8	-41	-19	-2
4-point gait	- 4	- 22	- 8	- 3	- 20	- 25	- 8	- 20	- 12	0	-12	-21	-9	-6
2-point gait	---	---	- 11	- 11	- 20	- 27	- 15	- 23	- 12	- 7	-22	-36	-9	-11
Δ [%]	M_{stem1}	M_{stem2}	M_{stem1}	M_{stem2}	M_{stem1}	M_{stem2}	M_{stem1}	M_{stem2}	M_{stem1}	M_{stem2}	M_{stem1}	M_{stem2}	M_{stem1}	M_{stem2}
3-point gait	46	70	- 51	- 68	- 12	- 20	- 27	33	- 6	40	-14	-58	-26	67
4-point gait	- 36	0	- 19	22	- 15	- 21	- 19	66	- 19	40	-26	0	-18	189
2-point gait	---	---	- 13	29	- 9	- 29	- 23	66	- 6	0	-37	-32	-14	104

Post-operative changes

The changes of $F_{res1}|F_{res2}$ and of the synchronous contralateral force F_{crutch} during 4-point walking were highest during the first pOP month (Figure 4). One week pOP, $F_{res1}|F_{res2}$ were 18|21% lower in comparison with the force levels 3 months pOP (numbers derived from the regression line), and one month pOP, $F_{res1}|F_{res2}$ were 7|8% lower. F_{res2} was always more reduced than F_{res1} was throughout the whole time of investigation, and this effect was most pronounced at early pOP times. In comparison with the first week pOP, the crutch forces $F_{crutch1}|F_{crutch2}$ decreased by 28|40% 4 weeks pOP, and by 38|49% 3 months pOP (numbers derived from the regression line).

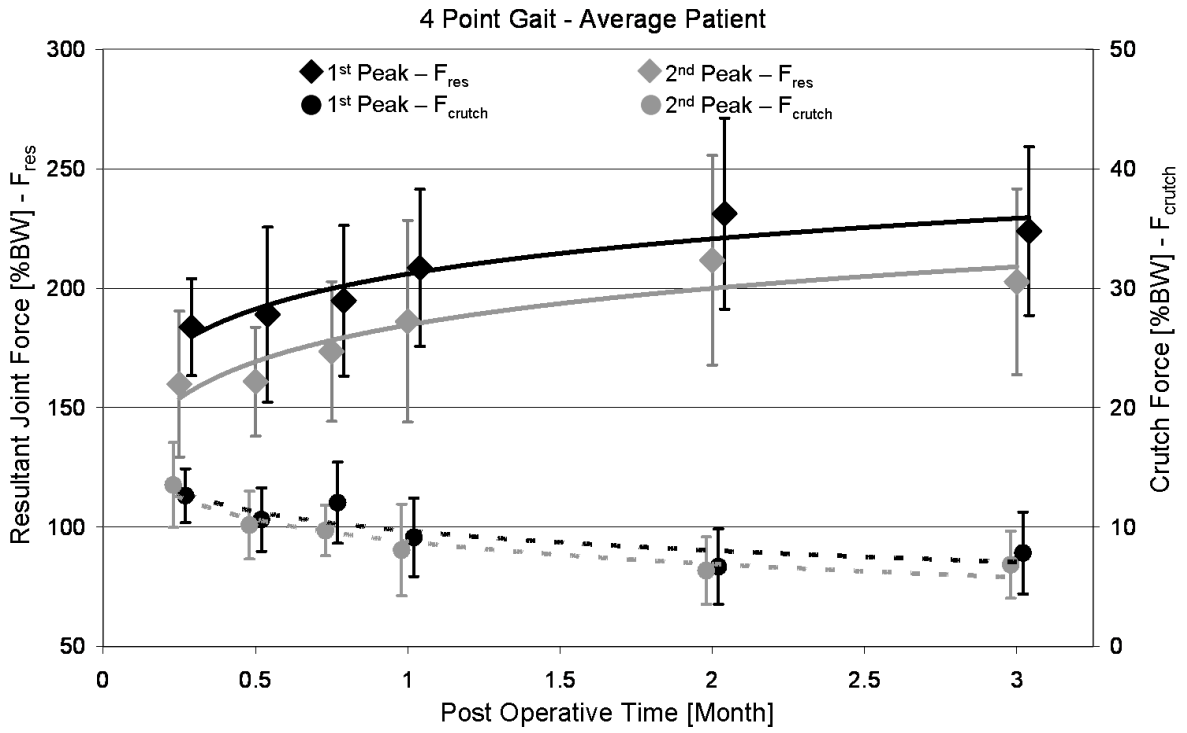

Figure 4: *Resultant peak joint force and simultaneous contralateral crutch forces during 4 point gait over the post-operative time; average data from 7 subjects ±1 SD, logarithmic best-fit curves*

Discussion

To the best of our knowledge, this is the first study reporting *in vivo*-measured hip contact forces, bending moments in the neck, torque around the stem axis, and synchronously acting crutch forces from a group of subjects. Special consideration was made to provide realistic measurement conditions. The patients were advised to load their crutches in the same way as they had done during their rehabilitation period. The aim of this study was to determine the joint load reduction during walking with crutches using a 3, 4, and 2-point gait. Based on previous literature and biomechanical considerations, three hypotheses were set forward:

I. F_{res}, M_{stem} and M_{neck} are reduced by no more than 25% for any kind of crutch use.

II. 4-point and 2-point gaits have a similar load-reducing effect.

III. The reduction of the hip contact force during walking with crutches depends on the post-operative time.

The first hypothesis could not be confirmed. Although the subjects reduced F_{res} by 17% on the average during a 3-point gait, by 12% during a 4-point, and by 13% during a 2-point gait (Figure 2), F_{res} reductions during a 3-point gait of up to 53% were observed in some patients (Figure 3). In a similar way, M_{Stem} was reduced by up to 19% on the average during a 3-point gait, and the bending moment M_{neck} by up to 16% (Figure 2). However, some patients achieved load reductions of up to 59% for M_{neck} and 68% for M_{Stem} (Table 2).

The second hypothesis could not be confirmed, either. The reduction of F_{res} was similar for both kinds of crutch walking (Figure 2). However, the average reduction of M_{Stem} was much larger during a 4-point than it was during a 2-point gait. Furthermore the intra-individual reductions of M_{Stem} and M_{neck} were very different between these two kinds of walking.

The third hypothesis could however be confirmed; the highest crutch forces and highest load reduction on the hip joint during walking with crutches was measured during the first four weeks pOP.

In the following, the most important findings of this study are summarized:

a) The 2nd force peak is more effectively decreased by crutches than the 1st peak is.

b) In a 3-point gait, the 2nd peak of F_{res} is reduced by approximately 50% more than it is in a 4-point or 2-point gait.

c) The reduction of F_{res} during a 2-point gait is just as effective as it is during a 4-point gait; M_{stem} is, however, best reduced by 4-point gait.

d) Average reductions of F_{res} in a 4-point gait of more than 20% are only achieved during the first 4 pOP weeks.

e) The 1st torque maximum M_{stem1} around the stem axis is much higher than the 2nd one is. In contrast to the reduction of F_{res1} and F_{res2} by crutches, only M_{stem1} was clearly reduced.

Based on these observations and other literature data, several conclusions can be drawn and clinical suggestions offered:

1) It could be shown that the load reduction at the first peak during a 3-point gait was similar to the load reduction during a 4-point gait (shown in Figure 2). A previous study has shown that patients typically load the affected leg during walking with crutches more than that expected by many physiotherapists and orthopaedic surgeons (Bergmann et al. 1978; Bergmann et al. 1979). Among the findings of the previous studies and our own measurement data we conclude that – as long as the patients themselves feel safe – they can walk just as well with a 4-point gait.

2) If the use of crutches after THR is ever advised after the 4th week, the patients should walk with a 2-point gait but only with 1 crutch. This handicaps them less than using 2 crutches and it was shown in Figure 2 and Figure 4 that force reduction during a 2 point gait is just as effective as it is during a 4 point gait. However if coordination is most important, a 4 point gait should be chosen to regain symmetric movement patterns (McDonough & Razza-Doherty 1988; Hesse et al. 1999). Otherwise the patients can walk with a 2-point gait with the crutch on the contralateral side.

3) In regard to the limited load reductions now observed, we assume that the use of crutches is more important in order to prevent extremely high loads than it is to reduce the peak forces during regular gait cycles. This is explained by the following three examples:

   a) After cementless implantation of hip prostheses, the bone needs several weeks to grow into the porous interface around the implant (Jasty et al. 1993). It is known that this can only proceed if the micro movement in the interface remains below a value of 20 to 40 µm (Bragdon et al. 1996; Pilliar et al. 1986). The maximum movement can rise with the maximum joint contact force and the torque around the stem axis. However a combination of low contact force and a high torsion moment can also be critical for the fixation, because of the reduced wedge stabilisation.

   b) Fresh fractures of the proximal femur or its neck, stabilised by implants, often cannot bear one's own normal body weight (Brumback et al. 1999). This is apparent because the risk of a non-union of the fracture depends not only on the high number of loading cycles with the average load, but also on the presence of extreme loads.

   c) Unsafe walking as a result of pain and stumbling can cause extremely high hip contact forces (Bergmann et al. 2004). Up to 870%BW were observed, and even higher levels must be expected in younger subjects. In contrast, occasional observations during everyday life and in rehabilitation clinics show that when walking with 2 crutches, patients often step fully with the affected leg, for example, when opening doors. The current study also indicates that joint forces having an average size or greater can act even when walking with crutches, especially in a 4-point or a 2-point gait. Based on these reports and observations, we assume that the main function of crutches and canes used after the fourth or sixth post-operative week is to remind the patients to walk cautiously and thus prevent potential injuries.

4) In some patients the hip joint load increased if they used the crutches in an incorrect manner (for an example, see www.OrthoLoad.com - H3L_140311_1_144). This underlines the importance of taking part in an initial training of crutch walking.

In contrast to the reduction of F_{res} and M_{neck} while walking with crutches, only the first peak of M_{stem} was clearly seen to be changed. This peak M_{stem1} was on the average decreased by up to 19% during a 3-point, 21% during a 4-point, and 10% during a 2-point gait. This torque is one of the most decisive factors for a stable implant fixation (Bergmann et al. 1995; Heller et al. 2001; McKellop et al. 1991; Nunn et al. 1989; Phillips et al. 1991). Fractures are in most cases stable after 6 weeks (Wehner et al. 2010), and bone ingrowth into implant interfaces is nearly complete after this time (Jasty et al. 1993). Furthermore the regression line in Figure 4 shows that the joint force reduction in the sixth week is only about 3% higher than it is in the eighth week. Thus a single crutch and 2-point gait can, according to our observations, be prescribed from the 5th and 6th pOP week on.

Limitations

The study was performed in order to measure the *in vivo* joint load reduction by using instrumented forearm crutches under realistic measurement conditions. The small number of investigated subjects and the large number of individual differences in joint force reductions achieved by crutches do not support any generalisation of the results. All patients were in good physical shape and younger than typical subjects after hip replacement. It cannot be excluded that patients who are older or weaker will load their crutches less than the subjects here did. No additional measurements were made, such as changes of muscle activities or ground reaction forces.

Acknowledgments

The authors gratefully acknowledge the voluntary collaboration of all subjects. The study was supported by the German Research Society (DFG - SFB 760, Be 804/19-1) and by Deutsche Arthrose-Hilfe e.V.

References

Barbour, P.S.M., Barton, D.C. & Fisher, J., 1995. The incluence of contact stress on the wear of UHMWPE for total replacement hip prostheses. *Methods*, 181-183, pp.250-257.

Bender, A. & Bergmann, G., 2011. Determination of Typical Patterns from Strongly Varying Signals. *Computer Methods in Biomechanics and Biomedical Engineering*, iFirst, pp.1-9.

Bergmann, G., Graichen, F. & Rohlmann, 2004. Hip joint contact forces during stumbling. *Langenbeck's archives of surgery*, 389(1), pp.53-59.

Bergmann, G., Graichen, F. & Rohlmann, 1995. Is staircase walking a risk for the fixation of hip implants? *Journal of biomechanics*, 28(5), pp.535-53.

Bergmann, G. et al., 1978. Das Gehen mit Stockstützen - II. Beinbelastung und Stützenkräfte bei Verwendung von zwei Unterarmgehstützen. *Zeitschrift für Orthopädie und ihre Grenzgebiete*, 116, pp.106-113.

Bergmann, G. et al., 1977. Walking with canes and forearm-crutches. I. Reduction of loads at the hip and proximal end of the femur by one sided use of cane/crutch (author's transl). *Zeitschrift fur Orthopadie und ihre Grenzgebiete*, 115(2), pp.174-182.

Bergmann, G. et al., 1979. Das Gehen mit Stockstütze - III. Kontrolle und Training der maximalen Auftrittskräfte mit einer instrumentierten Stütze. *Zeitschrift fur Orthopadie und ihre Grenzgebiete*, 118, pp.293-300.

Bergmann, G., Rohlmann & Graichen, F., 1989. In vivo Messung der Hüftgelenkbelastung 1. Teil: Krankengymnastik. *Z. Orthop.*, 127, pp.672-679.

Bragdon, C.R. et al., 1996. Differences in stiffness of the interface between a cementless porous implant and cancellous bone in vivo in dogs due to varying amounts of implant motion. *The Journal of arthroplasty*, 11(8), pp.945-951.

Brand, R.A. & Crowninshield, R.D., 1979. The effect of cane use on hip contact force. *Clinical Orthopaedics and Related Research*, (147), pp.181-184.

Brumback, R.J. et al., 1999. Immediate Weight-Bearing After Treatment of a Comminuted Fracture of the Femoral Shaft with a Statically Locked Intramedullary Nail. *The Journal of Bone and Joint Surgery*, 81(11), pp.1538-1544.

Buford, A. & Goswami, T., 2004. Review of wear mechanisms in hip implants: Paper I – General. *Materials & Design*, 25(5), pp.385-393.

Carter, D.R. et al., 2004. The Mechanobiology of Articular Cartilage Development and Degeneration. *Clinical Orthopaedics and Related Research*, (427), pp.69-77.

Dabke, H.V. et al., 2004. How Accurate Is Partial Weightbearing? *Clinical Orthopaedics and Related Research*, 421(421), pp.282-286.

Damm, P. et al., 2010. Total hip joint prosthesis for in vivo measurement of forces and moments. *Medical Engineering & Physics*, 32(1), pp.95-100.

Glaser, R. & Bornkessel, C., 2002. ISB recommendation on definitions of joint coordinate system of various joints for the reporting of human motion - part I: ankle, hip, and spine. *Journal of Biomechanics*, 35, pp.543-548.

Grace, L. et al., 1994. Outcomes after Displacement Fractures of the Femoral Neck. *The Journal of Bone and Joint Surgery*, 76-A(I), pp.15-25.

Graichen, F. et al., 2007. Implantable 9-channel telemetry system for in vivo load measurements with orthopedic implants. *IEEE transactions on bio-medical engineering*, 54(2), pp.253-61.

Graichen, F., Bergmann, G. & Rohlmann, 1994. Telemetric transmission system for in vivo measurement of the stress load of an internal spinal fixator. *Biomedizinische Technik Biomedical engineering*, 39(10), pp.251-258.

Hall, C.D. & Jensen, J.L., 2004. The effect of cane use on the compensatory step following posterior perturbations. *Clinical Biomechanics*, 19(7), pp.678-687.

Heller, M.O. et al., 2001. Influence of femoral anteversion on proximal femoral loading: measurement and simulation in four patients. *Clinical biomechanics*, 16(8), pp.644-9.

Hesse, S. et al., 1999. Das Gehen von Patienten mit voll belastbarem künstlichen Hüftgelenk auf dem Laufband mit partieller Körpergewichtsentlastung , im Kreuzgang und hilfsmittelfrei. *Z. Orthop.*, 137, pp.265-272.

Hol, A.M. et al., 2010. Partial versus unrestricted weight bearing after an uncemented femoral stem in total hip arthroplasty: recommendation of a concise rehabilitation protocol from a systematic review of the literature. *Archives of orthopaedic and trauma surgery*, 130(4), pp.547-55.

Iorio, R. et al., 2004. Displaced Femoral Neck Fractures in the Elderly Disposition and Outcome After 3- to 6-Year Follow-Up Evaluation. *The Journal of Arthroplasty*, 19(2), pp.175-179.

Jasty, M. et al., 1993. Comparison of bone ingrowth into cobalt chrome sphere and titanium fiber mesh porous coated cementless canine acetabular components. *Journal of Biomedical Materials Research*, 27, pp.639-644.

McDonough, A.L. & Razza-Doherty, M., 1988. Some biomechanical aspects of crutch and cane walking: the relationship between forward rate of progression, symmetry, and efficiency--a case report. *Clinics in Podiatric Medicine and Surgery*, 5(3), pp.677-693.

McKellop, H. et al., 1991. Comparison of the stability of press-fit hip prosthesis femoral stems using a synthetic model femur. *Journal of Orthopaedic Research*, 9, pp.297-305.

Mjöberg, B., Hansson, L.I. & Selvik, G., 1984. Instability of total hip prostheses at rotational stress. *Acta Orthop Scand*, 55, pp.504-506.

Moran, C.G. et al., 2005. Early mortality after hip fracture: is delay before surgery important? *The Journal of bone and joint surgery.*, 87(3), pp.483-9. Available at: http://www.ncbi.nlm.nih.gov/pubmed/15741611.

Neumann, D., 1999. An electromyographic study of the hip abductor muscles as subjects with a hip prosthesis walked with different methods of using a cane and carrying a load. *Physical therapy*, 79(12), pp.1163-76.

Neumann, D., 1998. Hip abductor muscle activity as subjects with hip prostheses walk with different methods of using a cane. *Physical Therapy*, 78(5), pp.490-501.

Nunn, D. et al., 1989. Torsional Stability of the Femoral Component of Hip Arthroplasty. *The Journal of Bone and Joint Surgery*, 71B(3), pp.452-455.

Phillips, T.W., Nguyen, L.T. & Munro, S.D., 1991. Loosening of cementless femoral stems: a biomechanical analysis of immediate fixation with loading vertical, femur horizontal. *Journal of Biomechanics*, 24(1), pp.37-48.

Pilliar, R.M., Lee, J.M. & Maniatopoulos, C., 1986. Observations on the effect of movement on bone ingrowth into porous-surfaced implants. *Clinical Orthopaedics and Related Research*, 208(208), pp.108-113.

Recnik, G. et al., 2007. Higher peak contact hip stress predetermines the side of hip involved in idiopathic osteoarthritis. *Clinical Biomechanics*, 22(10), pp.1119-24.

Roberts, S.E. & Goldacre, M.J., 2003. Time trends and demorgaphy of mortality after fractured neck of femur in an English population , 1968-98: database study. *British Medical Journal*, 327, pp.771-4.

Sonntag, D. et al., 2000. Gait with and without forearm crutches in patients with total hip arthroplasty. *International journal of rehabilitation research*, 23(3), pp.233-243.

Wehner, T. et al., 2010. Clinical Biomechanics Influence of the fixation stability on the healing time — A numerical study of a patient-specific fracture healing process. *Clinical Biomechanics*, 25, pp.606-612.

9. Summary of results

During walking the resultant contact force F_{res} had two peak values in all patients. The first one occurs at the instant of contralateral toe off (CTO) and has a value of 248%BW on average. With 240%BW the second peak was slightly lower and occurred at the contralateral heel strike (CHS). F_{res} was always higher than 35%BW during the swing phase of the leg (Figure 1). In contrast to F_{res}, the measured friction moment M_{res} increased nearly linearly during the whole extension phase, with the minimum value at the ipsilateral heel strike (HS) and an average maximum of 0.26%BWm shortly after the contralateral heel strike (CHS) at (Figure 9.1).

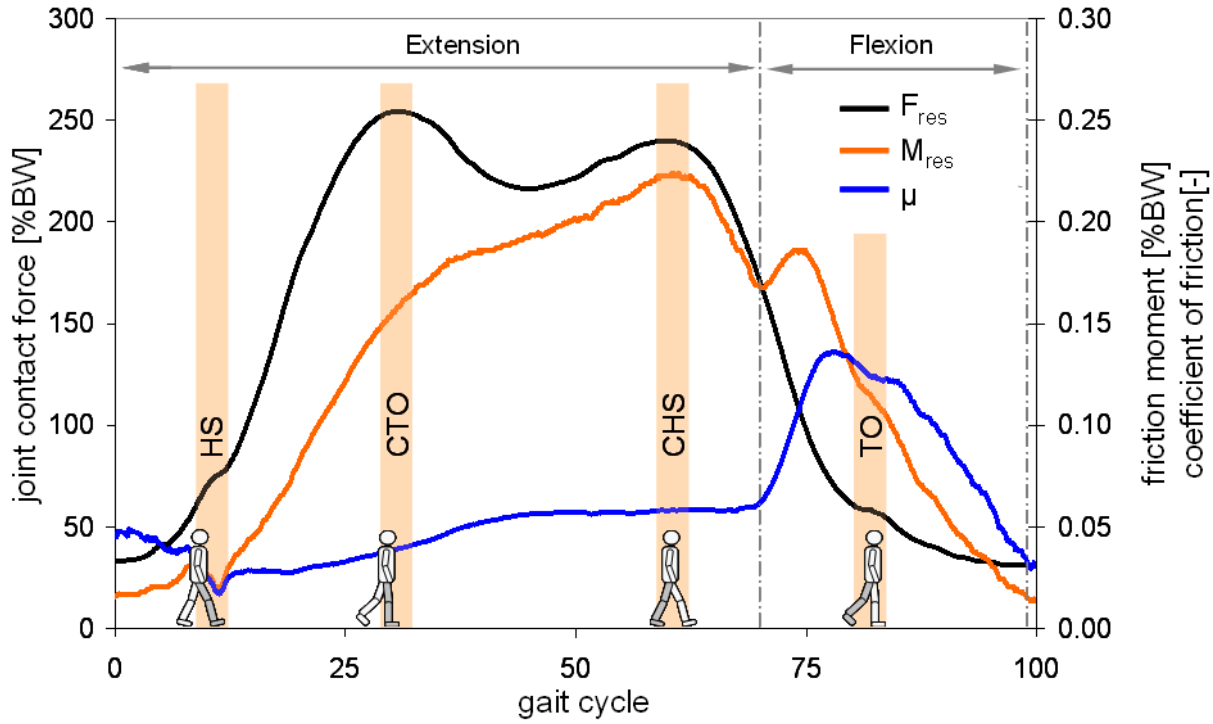

Figure 9.1: F_{res}, M_{res} and μ during walking; average subject, 3 month pOP

The three-dimensional coefficient of friction μ also increased during the extension phase, from 0.04 at CTO to 0.06 at CHS on average. During the flexion phase μ further increased to a maximum of 0.14 at toe off (TO) of the ipsilateral leg. The average friction-induced power throughout the whole gait cycle was 2.3W on average.

However, the contact forces and friction moments varied greatly between individuals. As a consequence, μ ranged from 0.03 to 0.06 at CTO and from 0.04 to 0.08 at CHS. The absolute peak values of μ lay between 0.09 and 0.23. Similarly to μ, the peak values of the friction-induced power varied between 1.4 W and 3.8 W. In seven out of

eight patients, the friction-induced power was greater during joint flexion than during joint extension, between 4% and 290%. Only one patient returned a lower value for friction-induced power during extension compared to joint flexion, with 21%.

See also publication: *Friction in Total Hip Joint Prosthesis Measured In Vivo during Walking* DOI:10.1371/journal.pone.0078373

The pattern of the bending moment M_{neck} at the femur neck during walking was nearly similar to that of the joint contact force, with two typical peak values. These peak values had the same average height of 3.5%BWm and acted at nearly the same times as those of F_{res}. The corresponding peak values of the torque M_{stem} around the stem axis were on average 1.7%BWm at CTO and 0.5%BWm at CHS. The second peak of M_{stem} was in all patients lower than the first one.

During walking with crutches the 2 peak values of F_{res} were reduced on average by -16|-33% during 3-point gait, -11|-14% during 4-point gait, and -12|-14% during 2-point gait. Related to joint contact force the bending moments in the implant neck at the instants of the two force peaks were also reduced by crutches. The average reductions were -19|-35% during a 3-point gait, -21|0% during 4-point gait, and -10|+15% during 2-point gait. The corresponding reductions of the torque were 16%, 11%, and 12%, while the maximum torque decreased by 19%, 21%, and 10% on average. However, the changes of torque and bending moments greatly depended on the investigated subject as well as on the method of crutch use.

The reduction of the 2 maxima of F_{res} linearly depended on the synchronous contralateral crutch force. Coefficients of determination (R^2) of 0.65|0.75 were calculated for 3-point gait, 0.74|0.62 for 4-point gait and 0.84|0.75 for 2-point gait. The regression lines revealed that the first force peak was reduced by 6|9|13%BW during 3-|4-|2-point gait if the contralateral force F_{crutch} increased by 1%BW. For the second peak of F_{res}, the reductions for each 1%BW of the crutch force increase were 6|11|12%BW.

The reductions of joint contact forces in comparison to walking without crutches were highest during the first four weeks after surgery (Figure 9.2). One and four weeks post surgery, respectively, the force maximum was 21% and 8% lower than it was after three months. When compared to the initial values of the first week, crutch forces decreased by 28% in the fourth week and by 38% in the third month. Average

reductions of the joint load by more than 20% are only achieved during the first four weeks following surgery.

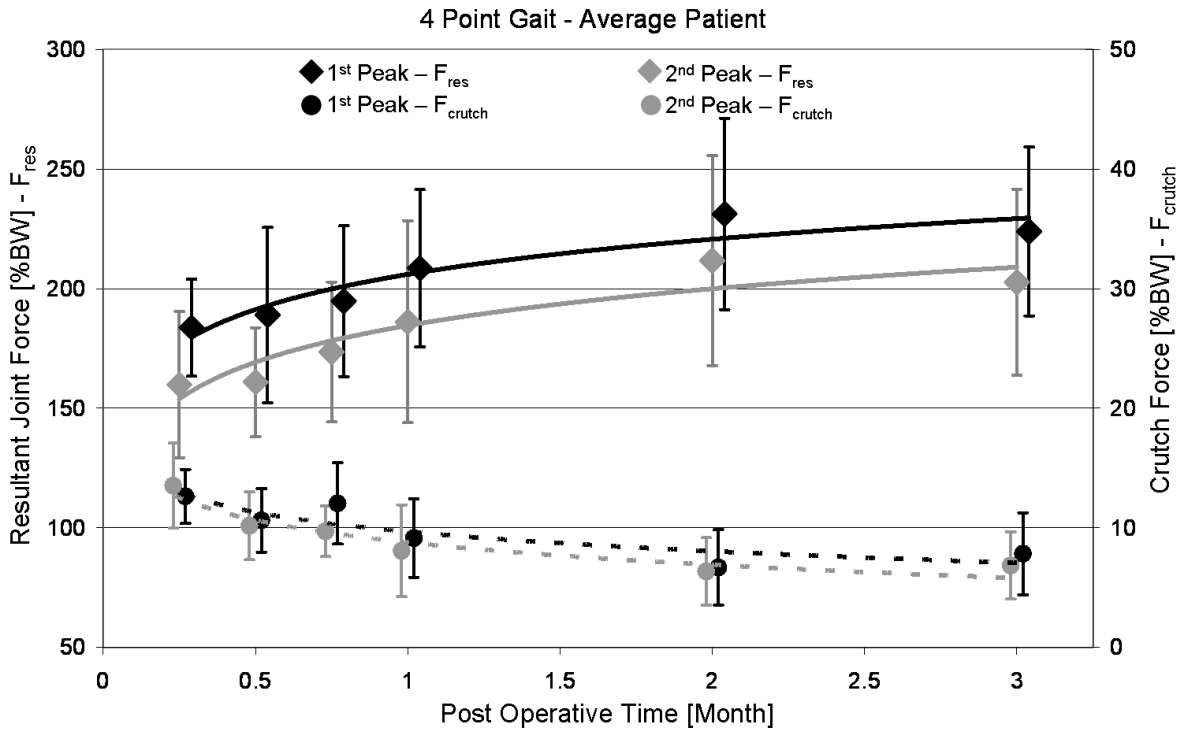

Figure 9.2: Resultant peak joint force and simultaneous contralateral crutch force during 4-point gait over the post-operative time; average data from 7 subjects ±1 SD, logarithmic regression curves (from publication "In vivo hip joint loads during three methods of walking with forearm crutches")

See also publication: *In vivo hip joint loads during three methods of walking with forearm crutches* DOI: 10.1016/j.clinbiomech.2012.12.003

The measurements during different physiotherapeutic exercises have shown that the joint contact forces F_{res} in all investigated patients were always lower than during walking, except during pelvis lifting with support only by ipsilateral leg. During this exercise the joint contact force was on average by up to 10% higher compared to walking. The bending moment M_{bend} in the femoral neck also increased by about 10% during this exercise. However, the peak torque value M_{tors}in the implant-bone-interface was comparable to the values during walking. Nevertheless, it was observed that weight-bearing exercises caused the highest joint contact forces

among all exercises with peak values of up to 441%BW. During voluntary isometric contractions, the peak loads ranged widely and potentially reached high levels, depending on the intensity of the contraction. Furthermore, exercises with long lever arms and dynamic exercises are able to cause hip joint loads with values up to 50% higher than those during walking.

See also publication: *In vivo hip joint loading during post-operative physiotherapeutic exercises* DOI:10.1371/journal.pone.0077807

10. Discussion

A previous study with only two patients [5] reported average hip contact forces during walking which were up to 20% lower than observed now. In the previous study the patients walked on a treadmill at 4 km/h, now they walked at 3.6 km/h on level ground. Another previous study [13] also investigated hip joint loads during free walking at velocities selected by the patient. In comparison to these *in vivo* measurements the differences of hip joint peak loads were only 5% lower.

Throughout the swing phase of walking the lowest values of F_{res} lay between 35%BW and 40%BW. This finding conflicts with a fluoroscopic study [14], which investigated the separation of the hip joint surfaces *in vivo*. It was reported that the joint surfaces of the unloaded leg separated with a displacement of 3.3mm on average during one-legged stance. However, a separation involves a total unloading of the hip joint, an effect which has never been observed in any of our patients. Because if this would have happened, fast changes in the directions of the resultant contact force or one of its components would have been observed during walking.

As part of our work the unloading effect of forearm crutches during three different types of crutch use was investigated. Previous research on the possibility to reduce hip joint loading by crutches was performed analytical methods. However, these studies have shown large differences between the calculated load reductions. Sonntag et al. reported a joint load reduction up to 15% [15]. In contrast to that, other studies have postulated quite higher load reductions at the hip joint of up to 35% [16], 15-20% [17] and 30-40% [18]. Unfortunately, all studies calculated the unloading of the hip joint only by indirect methods. In our study the hip joint load was measured *in vivo* during walking with different methods of crutch use. During walking with 4-point gait a maximum load reduction of 12% was measured. During 3-point gait the load reduction joint was only 5% better. It was shown that during walking with only one crutch used at the contralateral side (2-point gait), the load reduction of the hip joint was similar to 4-point gait (12% vs 13%). These results indicate that the possibility of forearm crutches to reduce hip joint loading is mostly overestimated.

For the physiotherapeutic exercises it was shown that weight-bearing activities caused the highest loads. Furthermore, movements against resistance or loads acting at long lever arms caused high torsional moments. The forces during isometric contractions depend on the contraction intensity, which is rather influenced by the

personal motivation than by the maximal muscle strength. Certainly joint contact forces during physiotherapeutic exercises can be increased by unexpected muscle co-contractions. We conclude that when deciding between partial and full weight-bearing exercises, physicians should consider the loads relative to those observed during walking. The data presented here should be used to optimise physiotherapy and post-operative treatment in order to enhance rehabilitation progress and minimise critical loads onto the implant or the femoral neck.

The *in vivo* friction in artificial hip joints was now measured for the first time ever. It could be shown that current state of the art hip simulators mimic the *in vivo* friction conditions insufficiently. In many simulator studies the implants only moved in the flexion-extension plane. It was now shown that the hip joint rotates around all axes during walking. Therefore abduction and adduction of the joint also have a significant influence on the friction conditions. Additionally, most *in vitro* friction studies applied a sinusoidal contact force, which not represents the physiological loading conditions with its two load peaks during walking.

Beside the possibility to measure friction *in vivo* in total hip joint replacements, it was also possible for the first time to calculate the *in vivo* coefficient of friction during the entire gait cycle. Because the hip joint moves around three axes during walking, the coefficient of friction was calculated using a three-dimensional approach. For this, the two-dimensional approach of Coulomb was used and transformed into a three-dimensional approach. It could be ascertained that the coefficient of friction was not constant during joint movement but almost linearly increased during walking from heel strike to contralateral heel strike. During the extension phase the determined *in vivo* coefficient of friction was nearly similar to the coefficients reported in previous studies (0.02-0.06). This indicates that *in vitro* simulator studies provide realistic test conditions during joint extension. However, when the joint movement changed from extension into flexion, the *in vivo* coefficient of friction increased drastically with an average peak of 0.14 around the instant of ipsilateral toe off. In previous studies, similar high coefficients were only obtained for dry condition [19] with ceramic/polyethylene as gliding partners. This let us assume that the lubrication of artificial hip joints with ceramic/polyethylene changes *in vivo* from mixed to dry friction condition. However, this effect has not been described in the literature to date. Thus, it can be concluded that typical *in vitro* simulator studies are not able to confidently describe the *in vivo* acting conditions during the flexion phase.

By using individual *in vivo* measured friction moments and corresponding coefficients of friction, the friction-induced power caused by the friction force was determined for each patient. This power heats up the implant. This temperature increase is transferred to the surrounding tissue and may cause tissue damage, depending on the final temperature. Potentially, loosening of the implant may be triggered. High temperatures may also destroy the macromolecules of the synovia, resulting in a further increase of joint friction.

The friction-induced power has shown a great variability between individuals. Similarly inter-individual differences were observed in another study [20]. In these study the friction induced heating of the total hip joint replacement was measured *in vivo* during walking. Thus we hypothesize that the large variance of the friction-induced power between the patients are eventually indicated by the individual synovial properties. However, the running-in effects of the gliding partner may depend on the individual physical activity levels of the patients and also attribute to these differences. The running-in effects and the expected decrease of friction in the joint over time following surgery will be part of a future study using the instrumented "T-Implant" (see publication: "High-tech hip implant for wireless temperature measurements *in vivo"* DOI:10.1371/journal.pone.0043489).

11. Conclusion

As part of the presented studies, *in vivo* joint loads and joint friction were measured simultaneously for the first time worldwide. Despite the small number of subjects and only one tribological pairing, this dataset presents an important scientific contribution to the understanding of *in vivo* loading of artificial hip joints. This exceptional insight into *in vivo* friction parameters of artificial hip joints will contribute to designing realistic parameters for *in vitro* implant testing.

Friction variability between individuals will require further *in vivo* measurements within a larger patient group as well as with different pairings. It is suggested to perform such investigations with the presented ‘Hip Implant for Wireless Temperature Measurements’ (see publication: "High-tech hip implant for wireless temperature measurements *in vivo*" DOI:10.1371/journal.pone.0043489).

12. Reverences

[1] Huch K., Müller K. A. C., Stürmer T., Brenner H., Puhl W. et al.; *„Sports activities 5 years after total knee or hip arthroplasty: the Ulm Osteoarthritis Study.”*; Annals of the Rheumatic Diseases 64: 1715–1720; 2005

[2] Chatterji U., Ashworth M.J., Lewis P. L., Dobson P.J.; *“Effect of total hip arthroplasty on recreational and sporting activity”*; ANZ journal of surgery 74: 446–449; 2004

[3] CJRR; *“CJRR report: Total hip and total knee replacements in Canada”*; Canadian Institute for Health Information; 2008

[4] Paul J. P.; *“The Biomechanics of the Hip-Joint and its Clinical Relevance”*; Proceedings of the Royal Society of Medicine, vol. 59, 943-48; 1966

[5] Bergmann G., Graichen F., and Rohlmann A.; *“Hip joint loading during walking and running, measured in two patients.”*; Journal of Biomechanics, vol. 26, no. 8, 969–90; 1993

[6] Davy D. T., Kotzar G. M., Brown R. H., Heiple K. G., Goldberg V. M., Berilla J., and Burstein A. H.; *“Telemetric force measurements across the hip after total arthroplasty.”*; The Journal of Bone and Joint Surgery, vol. 70, no. 1, 45–50; 1988

[7] Kotzar G. M., Davy D. T., Goldberg V. M., Heiple K. G., Berilla J., Heiple K. G., Brown R. H., and Burstein A. H.; *“Telemeterized In Vivo Hip Joint Force Data - A Report on Two Patients After Total Hip Surgery”*; Journal of Orthopaedic Research no. 21, 621-33; 1991

[8] Damm P., Graichen F., Rohlmann A., Bender A., Bergmann G.; *"Total hip joint prosthesis for in vivo measurement of forces and moments"*; Medical Engineering & Physics 32: 95–100; 2010

[9] Bergmann G., Graichen F., Rohlmann A., Westerhoff P., Heinlein B., et al.; *"Design and calibration of load sensing orthopaedic implants."*; Journal of Biomechanical Engineering 130; 2008

[10] Wu G., Siegler S., Allard P., Kirtley C., Leardini A., et al.; *“ISB recommendation on definitions of joint coordinate system of various joints for the reporting of human motion - part I: ankle, hip, and spine.”*; Journal of Biomechanics 35: 543–548; 2002

[11] Bender A. and Bergmann G.; *"Determination of typical patterns from strongly varying signals."*; Computer Methods in Biomechanics and Biomedical Engineering, vol. 15, no. 7, 761–9; 2012

[12] Damm P., Dymke J., Ackermann R., Bender A., Graichen F., Halder A., Beier A,, Bergmann G.; "Friction in total hip joint prosthesis measured in vivo during walking", PLoS ONE 8(11): e78373. doi:10.1371/journal.pone.0078373

[13] Bergmann G., Deuretzbacher G., Heller M., Graichen F., Rohlmann A., Strauss J., and Duda G.; *"Hip contact forces and gait patterns from routine activities."*; Journal of Biomechanics, vol. 34, no. 7, 859–71; 2001

[14] Dennis D., Komistek R. D., Northcut E. J., Ochoa J., and Ritchie A.; *"In vivo determination of hip joint separation and the forces generated due to impact loading conditions."*; Journal of Biomechanics, vol. 34, no. 5, 623–9; 2001

[15] Sonntag D., Uhlenbrock D., Bardeleben A., Kading M., and Hesse S.; *"Gait with and without forearm crutches in patients with total hip arthroplasty."*; International Journal of Rehabilitation Research, vol. 23, no. 3, pp. 233–243; 2000

[16] Neumann D.; *"An electromyographic study of the hip abductor muscles as subjects with a hip prosthesis walked with different methods of using a cane and carrying a load";* Physical Therapy, vol. 79, no. 12, 1163–76; 1999

[17] Bergmann G., Kölbel R., Rauschenbach N., and Rohlmann A.; *"Walking with canes and forearm-crutches. I. Reduction of loads at the hip and proximal end of the femur by one sided use of cane/crutch (author's transl)"*; Zeitschrift für Orthopädie und ihre Grenzgebiete, vol. 115, no. 2, 174–182; 1977

[18] Brand R. A. and Crowninshield R. D.; *"The effect of cane use on hip contact force."*; Clinical Orthopaedics and Related Research, no. 147, 181–184; 1979

[19] Xiong D. and Ge S.*; "Friction and wear properties of UHMWPE/Al_2O_3 ceramic under different lubricating conditions"*; Wear, vol. 250, 242–245; 2001

[20] Bergmann G., Graichen F., Rohlmann A., Verdonschot N., Van Lenthe G.H.; "*Frictional heating of total hip implants. Part 1: Measurements in patients.";* Journal of Biomechanics 34: 421–428; 2001

Statutory declaration

I hereby declare that I have authored this thesis independently, that I have not used other than the declared sources / resources, and that I have explicitly marked all material which has been quoted either literally or by content from the used sources. This PhD thesis has not been submitted for conferral of degree elsewhere.

_____ _____

Date and Location Signature

Eidesstattliche Erklärung

Hiermit versichere ich, dass ich die vorliegende Arbeit selbstständig verfasst und keine anderen als die angegebenen Quellen und Hilfsmittel benutzt habe. Alle Ausführungen, die anderen veröffentlichten oder nicht veröffentlichten Schriften wörtlich oder sinngemäß entnommen wurden, habe ich kenntlich gemacht.

Die Arbeit hat in gleicher oder ähnlicher Fassung noch keiner anderen Prüfungsbehörde vorgelegen.

_____ _____

Ort, Datum Unterschrift

Declaration to the contribution of the publications

Total hip joint prosthesis for in vivo measurement of forces and moments
Damm P. , Graichen F., Rohlmann A., Bender A., Bergmann G.;
Medical Engineering & Physics 32; 2010: p. 95-100; Impact: 1.62
Contribution in detail: conception, development, certification and fabrication of the implants, publication

High-tech hip implant for wireless temperature measurements in vivo
Bergmann G., Graichen F., Dymke J., Rohlmann A., Duda G.N., Damm P.;
PLoS ONE 7(8): e43489. doi:10.1371/journal.pone.0043489; Impact: 3.73
Contribution in detail: conception, development, certification and fabrication of the implants, data ascertainment, analyses and interpretation

Friction in total hip joint prosthesis measured in vivo during walking
Damm P., Dymke J., Ackermann A., Bender A., Graichen G., Bergmann G.,
PLoS ONE 8(11): e78373. doi:10.1371/journal.pone.0078373; Impact: 3.73
Contribution in detail: conception, data ascertainment, analyses and interpretation, publication

In vivo hip joint loading during post-operative physiotherapeutic exercises
Schwachmeyer V., Damm P., Bender A., Dymke J., Bergmann G.
PLoS ONE 8(10): e77807. doi:10.1371/journal.pone.0077807; Impact: 3.73
Contribution in detail: conception, data ascertainment, analyses and interpretation

In vivo hip joint loads during three methods of walking with forearm crutches
Damm P., Schwachmeyer V., Dymke J., Bender A., Bergmann G.
Clinical Biomechanics 28; 2013; 530-535; Impact: 1.869
Contribution in detail: conception, data ascertainment, analyses and interpretation, publication

List of publications

Journals

1. Damm P., Graichen F., Rohlmann A., Bender A., Bergmann G.
   Total hip joint prosthesis for in vivo measurement of forces and moments; Medical Engineering & Physics 32; 2010: p. 95-100; DOI: 10.1016/j.medengphy.2009.10.003

2. Kutzner I., Damm P., Heinlein B., Dymke J., Graichen F., Bergmann G.

   The effect of laterally wedged shoes on the loading of the medial knee compartment - in vivo measurements with instrumented knee implants.

   Journal of Orthopaedic Research, 2011: 29(12): p. 1910-1915;

   DOI: 10.1002/jor.21477

3. Bergmann G., Graichen F., Dymke J., Rohlmann A., Duda G.N., Damm P. *High-tech hip implant for wireless temperature measurements in vivo*

   PLOS One; 7 (8) 2012; e43489; DOI:10.1371/journal.pone.0043489

4. Damm P., Schwachmeyer V., Dymke J., Bender A., Bergmann G.
   In vivo hip joint loads during three methods of walking with forearm crutches; Clinical Biomechanics 28; 2013; 530-535; DOI: 10.1016/j.clinbiomech.2012.12.003

5. Damm P., Dymke J., Ackermann A., Bender A., Graichen G., Bergmann G.
   Friction in Total Hip Joint Prosthesis Measured In Vivo during Walking
   PLoS ONE 8(11): e78373; DOI:10.1371/journal.pone.0078373

6. Schwachmeyer V., Damm P., Bender A., Dymke J., Bergmann G.
   In vivo hip joint loading during post-operative physiotherapeutic exercises
   PLOS ONE 8(10); 2013; e77807; DOI:10.1371/journal.pone.0077807

7. Rohlmann A., Schmidt H., Gast U., Kutzner I., Damm P., Bergmann G.
   In vivo measurements of the effect of whole body vibration on spinal loads
   European Spine Journal; 2013; DOI: 10.1007/s00586-013-3087-8

8. Asseln M., Eschweiler J., Damm P., Al Hares G., Bergmann G., Tingart M., Radermacher K.
   Evaluation of biomechanical models for the planning of total hip arthroplasty
   Biomedical Engineering (58); 2013; DOI: 10.1515/bmt-2013-4116

Congresses

1. Damm P., Graichen F., Rohlmann A., Bergmann G.; *Frühbelastung ja/nein? - Lockerung des Schaftes*; AE-Dreiländerkurs Hüfte und Hüftrevision; 2009; Luzern; Swiss
2. Damm P., Rohlmann A.; Graichen F.; Bender A., Bergmann G.; *Entwicklung einer instrumentierten Hüftendoprothese zur Messung der in vivo auftretenden Kräfte und Momente*; 6. Jahrestagung der Deutschen Gesellschaft für Biomechanik; 2009; Münster; Germany
3. Damm P.; Graichen, F.; Rohlmann, A.; Bender, A.; Bergmann, G.; *An instrumented total hip joint prosthesis for in vivo measurement of forces and moment;* 17th Congress of the European Society of Biomechanics; 2010; Edinburgh, United Kingdom
4. Damm P.; Dymke J.; Bender A.; Graichen F.; Bergmann G. *Hip Joint Loading during Walking with Crutches*; Science Based Prevention – CSSB Symposium; 2009; Berlin; Germany
5. Damm P., Bender A., Dymke J., Graichen F., Bergmann G.; *Postoperative Änderung der in vivo Hüftgelenksbelastung beim Gehen mit Gehstützen;* 7. Jahrestagung der Deutschen Gesellschaft für Biomechanik; 2011; Murnau
6. Damm P., Bender A., Dymke J., Halder A.M., Beier A., Bergmann G.; *Belastung von Hüftendoprothesen beim Gehen mit Gehstützen;* Deutscher Kongress für Orthopädie und Unfallchirurgie; 2011; Berlin; Germany
7. Damm P., Ackermann R., Bender A., Graichen F., Bergmann G., *In-vivo measurements of the friction moment in total hip joint replacement during walking*; 18th Congress of the European Society of Biomechanics. 2012; Lisbon; Portugal
8. Damm P., Bergmann G., *Biomechanics of the hip - In vivo hip joint loads during different activities*; 1st Instructional Course - Anatomical Hip Reconstruction in Total Hip Arthroplasty; 2012; Zürich; Swiss
9. Damm P., Bergmann G.; *Sport und Endoprothetik - In vivo Belastungsmessungen am künstlichen Hüftgelenk bei sportlichen Aktivitäten*; 3. Bergedorfer Sportmedizin Symposium; 2012; Hamburg; Germany
10. Damm P., Bergmann G.; *Mechanische Belastung der Gelenke - In vivo Belastungsmessungen am künstlichen Hüftgelenk*; Sportmedizin Symposium; 2012; Tübingen; Germany

11. Damm P., Dymke J., Schwachmeyer V., Bender A., Halder A., Beier A., Graichen F., Bergmann G.; *In vivo Hüftgelenkbelastung beim Sport*; Deutscher Kongress für Orthopädie und Unfallchirurgie; 2012; Berlin; Germany
12. Damm P., Dymke J., Bender A., Halder A., Beier A., Graichen F., Bergmann G.; *Belastung des künstlichen Hüftgelenkes bei sportlichen Aktivitäten*; Endoprothetik Kongress Berlin; 2012; Berlin; Germany
13. Damm P., Dymke J., Bender A., Halder A., Beier A., Graichen F., Bergmann G.; *Hip Joint Loading during Walking with Crutches*; 13th Congress of European Federation of National Association of Orthopaedics and Traumathology; 2012; Berlin; Germany
14. Schwachmeyer V., Damm P., Bergmann G.; *In vivo hip joint loading during post-operative physiotherapeutic exercises*; 59th Annual Meeting of the Orthopaedic Research Society; 2013; San Antonio; USA
15. Damm P., Bender A., Graichen F., Bergmann G.; *In vivo friction in total hip replacement during walking*; 59th Annual Meeting of the Orthopaedic Research Society; 2013; San Antonio; USA
16. Damm P., Ackermann R., Bender A., Graichen F., Bergmann G.; *Die in vivo wirkende Reibung am künstlichen Hüftgelenk*; Endoprothetik Kongress Berlin; 2013; Berlin; Germany
17. Damm P., Bender A., Bergmann G.; *Die in vivo wirkende Reibung im künstlichen Hüftgelenk*; 8. Jahrestagung der Deutschen Gesellschaft für Biomechanik; 2013; Neu-Ulm; Germany
18. Eschweiler J., Asseln M., Damm P., Al Hares G., Bergmann G., Tingart M., Radermacher K.; *Evaluierung biomechanischer Hüftgelenksmodelle zur Planung von Endoprothesenversorgungen*; 8. Jahrestagung der Deutschen Gesellschaft für Biomechanik; 2013; Neu-Ulm; Germany
19. Kutzner I., Damm P., Schulze H. , Bergmann G., *Die Belastung des Knie- und Hüftgelenks beim Vibrationstraining;* 8. Jahrestagung der Deutschen Gesellschaft für Biomechanik; 2013; Neu-Ulm; Germany
20. Eschweiler J., Asseln M., Damm P., Al Hares G., Bergmann G., Tingart M., Radermacher K.; *Evaluation of Biomechanical Models for the Planning of Total Hip Arthroplasty*; Congress of the International Society for Computer Assisted Orthopaedic Surgery; 2013; Lake Buena Vista; USA

21. Damm P., Bender A., Graichen F., Bergmann G.; *In vivo measurements of friction in total hip joint prostheses during walking 3 and 12 months post-operatively*; XXIV Congress of the international society of biomechanics; 2013; Natal; Brasil
22. Bergmann G., Bender A., Graichen F., Damm P.; *Is insufficient joint lubrication a co-factor for development and progression of arthrosis?*; 19th Congress of the European Society of Biomechanics; 2013; Patras; Greece
23. Damm P.; Bender A., Bergmann G*., Influence of the resting period on the in vivo friction in hip joint replacement*; 19th Congress of the European Society of Biomechanics; 2013; Patras; Greece
24. Damm P., Kutzner I., Schulze H., Bergmann G., *Die Belastung der Hüft- und Kniegelenke beim Vibrationstraining mit einem Galileo-2000-System*; Deutscher Kongress für Orthopädie und Unfallchirurgie; 2013; Berlin; Germany
25. Damm P., Bergmann G., *In vivo Belastungsmessungen am künstlichen Hüftgelenk;* Kolloquium Biomedizinische Technik, Helmholtz-Institut für Biomedizinische Technik der RWTH Aachen; 2013; Aachen; Germany
26. Damm P., Schwachmeyer V., Krump A., Dymke J., Bergmann G., *In vivo Hüftgelenkbelastungen beim Training an Fitnessgeräten,* Endoprothetik Kongress Berlin; 2014; Berlin; Germany
27. Damm P., Bender A., Bergmann G., *Postoperative Änderung der in vivo Reibung im künstlichen Hüftgelenk beim Fahrradfahren*, Endoprothetik Kongress Berlin; 2014; Berlin; Germany
28. Schuster S., Bergmann G., Dymke J., Damm P., *Die in vivo Hüftgelenkbelastung beim Nordic Walking,* Endoprothetik Kongress Berlin; 2014; Berlin; Germany
29. Schmuck D., Bergmann G., Dymke J., Damm P., *Untersuchung des Einflusses unterschiedlichen Schuhwerks auf die in vivo Hüftgelenksbelastung beim Gehen*, Endoprothetik Kongress Berlin; 2014; Berlin; Germany

Awards

2011

Young Investigator Award (2. Place)

7. Jahrestagung der Deutschen Gesellschaft für Biomechanik; Murnau; Germany

„Postoperative Änderung der in vivo Hüftgelenksbelastung beim Gehen mit Gehstützen“

Damm P., Bender A., Dymke J., Graichen F., Bergmann G.

2012

ESB Clinical Biomechanics Award (nominated)

18th Congress of the European Society of Biomechanics; Lisbon; Portugal

“In-vivo measurements of the friction moment in total hip joint replacement during walking”

Damm P., Ackermann R., Bender A., Graichen F., Bergmann G.,

2013

Poster Award

6. Endoprothetikkongress; Berlin, Germany

„Die in vivo wirkende Reibung am künstlichen Hüftgelenk“

Damm P., Ackermann R., Bender A., Graichen F., Bergmann G.

Best Experimental Study Award

8. Jahrestagung der Deutschen Gesellschaft für Biomechanik; Neu-Ulm; Germany

„Die Belastung des Knie- und Hüftgelenks beim Vibrationstraining“

Kutzner I., Damm P., Schulze H. , Bergmann G.